ΠΑΝΕΠΙΣΤΗΜΙΟ ΚΡΗΤΗΣ
ΣΧΟΛΗ ΘΕΤΙΚΩΝ ΚΑΙ ΤΕΧΝΟΛΟΓΙΚΩΝ ΕΠΙΣΤΗΜΩΝ
ΤΜΗΜΑ ΒΙΟΛΟΓΙΑΣ

ΚΑΙ

ΕΥΡΩΠΑΙΚΟ ΕΡΓΑΣΤΗΡΙΟ ΜΟΡΙΑΚΗΣ ΒΙΟΛΟΓΙΑΣ ΧΑΙΔΕΛΒΕΡΓΗ
EUROPEAN MOLECULAR BIOLOGY LABORATORY
(EMBL HEIDELBERG)

THE ROLE OF THE HOMEOBOX TRANSCRIPTION FACTOR BSX IN THE REGULATION OF ENERGY HOMEOSTASIS IN MICE

ΜΑΡΙΑΣ ΣΑΚΚΟΥ

ΔΙΔΑΚΤΟΡΙΚΗ ΔΙΑΤΡΙΒΗ

ΥΠΟΒΛΗΘΗΚΕ ΣΤΟ ΤΜΗΜΑ ΒΙΟΛΟΓΙΑΣ ΤΟΥ ΠΑΝΕΠΙΣΤΗΜΙΟΥ ΚΡΗΤΗΣ

ΗΡΑΚΛΕΙΟ 2006

ΕΠΙΒΛΕΠΟΥΣΑ ΕΠΙΤΡΟΠΗ ΣΤΟ ΕΥΡΩΠΑΙΚΟ ΕΡΓΑΣΤΗΡΙΟ ΜΟΡΙΑΚΗΣ ΒΙΟΛΟΓΙΑΣ - **EMBL HEIDELBERG**

Dr MATHIAS TREIER (DEVELOPMENTAL BIOLOGY UNIT)
Dr MANOLIS PASPARAKIS (MOUSE BIOLOGY UNIT, MOTEROTONTO)
Dr IAIN MATTAJ (GENE EXPRESSION UNIT- DIRECTOR GENERAL EMBL)
Καθ.ΙΩΣΗΦ ΠΑΠΑΜΑΤΘΑΙΑΚΗΣ (ΚΑΘΗΓΗΤΗΣ, ΠΑΝΕΠΙΣΤΗΜΙΟ ΚΡΗΤΗΣ)

Η ΕΠΤΑΜΕΛΗΣ ΕΞΕΤΑΣΤΙΚΗ ΕΠΙΤΡΟΠΗ

ΙΩΣΗΦ ΠΑΠΑΜΑΤΘΑΙΑΚΗΣ, ΚΑΘΗΓΗΤΗΣ ΠΑΝΕΠΙΣΤΗΜΙΟΥ ΚΡΗΤΗΣ
ΑΧΙΛΛΕΑΣ ΓΡΑΒΑΝΗΣ, ΚΑΘΗΓΗΤΗΣ ΠΑΝΕΠΙΣΤΗΜΙΟΥ ΚΡΗΤΗΣ
ΑΘΑΝΑΣΣΙΟΣ ΠΑΠΑΒΑΣΣΙΛΙΟΥ, ΚΑΘΗΓΗΤΗΣ ΠΑΝΕΠΙΣΤΗΜΙΟΥ ΑΘΗΝΑΣ
ΔΕΛΙΔΑΚΗΣ ΧΡΗΣΤΟΣ, ΑΝ. ΚΑΘΗΓΗΤΗΣ ΠΑΝΕΠΙΣΤΗΜΙΟΥ ΚΡΗΤΗΣ
ΧΑΛΕΠΑΚΗΣ ΓΙΩΡΓΟΣ, ΑΝ. ΚΑΘΗΓΗΤΗΣ ΠΑΝΕΠΙΣΤΗΜΙΟΥ ΚΡΗΤΗΣ
ΜΑΡΙΑ ΚΟΦΦΑ, ΕΠ.ΚΑΘΗΓΗΤΗΣ ΠΑΝΕΠΙΣΤΗΜΙΟΥ ΑΛΕΞΑΝΔΡΟΥΠΟΛΗΣ
Dr MATHIAS TREIER (EMBL)
Dr MANOLIS PASPARAKIS (EMBL)

Η ΜΕΛΕΤΗ ΑΥΤΗ ΔΙΕΚΠΕΡΑΙΩΘΗΚΕ ΣΤΟ ΕΥΡΩΠΑΙΚΟ ΕΡΓΑΣΤΗΡΙΟ ΜΟΡΙΑΚΗΣ ΒΙΟΛΟΓΙΑΣ –

THIS STUDY WAS CARRIED OUT AT THE EUROPEAN MOLECULAR BIOLOGY LABORATORY IN HEIDELBERG

Acknowledgements

I would like to thank my supervisor Mathias for having me in his lab and for providing me with stimulating ideas and discussions throughout my PhD. His expertise, scientific advice, endless good ideas and the high standards of his demands, have been of great value for my development as a person and as a scientist.

I 'm grateful to the members of my thesis committee Iain Mattaj, Manolis Pasparakis and Sifis Papamathaiakis for the suggestions, the challenging discussions and the advices about my work.

Thanks to past and present members of the Treier lab. Special thank goes to Katrin and Eve, with whom I worked more closely, for supporting helping and teaching me many things especially at the beginning of my PhD, Petra Wiedmer from Matthias's Tschoep lab for collaborating with us for the physiological measurements of the mice and to Henry who helped me with the microarray experiment. Thanks a lot the rest of the lab especially Vitor, Lars, Uli, Dirk, Sandra, Thomas, Claudia, Tobias and Anne for the constructive discussions, comments, advices, support and fun in and out of the lab.

Thanks to Christian Klassen from the transgenic facility for the injections and production of chimeric mice. Thanks to everybody from the Laboratory of Animal Resources for the expert handling of the mouse colonies, the help they gave me for weighing the mice and special thanks to Klaus Schmidt for performing the iv and ip injections.

I would like to thank all my friends for making these 4 years of my PhD in Heidelberg complete. Thanks to my swimming buddies, David, Dagmar, Stephanie, Aurelio, Felix and Johan. Special thanks to my friends Karsten, Caroline, Manuela, Dilem, Tassos, Kat. Pam, Giovanni, Nadine, Angela, Nancy, Kristin and all the others.

Very special thanks to my mom my dad and Alexandros for their love, support and advice, without them nothing would have been possible.

Thank you, Will, for your love and for standing by my side, "there is no delight in owning anything unshared" (Seneca), I dedicate this thesis to you.

Summary

Consuming sufficient food to maintain adequate energy stores is critical for survival for all species in the animal kingdom. To ensure that this activity takes a high priority in brain function, mammalian brains have evolved several potent and inter-related neuronal circuitries that drive and control the balance between food consumption and energy expenditure, and this is a fundamental aspect of energy homeostasis. The neuronal circuitries that regulate energy balance include the hypothalamic neuropeptide Y, Agouti related peptide (NPY/AgRP) and pro-opiomelanocortin, cocain-amphetamin regulated transcript (POMC/CART) expressing neurons. NPY/AgRP neurons constitute a potent feeding system that is activated during a negative energy balance situation. This is actively opposed by the POMC/CART satiety system which is stimulated upon excess of energy storage. Peripheral hormones like Leptin, an adipocyte derived cytokine that signals starvation of the body to the brain upon down-regulation, Insulin, a pancreas derived hormone signaling glucose levels or Ghrelin, a gut secreted peptide that triggers the feeling of hunger, utilize both NPY/AgRP and POMC/Cart expressing neurons to mediate their functions. They achieve this by modifying the activity of these neurons at both the physiological and transcriptional level.

To investigate the transcriptional network underlying the function of NPY/AgRP and POMC expressing neurons we identified Bsx, a homeodomain transcription factor that exerts specific expression in the orexigenic NPY/AgRP neurons of the arcuate nucleus. In order to characterize genetically the role of *Bsx* in the orexigenic neurons I generated two mouse strains deficient for the gene. I could show by this loss of function experiment in mice, that Bsx is required in the NPY/AgRP neurons both to maintain the expression of *Npy* and *Agrp* peptides, and to modulate spontaneous physical activity at the physiological level. In addition, mutant mice lacking *Bsx* can partially rescue the obesity phenotype caused by Leptin deficiency in *ob*/*ob* mutant mice. Food intake is reduced in these mice, due to the down-regulation of *Npy,* but the locomotory activity defect that *ob*/*ob* mice display is not rescued. These results provide evidence that the proposed relationship between levels of physical activity, resting thermogenesis, food intake and body weight can be genetically uncoupled and suggests the existence of a specific molecular control for subcomponents of energy balance regulation within subsets of hypothalamic neurons.

List of Abbreviations

AgRP	Agouti Related Peptide
αMSH	α-Melanin stimulating hormone
ARH	Arcuate nucleus of hypothalamus
BAC	Bacterial Artificial Chromosome
Bsh	Brain specific homeobox (Drosophila gene)
Bsx	Brain specific homeobox (murine protein)
Bsx	Brain specific homeodomain (murine gene)
cAMP	cyclic Adenosine Mono Phosphate
CART	cocaine amphetamine transcript
CCK	cholecystokinin
cDNA	complementary DNA
cm	centimeter
CNS	Central nervous system
CRE	cAMP response element
CREB cAMP	Response Element Binding protein
CRH	Corticotropin Releasing Hormone
DIO	Diet induced obesity
DNA	desoxyribonucleic acid
DMC	Dorsomedial hypothalamic nucleus, compact
DMH	Dorsomedial hypothalamus
DMSO	dimethyl sulfoxide
DTR	Diphteria toxin
EGFP	Enhanced Green Fluorescent Protein
g	gram
GABA	Gamma aminobutyric acid
GAD	glutamic acid decarboxylase
GH	Growth Hormone
GHRH	Growth hormone releasing hormone
GHRP-6	His-D-Trp-Ala-Trp-D-Phe-Lys-amide
GHS-R	Growth hormone secretagogue receptor
GLP-1	glucagon like peptide 1
GPCR	G protein-coupled receptor

GST	glutathione S-transferase
IR	Immunoreactivity
IRES	internal ribosomal entry site
IRS	insulin receptor substrate
JAK	Janus Kinase
Kb	Kilobase
KO	Knock Out
L	Litre
LB	Luria-Bertani
LHA	Lateral hypothalamic area
MAP	kinase Mitogen Activated kinase
ml	milli litre
μl	micro litre
M	Molar
mM	milli Molar
μM	micro Molar
MCH	Melanocortin-concentrating Hormone
MC4R	Melanocortin 4 receptor
MSH	Melanocyte Stimulating Hormone
NPY	Neuropeptide Y
NTP	nucleotide tri-phosphate
ObRb	leptin receptor
ORF	Open reading frame
PBS	phosphate buffered saline
PCR	polymerase chain reaction
PH	potential of Hydrogen
PI3K	phosphoinositol-3 kinase
PKA	Protein kinase A
PMA	Phorbol 12-myristate 13-acetate
POMC	Pro-opiomelanocortin
PP	pancreatic peptide
rpm	revolutions per minute
s	second

SOCS3	suppressor of cytokine signaling 3
STAT3	signal transducer and activator of transcription 3
TR	Thyroid Hormone Receptor
TRH	Thyrotropin Releasing Hormone
TSH	Thyroid Stimulating Hormone
U	unit
V	volt
VMH	Ventromedial hypothalamus
wt	wild type
^{o}C	degrees centigrade

1 Introduction

In the developed world, obesity prevalence is increasing at an alarming rate with major derivative health complications. The easy availability of high caloric food in combination with a general decrease in physical activity promotes obesity, diabetes, hypertension and heart diseases. Body weight is determined by both inheritance and environment and intensive studies in the last decade have revealed the identity of some genes involved in these processes. Products of these genes are expressed in the hypothalamic area of the brain and are responsible for regulating the physiology of energy homeostasis. Cloning of two recessive mutations in mouse, the *obese* (*ob*) and *diabetes* (*db*), resulting in morbid obesity, hyperglycemia and diabetes was the first insight in the molecular events underlying obesity and furthermore gave new perspectives for drug discovery and development.

1.1 Hypothalamic circuits and their role in regulating energy homeostasis

Feeding is a behavior critical for the survival of the organism. Feeding behavior does not only provide all of the body's macronutrients (carbohydrates, proteins and lipids) and micronutrients (minerals and vitamins) but in addition it is a fundamental aspect of energy homeostasis, a process ensuring that energy stores in the form of adipose tissue is kept constant over long intervals. For this process to occur a physiological system exists, that has as primary function to maintain homeostasis of energy stores in response to variable access to nutrition and demands for energy expenditure. This system has both afferent sensing components and efferent output (Figure 1.1). The afferent system contains mainly two types of signals, short-term signals that regulate initiation and termination of individual meals, and long-term signals that inform the central nervous system (CNS) about the status of the body's energy stores. These two categories of signals are not exclusive, since signals

relating to long-term energy stores, including insulin and leptin can modulate responses to short-term nutritional inputs. All of the signals of the afferent system converge in the hypothalamus, a neural structure situated at the mediobasal area of the brain. Efferent outputs of the hypothalamus exert homeostatic control over food intake, levels of physical activity, basal energy expenditure and endocrine systems, including those that determine reproductive competence.

The primary locus for integration of the signals influencing energy balance is neurons situated in the Arcuate nucleus (Arc) of hypothalamus. Arc nucleus is the sentinel of hypothalamus since it occupies a strategic place in the brain at the floor of the third ventricule next to the median eminence (ME), which lacks the blood-brain barrier (Banks et al., 1996; Korner et al., 1999). Neurons of the Arc nucleus express a large number of receptors enabling them to sense and integrate all the hormonal and peptidergic signals related to energy balance. The circulating hunger and satiety signals penetrate the brain via ME and initiate their actions by engaging the adequate receptors on the Arc nucleus neurons.

Within the Arc nucleus two distinct populations of neurons have been characterized (Elias et al., 1998) (Figure 1.2). One population that synthesizes neuropeptide Y (NPY) and agouti-related peptide (AgRP) (thereafter called as NPY/AgRP neurons) (Bagnol et al., 1999; Baskin et al., 1999; Hahn et al., 1998) and the other synthesizes pro-opiomelanocortin (POMC) and cocaine amphetamine regulated transcript (CART) (thereafter called POMC/AgRP neurons) (Kristensen et al., 1998; Vrang et al., 1999). The two populations have opposite functions in the regulation of energy homeostasis and body weight, NPY/AgRP neurons stimulating feeding, called for this reason “orexigenic” and POMC/CART neurons stimulating satiety and ihibiting food intake, called “anorexigenic”. The outlines of the hypothalamic circuits in which NPY/AgRP and POMC/CART neurons are involved have been revealed by numerous genetic studies presented in the next two paragraphs.

1.1.1 Central Melanocortin system

POMC produces two different classes of peptides post-translational, melanocortins and β-endorphins (Figure 1.2). Both of them exert various functions

since they act as hormones or neuropeptides. Melanocortin peptides including the adrenocorticotropin and α- β- γ- melanocyte-stimulating hormones (MSH) mediate their effect by binding specifically with high affinity on G protein-coupled-melanocortin receptors, MC1R to MC5R. POMC is expressed in the periphery, primarily in the pituitary, skin and hair follicle (Cone, 2005).

In the Central Nervous System (CNS) the melanocortin system includes a circuitry of neurons in the hypothalamus where it includes the two neuronal populations of the Arc nucleus expressing AgRP and POMC, in the nucleus of the solitary tract (NTS) of the brainstem and secondary downstream target neurons innervated by POMC and AgRP containing fibers, that express the MC3R and MC4R. POMC and the melanocortin peptides produced in the CNS function as agonists of MC3 and MC4R, whereas AgRP is a high affinity antagonist of these receptors. Receptors sites in the brain receive most of the case projections from both agonist and antagonist expressing fibers (Haskell-Luevano et al., 1999). Genetic and pharmacological studies performed in mice and humans give evidence for the implication of the melanocortin system in signaling satiety and suppression of feeding. A unique feature of this system is that it functions as a rheostat of energy stores since it has been shown that POMC and MC4R have dosage effect in which loss of one of the alleles of the genes produces intermediate phenotypes (Huszar et al., 1997).

An indication for the role of melanocortin system in energy homeostasis came with the elucidation of the genetic mechanisms underlying the obesity in the mutant A^y/a mouse strain (Yen et al., 1994). Ectopic over expression of the Agouti gene was found to be the cause of the obese and of the yellow color coat phenotypes. Agouti does that by acting as an aberrant antagonist of the melanocortin receptors, the MC1R in the skin and the MC4R in the hypothalamus of the brain. In addition it has been shown that intra cerebellar administration of AgRP results to chronic hyperphagia and to weight gain (Ollmann et al., 1997). Furthermore targeted deletions of the genes encoding POMC and either of the two melanocortin receptors expressed in the brain results to obesity, hyperphagia, hyperinsulemia and hyperglycemia confirming the interpretation for the A^y/a mouse phenotype (Butler et al., 2000; Challis et al., 2004; Yaswen et al., 1999). Inactivation mutations in the POMC locus have been identified in obese human individuals, being hyperphagic and show altered skin pigmentation

just like the mouse model does, that will be very useful for the determination of the role of all the individual cleavage products of POMC on energy homeostasis (Krude et al., 1998; Vaisse et al., 1998). Mice lacking functional MC3R display increased adiposity, despite that their metabolic rate and food intake seem to be normal. MC4R deficient mice in the opposite develop similar phenotype o the one of Ag^{y} mice, notably obesity, hyperphagia, increased longitudinal growth and type 2 diabetes in some of the cases. Therefore it was predicted that loss of function for the AgRP, would induce starvation and severe weight loss. It was a big surprise in the obesity field that loss of function of AgRP via knockout of the *Agrp* gene in mice ($Agrp^{-/-}$) produced no metabolic phenotype (Gropp et al., 2005; Wortley et al., 2005). KO mice have normal body weight, adiposity and unchanged food intake, raising the question if this neuropeptide was essential for energy homeostasis as initially has been speculated.

1.1.2 NPY/AgRP expressing neurons

NPY has been implicated by many studies using different approaches in the regulation of feeding and body weight (Hokfelt et al., 1998). NPY is a 36-amino-acid neurotransmitter widely expressed throughout the central and the peripheral nervous system. Other related family members of the NPY are the peptide YY (PYY) and the pancreatic polypeptide (PP) that are produced by L type cells in the small intestine and colon and in F type cells in the pancreas respectively (Hazelwood, 1993). Both PYY and PP recognize, bind and are able to access on the Y receptors expressed in the hypothalamus and the brain stem. All the Y receptors are seven trans-membrane GPCR receptors, and their activation results to inhibitory responses such as the inhibition of cAMP accumulation (Shimizu-Albergine et al., 2001). NPY and PYY have identical affinity onto all six known Y receptors (Y1-Y5 and in mouse the Y6) (Blomqvist and Herzog, 1997).

Icv of NPY or NPY related peptides stimulate robust long-term feeding (Clark et al., 1984; Marsh et al., 1998; Woods et al., 1998). Furthermore NPY expression is strongly induced in conditions of either energy deprivation, like starvation, or increased energy demands, like lactation (Chen et al., 1999; Rizk et al., 1998;

Schwartz et al., 1998; Wilding et al., 1993). Various rodent genetic models for obesity exhibit hyperphagia and strong up-regulation of *Npy* expression levels, just like in the case of *Agrp*. In addition both *Agrp* and *Npy* are induced by various pharmacological treatments that stimulate feeding. Furthermore blockage of their action in the hypothalamus by pharmacological means inhibits feeding.

Despite the fact that all the previous results about NPY and its function in feeding regulation are appealing, genetic evidence for the role of NPY does not support the model of NPY/AgRP neurons being orexigenic. Transgenic mice over-expressing NPY in the Arc nucleus (18% more compared to basal expression levels in wt mice) show no change in food intake and body weight (Kaga et al., 2001). However an obese phenotype with transiently increased food intake have been observed when the transgenic mice are fed with high sucrose diet. Markedly mice unable to produce NPY ($Npy^{-/-}$) have normal body weight and show no reduction in food intake. $Npy^{-/-}$ mice respond to starvation and re-feeding normally and they show no difference to wild type mice when they are fed with high fat diet (Erickson et al., 1996a). Later on, detailed analysis of the $Npy^{-/-}$ mice revealed some deficits. For example $Npy^{-/-}$ mice are slower to initiate feeding after a period of starvation and they show a transient blunting of feeding response in hypoglycemic challenges, nevertheless daily food intake measurements showed no difference between the different genotypes (Bannon et al., 2000). Furthermore high fat diet doesn't influence the body weight of $Npy^{-/-}$ mice in a significant manner, but increases the fat pad depots in the KO mice compared to wt ones (Hollopeter et al., 1998). Thus contrary to expectations genetic disruption of *Npy* has little effect on feeding. The discrepancies found between the icv injection studies in wt mice and the phenotype of *Npy* deficient mice lead to a confusion in the field about the role of NPY in the regulation of feeding and energy balance. However other genetic studies gave more obvious evidence about the role of NPY in feeding regulation. Crossing of the $Npy^{-/-}$ mouse in the *ob*/*ob* background, a leptin deficient severely obese mouse, leads to a significant attenuation of the obesity phenotype and to amelioration of the diabetes developed in the *ob*/*ob* mutant mice. This genetic analysis is direct evidence that NPY mediates increase of food intake and obesity in this obesity model mouse and that it is a necessary component of the feeding behavior regulation (Erickson et al., 1996b).

Pharmacological studies performed on the Y receptors in wt mice gave similar results as the initial studies on NPY. Icv injections of the Y1/Y5 preferring ligand Leu^{31}/Pro^{34} NPY into rodents strongly stimulates feeding behavior. However *Y1 receptor* KO mice do not display any abnormalities in respect of feeding and body weight (Kanatani et al., 2000; Kushi et al., 1998; Pedrazzini, 2004). The only defect detected was that the fasting induced re-feeding was impaired in the Y1 deficient mice compared to wt littermates. Y5 receptor KO does similarly feed and grow in a normal way. In the same lines body weight and adiposity of $Y5^{-/-}$ receptor mice are normal and they show no defect in fasting induced re-feeding (Marsh et al., 1998; Marsh et al., 1999).

For the Y2 receptor, the PYY (3-36) has been identified as an endogenous agonist. PYY belongs to the NPY related peptide family and is secreted postprandial from cells of the gastrointestinal tract. When PYY is injected in mice, inhibits food intake and this effect is impaired in Y2 receptor KO mice. Another interesting feature of Y2 receptor is that it is the only Y receptor expressed in the NPY/AgRP neurons, and given that the intracellular signaling pathways activated by the Y receptors are inhibitory ones, Y2 might be involved in an inhibitory feedback loop for these neurons. However Y2 receptor KO mice have no major phenotype in respect to feeding, in the opposite of what expected it has been measured that they have increased food intake instead. Nevertheless, like in the case of NPY the double mutant $Y2^{-/-}$ *ob*/*ob* mice show attenuation in the obesity and the diabetes phenotype (Naveilhan et al., 1999; Sainsbury et al., 2002a; Sainsbury et al., 2002b).

Germline deletion of the Y4 receptor gives rise to mice that show reduced food intake and significantly reduced body weight. Y4 KO mice display in addition other phenotypes; they have a smaller heart and lower basal blood pressure. Interestingly though generation of the double $Y4^{-/-}$ *ob*/*ob* mice does not ameliorate the obesity phenotype (Sainsbury et al., 2002c). In addition the double KO $Y2R^{-/-}$ $Y4R^{-/-}$ was produced and the mice retained the lean phenotype with reduced body weight and fat mass, due to the increase of thermogenesis and locomotor activity. This experiment reveals in parallel that the two receptors function in synergy to regulate locomotor activity and food intake since they interact genetically (Sainsbury et al., 2003).

Despite the fact that clearly NPY and Y receptors mediate induction of food intake in both pharmacological experiments and obesity mouse models they seem to have a high redundancy since none of the single gene deficiency developed any eating disorder. For the Y receptors this redundancy is due to the multiple different ones that are expressed in overlapping patterns in the brain. Various combinations of KO alleles for these genes and generation of double KO mice showed no major defect in feeding behavior. Both compound *Npy*$^{-/-}$ *AgRP*$^{-/-}$ (Qian et al., 2002) and *Y1*$^{-/-}$ *Y2*$^{-/-}$ mutant mice display normal food intake, body weight and adiposity (Naveilhan et al., 2001; Naveilhan et al., 1999; Naveilhan et al., 1998). The only combination of alleles that generated lean mice that ate less is the double mutant mice for *Y2*$^{-/-}$ *Y4*$^{-/-}$ (Naveilhan et al., 2001)

A prominent explanation of the bland metabolic phenotypes in the *Npy*$^{-/-}$ *AgRP*$^{-/-}$ double KO or the single *Npy*$^{-/-}$ and *AgRP*$^{-/-}$ is that the ablation of these genes early on in development promotes compensatory mechanisms to ensure survival and normal body weight. Starvation is a bigger threat for survival rather than obesity. Thus this system is organized and developed in a more robust way in response to deficient energy intake rather than excess of energy. Evolution in these circumstances favored genotypes that are efficiently storing energy in periods of pour food supplies in both humans and rodents (Neel, 1999). The evolutionary advantage of the energy intake and storing system is reflected during development, since the NPY/AgRP system is established between 8 and 45 days after birth in mouse, before the melanocortin circuitry is. Nevertheless, animal have developed adaptive responses to avoid obesity in the case of over-storing energy and fat by suppressing feeding and increasing energy expenditure (Weigle, 1994). This system though of obesity avoidance is not that strongly galvanized as the one of stimulating appetite. Thus, it is easy to explain the existence of high number of obesity models in rodents compared to lean ones and the increase of obesity prevalence in humans the last decades, given the high fat diet environment.

Physiological analysis of the Arc nucleus circuitry revealed that the two neuronal populations NPY/AgRP and POMC/CART are functionally related (Figure) (Elmquist et al., 1998a; Elmquist et al., 1999). Electrophysiological recordings using mouse hypothalamic slices in which POMC/CART neurons and NPY/AgRP neurons were identified by the expression of GFP-POMC and Saphire-NPY transgenes have

been performed to characterize the responsiveness of the neurons. Whole-cell patch-clamp recordings demonstrated that the POMC/CART cell bodies receive synapses by neuronal terminals containing both the inhibitor neurotransmitter GABA and the neuropeptide NPY (Roseberry et al., 2004). Within the Arc nucleus The NPY/AgRP neurons exert presynaptic inhibition onto the POMC neurons via GABAergic projection on their cell bodies. Depolarization and electrical activation of the orexigenic NPY/AgRP neurons by peripheral hunger signals leads to inhibition of the anorexigenic POMC/AgRP neurons, a necessary coordination of the circuitry in order that the two opposite pathways are mutually exclusive and that the circuitry either induces feeding or satiety.

Sensory peripheral and central afferent inputs related to energy stores bind to their respective receptor on the POMC and NPY/AgRP expressing neurons and are able to change the activity and/ or their transcriptional program of these neurons via various intracellular signaling pathways activated. The convergence of these signals in the brain is accomplished by projections of the first order neurons in the Arc nucleus to second order neurons situated in various other hypothalamic. NPY/AgRP and POMC neurons project and innervate neurons situated at the Paraventricular nucleus (PVH) and the lateral hypothalamic area (LHA), both of which provide the main descending outputs that regulate autonomic, and endocrine responses contributing to feeding.

The next paragraphs will outline the role of the various peripheral signals in modifying the activity of the Arc nucleus neuronal circuitry described.

1.2 Afferent peripheral signals

1.2.1 Leptin

Large number of studies support the hypothesis that food intake and body weight in long term is controlled by a lipostatic system (Kennedy, 1953). Since fat

mass tends to be relatively stable over long periods in mammals, it has been speculated that there should be a homeostatic mechanism that monitors changes in energy stores and drives compensatory changes in food intake and energy expenditure in order to maintain adipose mass at a set point. This adipostatic model is consistent with the observation that a decrease in the fat mass from fasting or surgical operation causes hyperphagia, decreases energy expenditure, and eventually resets body weight in the previous level (Faust et al., 1977; Harris, 1990; Harris et al., 1986). Conversely, weight gain due to forced overfeeding inhibits voluntary food intake (Harris, 1990; Harris et al., 1986). Based on these data it has been suggested that a circulating satiety factor exists regulating both food intake and energy expenditure according to the levels of the energy stores of the body. That concept was further strengthened by the discovery and characterization of two recessive mutations in mice, the *obese* (*ob*) and the *diabetes* (*db*), both leading to obesity and diabetes (Ingalls et al., 1950).

The *ob* gene was identified by positional cloning 11 years ago, and shown to encode leptin, a cytokine like hormone named from the Greek root leptos that means thin (Zhang et al., 1994). The gene is transcribed to a 4.5 Kb mRNA transcript with a highly conserved 167 amino acid open reading frame (ORF) expressed and secreted almost exclusively by adipocytes and to lower levels by brown adipose tissue, stomach, skeletal muscles, placenta and mammary tissues (Gong et al., 1996). The *ob* gene expands on 650 Kb and consists of 3 exons. Within the *ob* gene promoter several regulatory elements have been identified including, cAMP and glucocorticoid response elements, and CCATT/enhancer and SP-1 binding sites. Ob gene product shows a high homology among mouse, rat and human.

Leptin mRNA levels is positively strong correlated with leptin protein levels in adipose tissue and circulating leptin levels (Considine et al., 1996b; Frederich et al., 1995; Maffei et al., 1995). The changes in leptin expression in response to fasting or feeding correlate to changes in body weight or fat mass and fat cell size, suggesting that leptin serves as indicator of energy stores in the adipose tissue (Boden et al., 1996). Leptin expression though do not increase in response to individual meals, indicating that it has a long-term satiety function rather than a short-term meal related one. It has been reported that regulation of leptin expression by nutrition is regulated by insulin, since leptin expression increases after the peak of insulin secretion during the feeding cycle (Saladin et al., 1995). Cell culture experiments performed on

isolated adipocytes showed that insulin treatment induces increase of leptin expression (Saladin et al., 1995). Additionally insulin administration in rodents induces increase of blood leptin levels (Saladin et al., 1995).

Early studies have shown that intracranial and peripheral administration of leptin in rodents and humans respectively reduced body weight and fat mass, and the reduction was mainly due to a marked decrease of food intake (Halaas et al., 1995). Furthermore, the involvement of leptin in feeding regulation has been supported by the analysis of three genetic models of obesity, the *ob*/*ob* and *db*/*db* mice and the *fa*/*fa* Zucker rat . Lack of functional leptin, in the *ob*/*ob* mutants or lack of functional leptin receptor in the *db*/*db* and *fa*/*fa* mutant animals results to morbid severe obesity and diabetes due to hyperphagia and reduced energy expenditure (Chen et al., 1996; Considine et al., 1996a; Halaas et al., 1995). In both *ob*/*ob* and *db*/*db* mutant mice, where leptin signaling is deficient, the brain senses constitutively starvation and lack of energy fat stores despite the obesity. Both mutant mice strains have reduced energy expenditure and very efficient metabolism, such that obesity develops even without overeating. In adulthood they even develop diabetes since they exhibit hyperglycemia and hyperinsulinemia (Ahima et al., 1996) as a result of the constant feeding.

As already mentioned above, hypothalamus is the primary locus for the integration of energy store related signals. Gene expression analysis in the *ob*/*ob* and *db*/*db* mice have showed that *Npy* and *Agrp* transcripts are constantly induced, whereas *Pomc1* transcriptions seem to be suppressed. Genetic analysis have indicated the importance of NPY in feeding behavior since the generation of the compound mutant $Npy^{-/-}$ *ob*/*ob* exhibits an attenuated obesity (Erickson et al., 1996b). *Npy* deficiency in the *ob*/*ob* background leads to improve feeding and energy metabolism and to a partial rescue of the obese phenotype that *ob*/*ob* mice exert. Despite the lack of genetic data supporting the role of NPY in stimulating feeding which aroused from the analysis of the $Npy^{-/-}$ mice, generation of the compound mutant proved that it is an essential component of regulating energy homeostasis and mediator of leptin effect on the body weight.

Leptin receptor (ObR) has been identified by expression cloning using mouse brain and by positional cloning from the *db* locus in mice (Chen et al., 1996; Tartaglia et al., 1995). ObR belongs to the family of class 1 cytokine receptors which includes, the gp130, signal transducing membrane protein of the interleukin-6 (IL-6) signaling

complex, the leukemia inhibitory factor (LIF) receptor and the granulocyte colony-stimulating factor (G-CSF) receptor (Tartaglia, 1997). In mice *db* locus produces six different spliced forms for ObR (a, b, c, d, e, f) with different carboxy-termini length (Lee et al., 1996). The ObRe isoform that does not contain a transmembrane domain neither intracellular motifs and circulates as a soluble receptor. ObRb it's the only isoform fully capable of activating intracellular signaling. Its importance is demonstrated by the fact that *db*/*db* obesity is due to a premature stop codon inserted in the 3'-end of the ObRb mRNA transcript that leads to a synthesis of a truncated receptor that replaces the ObRb isoform with the ObRa one, which is incapable in activating intracellular signaling pathway.

ObRa is expressed in the CNS with highest levels in the choroid plexus and the microvessels (Bjorbaek et al., 1998b). Leptin enters the brain by a saturable transport mechanism, possibly by receptor-mediated endocytosis across the hemato-encephalic barrier. ObRa due to its expression pattern is a good candidate for binding and internalizing leptin.

Analysis of the *ObRb* expression pattern revealed dense mRNA levels in the CNS. More precisely, within the hypothalamus high mRNA levels have been detected in the arcuate (ARC), dorsomedial (DMH), ventromedial (VMH) and premammilary gland nuclei (PMV); moderate expression has been found in the lateral hypothalamic area (LHA) and even lower levels in the paraventricular nucleus (PVH) (Elmquist et al., 1997; Elmquist et al., 1998b; Mercer et al., 1996b). ObRb is expressed in other brain regions, namely in the cortical area of the cerebellum, in the Purkinje and granular neuronal populations and the thalamus, but its function remains to be studied. Immunohistochemical analysis on brain sections of leptin administrated mice and detailed mapping studies revealed rapid and robust signal transducer and activator of transcription 3 (STAT3) activation (Hosoi et al., 2002; Hubschle et al., 2001; Munzberg et al., 2003) and nuclear translocation and induction of the early response Fos proteins in hypothalamic nuclei (Elias et al., 2000; Elmquist et al., 1997). The hypothalamic nuclei where STAT3 and Fos activation are detected overlap with the nuclei where *ObRb* is expressed, namely the Arc, the DMH, the VMH, the LHA, the PMN and the PVN. Leptin responsiveness by studies of Fos immunoreactivity has been detected in extra-hypothalamic areas including the dorsal raphae nucleus and in the midbrain the nucleus of the solitary tract.

Leptin enters the brain via the mediobasal hypothalamus and the Arc nucleus, where the blood brain barrier is specifically modified in order to allow the passage of large molecules. Double immunohistochemistry revealed that both of the Arc neuronal populations NPY/AgRP and POMC/CART express the ObRb isoform (Cheung et al., 1997; Mercer et al., 1996a). Leptin signals in the hypothalamus by stimulating *Pomc1* expression and inhibiting *Npy* and *Agrp* as demonstrated by quantification of gene expression and genetic analysis. The molecular basis for the stimulation of *Pomc1* transcription involves activation of the JAK-STAT3 pathway (Vaisse et al., 1996) (figure 1.3). More specifically binding of leptin onto ObRb on the POMC/CART expressing neurons, leads to a rapid activation of Janus kinase 2 (JAK2) that is constitutively associated with a conserved trans-membrane domain in the carboxy-terminal of the receptor (Ghilardi and Skoda, 1997). JAK2 is a tyrosine, threonine-kinase and its activation leads to phosphorylation of Y 985 and Y 1138 of the ObRb (Bjorbaek et al., 1997). This phosphorylation event provide binding motif for src homology 2 (SH2)- domain-containing proteins like STAT3 and SH2-domain-phosphotyrosine phosphatase (SHP-2). STAT3 binds to Y 1138 of the ObRb, and become tyrosine phosphorylated by JAK2, then it dissociates from ObRb, form homodimers in the cytoplasm and translocate into the nucleus where it activates gene transcription (Bjorbaek et al., 2001). Transcriptional circuitry activated by STAT3 is a crucial component for the regulation of energy homeostasis, since a KO mouse containing a deletion of the Y 1138 residue in the ObRb locus develops severe obesity. SHP-2 binds to Y 985 of the ObRb and activates the extracellular signal-regulated kinase (ERK) signaling pathway and induces the early response gene c-Fos (figure 2) (Banks et al., 2000). Except of the JAK/STAT pathway leptin activates the phosphoinositol-3 kinase (PI3K) signaling pathway that is suggested to play an important role in the suppression of *Npy* and *Agrp*. Insulin receptor substrate 1 and 2 (IRS-1, IRS-2) are activated and have been involved in this signaling pathway (Niswender et al., 2001; Zhao et al., 2002), however the exact mechanism by which ObRb activates PI3-K and cAMP signaling pathway is not yet characterized. Latest studies performed on the *fa/fa* leptin receptor defective rats, provided evidence that leptin regulates insulin sensitivity and glucose metabolism via the PI3K signaling pathway in neurons of the Arc nucleus. Leptin does not only regulate energy homeostasis via transcriptional regulation of the neurons expressing ObRb, but

modifies the neuronal firing rates of the neurons, either by activating them or by inhibiting them. In this way leptin does not only regulate in long term the function of these neurons but exerts rapid physiological effects. It has been demonstrated that leptin induces Fos immunoreactivity and increases the frequency of action potentials in POMC neurons both directly (Cowley et al., 2001). Leptin directly hyperpolarizes NPY/AgRP neurons (Schwartz et al., 1996), inhibiting their activation and NPY or AgRP secretion and decreasing the GABAergic inhibitory tone that NPY/AgRP neurons exert onto POMC cells. Decrease of the GABAergic inhibitory tone leads indirectly to activation of the POMC neurons. Despite the fact that Kir6.2 K^+-ATP channels have been involved in mediating the anorexigenic effects of leptin in both POMC and NPY/AgRP neurons (Miki et al., 2001), molecular events underlying their function are still unclear.

In situ hybridization has shown that suppressor of cytokine signaling (SOCS) 3 mRNA is strongly induced by leptin (Bjorbaek et al., 1998a; Elmquist et al., 1998b). Furthermore promoter analysis of SOCS-3 resulted to identification of functional STAT3 DNA binding elements, supporting that SOCS-3 is a direct target of leptin signaling pathway (Auernhammer et al., 1999). It has been suggested that SOCS-3 regulates negatively leptin intracellular signaling by either binding on Y 985 of the activated ObRb via its SH-2 domain, or by binding directly on JAK2 and inhibiting its tyrosine kinase function (Bjorbaek et al., 1998a). Based on studies carried out until now, SOCS-3 plays an important role in the development of leptin resistant obesity syndrome, which is the case for most of the human obesity cases. Another important negative regulator of leptin signaling pathway is protein tyrosine phosphatase 1 B (PTP1B) that has been shown to dephosphorylate and inactivate JAK2 in cell culture studies (Cheng et al., 2002; Elchebly et al., 1999; Klaman et al., 2000). In addition mice deficient for PTP1B are resistant in developing diet induced obesity (DIO) and are not hyper-phagic despite having low serum leptin levels (Zabolotny et al., 2002).

1.2.2 Signals from the gastrointestinal tract

Ghrelin belongs to the short-term afferent signals, since it is synthesized and secreted from cells situated in the gastrointestinal tract, in response to fasting and

regulates meal initiation (Cummings et al., 2001). Ghrelin is the endogenous ligand of Growth Hormone secretagogue receptor (Ghsr), a seven trans-membrane GPCR receptor (Kojima et al., 1999; Kojima et al., 2001). *Ghsr* is expressed mainly in the NPY/AgRP neurons, and the somatostatin expressing neurons of the Arc nucleus (Nakazato et al., 2001). It has been shown that except of being an orexigenic signal, it is stimulating growth hormone release (Hosoda et al., 2000). Systemic and icv administration of ghrelin causes increase of food intake that leads to weight gain if the administration is chronic (Okada et al., 1996; Torsello et al., 1998; Tschop et al., 2000). In the molecular level it has been shown that icv administration has a stronger effect supporting that ghrelin act in the CNS. Indeed, ghrelin induces the early response genes Fos and Egr1 (early growth response 1) exclusively in the NPY/AgRP expressing neurons in the Arc nucleus (Hewson and Dickson, 2000). Increase of Fos immunoreactivity is a molecular marker for electrophysiological neuronal activation. Recently it has been demonstrated that ghrelin activates exclusively NPY/AgRP neurons since *Ghsr* is only expressed in this population and that ghrelin induces a 300% increase of the spontaneous action potential frequency (Dickson et al., 1993; Dickson and Luckman, 1997). Simultaneously a 50% decrease of the POMC spontaneous activity have been measured but this decrease is an indirect effect from the NPY/AgRP neurons, since blockage of NPY-R1 receptors abolishes this inhibitory effect (Willesen et al., 1999). An additional proof for the implication of ghrelin in the regulation of body weight is that *ghrelin* expression has been shown to be strongly up-regulated in the stomach of *ob*/*ob* mice (Asakawa et al., 2001). Recent studies have indicated that ghrelin plasma levels during fasting were decreased in obese humans; this of course might represent an adaptation mechanism to the positive energy balance associated with the establishment of obesity in these persons.

Glucagon like peptide-1 (GLP-1), cholecystokinin (CCK), PYY and PP, 2 peptides that belong to the same family with the central NPY are satiety signals secreted by endocrine cells of the stomach and the intestin. More precisely GLP-1 is one of the products of the preproglucagon gene. GLP-1 is secreted postprandial from the L-cells of the gastrointestinal tract and acts onto neurons of the hypothalamus via binding onto their receptor, and inhibits food intake (Yamamoto et al., 2002), long lasting GLP-1 infusion leads to weight loss and blockage of the CNS GLP-1 receptors increases food intake and obesity (Farooqi et al., 1999).

CCK is a satiety hormone secreted by mucosal enteroendocrine cells, in response to the presence of food in the gut. CCK coordinates postprandial contraction and gut motility and pancreatic secretion in order to empty the stomach and gut. It does that via CCK1 receptors expressed in the gut in neurons of the arcuate nucleus and on the peripheral vagal afferent terminals which transmit neural signals to the brainstem (Moran, 2000). CCK is secreted in response to various luminal nutrients, such as fatty acids and promotes satiety and inhibits food intake. Latest studies on CCK neurons have been established that afferent CCK vagal afferent fibers that express the CCK receptor, innervate POMC expressing neuronal population situated in the nucleus tractus solitarius (NTS). NTS is a structure of the brainstem where a POMC neuronal population has been characterized via GFP immunostaining on eGFP-POMC transgenic mice, shown to be activated by CCK and mediating partially the anorectic effects of CCK via the CNS (Fan et al., 2004).

In the opposite peptide YY (PYY) and pancreatic polypeptide (PP) are potent short-term appetite inhibitors (Batterham et al., 2002; Schwartz and Morton, 2002). They are recognized by the Y family receptors expressed in the CNS. PYY binds onto the Y2 receptors expressed on the NPY/AgRP neurons and inhibits their activation and NPY release. Inhibition of the NPY/AgRP neuronal activity results to disinhibition of the POMC neurons since the collateral inhibitory tone decreases(Batterham et al., 2002; Cowley et al., 2001). PP is released from the pancreas under nutrient control and acts on Y4 and Y5 receptors in the brain (Cowley et al., 2001; Katsuura et al., 2002). Chronic peripheral PP administration reduces food intake in both lean and obese mice, conversely central administration induces increase of food intake, most probably by acting on Y4 and Y5 in the CNS.

All these gut derived satiety signals is a very interesting system that have been evolved in order to acutely suppress food intake. Integrating the action of the gut hormones into the system of energy homeostasis in a more precise manner, further genetic and pharmacological approaches will be necessary.

1.3 Efferent Outputs

NPY/AgRP and POMC expressing neurons from the arcuate nucleus integrate information about energy levels of the body to other brain structures by divergent projections throughout the hypothalamus. They initially project and innervate the Lateral Hypothalamic area (LHA), the Dorsomedial hypothalamus (DMH) and the paraventricular hypothalamic nucleus.

The LHA contain spatially overlapping neuronal populations expressing melanin concentrating hormone (MCH) (Bittencourt et al., 1992) orexins (ORX) (Sakurai et al., 1998). mRNA levels of both of these peptides are up-regulated upon starvation (Qu et al., 1996), when leptin serum levels are decreased (Ahima et al., 1996); they are normalized by refeeding or leptin administration. Injection of either MCH or ORX, induce increase of food intake. These data in combination with data obtained from genetic analysis of the ORX and MCH (Shimada et al., 1998) deficient mice provide evidence that they are both strong food intake stimulators. In addition CART (Kristensen et al., 1998)and corticotropin releasing hormone (Kelly and Watts, 1996) (CRH) are expressed in the LHA and their induction leads to decrease of food intake (Kelly and Watts, 1998). Both of these peptides induce satiety and anorexia when injected centrally (Sawchenko, 1998). Despite the fact that leptin and other peripheral hormones modify their activation and expression profiling, it is not yet clarified if this is a direct effect of leptin onto these neurons, or if it an indirect effect due to the Arc nucleus neuronal projections (Elmquist et al., 1998a). Specific target sites for these neuronal populations involved in regulating efferent outputs of the energy homeostasis network are not yet known. It has been speculated that neurons of LHA integrate body weight and food intake by innervating regions like the PVH, the prefrontal cortex,the parabranchial nucleus, and the dorsal vagal complex as well as neurons in the brainstem and the spinal cord, which might control stereotypical feeding motor patterns (Saper et al., 1976), (Swanson and Kuypers, 1980)

PVH is the main output of the hypothalamus, since it is coordinating the activity of the pituitary gland (Treier and Rosenfeld, 1996), which then signals to peripheral endocrine organs such as the thyroid, adrenal and gonad glands in order to regulate metabolism, growth and reproduction according to the energy levels

available (Figure 1.4). Neurons from the magnocellular system of PVH that synthesize oxytocin (OT) and vasopressin (VP) hormones, release them in an activity dependent manner in the posterior part of the pituitary gland. The parvocellular neuronal population in the PVH, synthesizes thyrotropin-releasing hormone (TRH) and corticotropin-releasing hormone (CRH) which are secreted in the median eminence. From the median eminence they access to the anterior lobe of the pituitary gland via the portal vascular system, where they regulate the synthesis and release of adrenocorticotropin hormone (ACTH) and thyroid –stimulating hormone (TSH).

PVH is in a strategic position to coordinate in parallel the endocrine system, via modulating pituitary activity and the autonomic nervous system. It has been demonstrated that PVH innervates directly vagal parasympathetic preganglionic neurons that regulate the function of gastrointestinal function (Tannenbaum et al., 1998).

1.5 Aim of study

Although the neural hypothalamic control of energy homeostasis has been the subject of intense research the last 10 years since the cloning of leptin and leptin receptor, the molecular events mediating integration of the peripheral signals in the hypothalamic neurons are still largely unknown. Leptin has the capacity to suppress the transcription of both orexigenic peptides NPY and AgRP and in parallel to induce transcription of the anorectic POMC via binding onto ObRb. Very little is known about how in the fist place the two cell lineages are defined and which are the factors responsible for the differential regulation of the peptides since the until now transcription factors identified downstream various hormonal signaling pathways, STAT3, SOCS3, Fos, Erg-1, are induced in both neuronal populations. In this context we became very interested about studying the role of Bsx in the regulation of energy homeostasis.

Bsx is a homeodomain containing transcription factor that exerts hypothalamic specific expression pattern. From early on during development expression of *Bsx* is restricted in the diencephalic area of the mouse brain. During adulthood *Bsx* expression is restricted in a very specific and small populations of neurons in the mediobasal and the Dorsomedial hypothalamus. Intriguingly, Bsx is highly conserved between human, rodents, Drosophila, C.elegans and fish, both in sequence and expression pattern. In all species *Bsx* is expressed specifically in a limited number of neurons of the CNS. This provided us with an indication that Bsx could take part in an evolutionary conserved system playing an important role in regulation of homeostatic functions. More specifically given the expression of *Bsx* in neuronal populations situated within Arc and DMH and the importance of these areas of hypothalamus in regulating energy homeostasis we wanted to investigate the role of Bsx in shaping the hypothalamus and regulating food intake.

In the light of the importance the two nuclei where *Bsx* is expressed in integrating hormonal afferent signals, we decided to study genetically the role of Bsx in the hypothalamic area of mice. To this end we generated mice with abolished *Bsx* expression, by homologous recombination and gene targeting and analyzed the phenotype of the mutant mice for deregulation of any of the hypothalamic

components important for energy homeostasis regulation and for any physiological defect.

2 Results

2.1 Expression pattern of murine *Bsx* in the hypothalamus

The murine *Brain Specific Homeobox (Bsx)*, has been identified and cloned in the lab by a screen performed for characterization of new factors in the hypothalamic-pituitary axis. *Bsx* displays an ORF of 699 nucleotides that code for a protein of 232 amino acids. Among the homeodomain containing proteins, *Bsx* displays a high similarity with Barx, Barh1 and Nkx sub families. In mouse the genomic structure analysis showed that the Bsx coding sequence spans in 3 exons in a genomic DNA area of approximately 5 Kb.

Bsx expression as detected by in situ hybridization (Figure 2.1) is on early in development. At embryonic day e10.5 in *Bsx* is expressed in a few cells located bilaterally in the developing diencephalon that will give rise to the adult hypothalamic area (Figure 2.1 A). *Bsx* as detected, on transversal section of a mouse at e13.5 is expressed in a symmetrical way around the 3rd ventricule of the brain, in the area of the developing diencephalon (Figure 2.1 B) and on coronal section of an e17.5 mouse brain *Bsx* is expressed in limited number of cells surrounding the 3rd ventricule of the brain (Figure 2.1 C). In adult mice in situ hybridization for *Bsx* on sagital (Figure 2.1 D) and coronal (Figure 2.1 E) sections revealed expression in the medial area of the Arc nucleus of hypothalamus situated next to the ME, and the compact area of the DMH. The expression of *Bsx* is symmetrical in both hemispheres of the brain and expands in an area of 1mm from rostral to caudal. Precisely *Bsx* expression in adult can be detected in the hypothalamic area from Bregma –1.26 mm to Bregma –2.26 mm according to the mouse brain atlas in stereotaxic coordinates.

2.2 Bsx is expressed in the NPY/AgRP neurons but not in the POMC neurons in the arcuate nucleus of hypothalamus.

Bsx expression is mainly restricted in the compact area of the Dorsomedial nucleus (DMC) and the medial area of the Arc nucleus of the hypothalamus in adult mice, as demonstrated by *Bsx* mRNA distribution studies (Figure 2.2.1 A). To analyze the distribution of Bsx protein, I generated a specific antibody against the carboxy-terminus of Bsx and performed immunohistochemistry on adult brain sections. Bsx – immunoreactive nuclei were detected in the Arc and the DMC (Figure 2.2.1 B), confirming that the factor is produced in the hypothalamus of the adult mouse brain. The specificity of the Bsx antibody enabled me to further characterize the Bsx expressing population in the hypothalamus by performing immunohistochemistry. I performed double immunohistochemistry on colchicines - treated animals, since the neuropeptides expressed in the arcuate nucleus are translated in the soma of the neurons but are rapidly transported on the axons, for Bsx and NPY, AgRP, β-endorphin and α-MSH, which are two of the posttranslational products of POMC in the hypothalamus. We found that Bsx highly co-localizes within the orexigenic NPY and AgRP expressing neuronal population (Figure 2.2.1C –2.2.1D) however there was no overlap between the Bsx and the anorexigenic POMC/CART expressing neuronal populations as detected by using antibodies against β-endorphin and α-MSH (Figure 2.2.1G-H). A percentage of 95 % of the NPY expressing neurons are Bsx positives, nevertheless none of the β-endorphin and α-MSH positive neurons are Bsx stained. As mentioned β-endorphin and α-MSH are two peptide cleavage products derived from POMC, usage of antibodies raised against the two peptides stains the anorexigenic POMC/CART expressing population. I furthermore showed the co-localization of Bsx in the orexigenic NPY/AgRP neurons in second independent way, by using heterozygote mice for the Histone2BeGFP cassette and performing a double immunofluorescence/in situ hybridization for GFP and *Npy* or *Agrp* (Figure 2.2.1 E-2.2.1F). In addition to the arcuate nucleus, Bsx seems to be expressed in some scattered neurons of the Lateral hypothalamus (LH), where Melanocortin-concentrating hormone (MCH) and Orexin peptides are expressed. Double immunofluorescence for Bsx and MCH or Orexin A revealed that Bsx expressing

neurons intermingle in proximity with MCH and Orexin expressing ones, two neuronal populations that has been shown to regulate feeding behavior and energy expenditure by modulating levels of locomotory activity. In conclusion we identified for the first time a transcription factor that has a specific expression in the orexigenic NPY/AgRP neurons of the hypothalamus.

To assess the role of Bsx in mouse development and within the NPY/AgRP expressing neuronal subpopulation of the arcuate nucleus we generated two different *Bsx* alleles via homologous recombination in murine embryonic stem (ES) cells, the Bsx^{lacZ} and the $Bsx^{H2BeGFP}$ alleles.

The Bsx^{lacZ} allele has deleted exon two of the *Bsx* coding sequence containing a major part of the homeodomain coding sequence of the transcription factor, which should result in a truncated protein unable to bind DNA. A 192BAC was isolated and a 8 Kb BamHI-fragment was subcloned containing the *Bsx* genomic locus. (Figure 2.2.2) The flanking arms of the targeting vector were generated by PCR using the 8 Kb genomic BamHI-fragment in pBluescript SK with specific primers. The 5' homology arm was fused in frame with a lacZ-Neo cassette for selection in the ES cells and a DTA cassette was added to the 3' arm for negative selection. Germ-line transmission of the targeted Bsx^{lacZ} allele was obtained from two independent ES cell clones.

A second *Bsx* allele was constructed by replacing exon 1 of the *Bsx* coding sequence with a sequence coding for the Histone2BeGFP fusion protein followed by a polyA signal, which should result in the absence of functional Bsx protein.

For both alleles we obtained homozygous adult mutants Bsx^{lacZ} and $Bsx^{H2BeGFP}$ mice or mice trans-heterozygous for both alleles in the expected mendelian ratio. Immunostaining on adult coronal brain sections from homozygous mutant mice (Figure 2.2.3 A) with the rat polyclonal antiserum showed no signal demonstrating that the targeting strategy was successful. GFP emission from heterozygous $Bsx^{H2BeGFP}$ coronal brain section (Figure 2.2.3B) and double immuno- in situ staining for GFP and *Npy* or *Agrp* demonstrated that the nuclear reported H2BeGFP cassette faithfully reflected the endogenous Bsx expression in the NPY/AgRP neurons of the arcuate nucleus and the DMH area. We next asked if the deletion of *Bsx*, due to its specific expression during embryonic development, leads to the loss of *Bsx* expressing neurons in adult homozygous mutant brains. To this end I counted H2BeGFP

positives neurons throughout the arcuate nucleus and the DMH of heterozygous *Bsx*^{H2BeGFP} and trans-heterozygous *Bsx*$^{H2BeGFP/lacZ}$ mouse brains (Figure 2.2.3E-F) and found no difference in cell number, demonstrating that the loss of Bsx function does not lead to a loss of *Bsx* expressing neurons.

Figure 1

Figure 2

2.3 Downregulation of *Npy* and *Agrp* in the arcuate nucleus of Bsx mutant mice.

Mice homozygous mutant for *Bsx*, didn't show any anatomical defect nor obvious phenotype and were fertile. We therefore wondered if loss of *Bsx* leads to change of the transcriptional program in the NPY/AgRP expressing neurons. Radioactive quantitative In situ hybridization revealed a significant strong down-regulation of *Npy* expression in *Bsx* mutant mice (Figure 2.3.1 A). The upper panel is a scan of the film from the in situ hybridization revealing that despite *Npy* being expressed in the cortical area and the arcuate nucleus the down-regulation is specific for the arcuate nucleus where *Bsx* is normally expressed. Similarly immunofluorescence staining for NPY revealed a strong reduction of the NPY staining in the arcuate nucleus (Figure 2.3.1B). NPY staining in other hypothalamic areas, although it is weaker than the one seen in wt control sections is unchanged, suggesting that the projections of the NPY/AgRP neurons were not altered in the mutant $Bsx^{lacZ/lacZ}$ mice.

The orexigenic melanocortin receptor antagonist *Agrp* that co-localizes with both *Npy* and *Bsx*, was also strongly down-regulated in the *Bsx* mutant brain section (Figure 2.3.1C). Conversely to the changes in the expression of the two orexigenic peptides *Npy* and *Agrp*, the anorexigenic hypothalamic peptides *Pomc1* and *Cocain-amphetamin regulated transcript* (*Cart*) were unchanged in the arcuate nucleus of homozygous $Bsx^{lacZ/lacZ}$ mice compared to basal *wt* expression levels (Figure 2.3.1D-E).

2.4 Downregulation of *Somatostatin* in the arcuate nucleus of Bsx mutant mice.

Interestingly Somatostatin (Sst) neurons that are situated in the arcuate nucleus express the GABA neurotransmitter. The role of *Sst* in the energy homeostasis regulation hasn't been yet addressed; it has been though shown that activation of Sst neurons and Sst secretion inhibits growth-hormone releasing hormone neuronal activation and eventually secretion of growth hormone from the pituitary gland (Tannenbaum et al., 2003). Nevertheless mice deficient for *Sst* have no obvious phenotype, since the mice develop normally and they have no obvious metabolic or feeding related defect (Low et al., 2001; Zeyda et al., 2001). Quantitative in situ hybridization analysis for *Sst* revealed a strong and specific decrease of the *Sst* transcripts in the arcuate nucleus of *Bsx* mutant mice (Figure 2.4.1A). The upper panel is a scan of the film showing expression of *Sst* in the cortical area, the Paraventricular hypothalamus (PVH) and the arcuate nucleus; in the $Bsx^{lacZ/lacZ}$ section *Sst* expression is specifically impaired in the arcuate where it co-expressed with Bsx.

2.5 Ghrelin responsiveness is impaired in the *Bsx* mutant mice

A large number of afferent inputs related to body energy levels are integrated by the NPY/AgRP neuronal population. Leptin, the adipocyte derived hormone activates the JAK-STAT pathway in the neurons of the arcuate nucleus that leads to phosphorylation of STAT3 and translocation of the factor from the cytoplasm to the nucleus (Munzberg et al., 2003). To investigate if the NPY/AgRP neurons are responsive to leptin, wt and Bsx mutant mice were starved for 48 hours in order to induce intrinsic leptin levels and potentate leptin responsiveness of the mice. I next administrated intra-venous leptin, sacrificed the mice 45 min later and performed a phospho-stat3 immunostaining (Figure 2.5.1A). Counting the number of the P-STAT3 immunoreactive nuclei revealed no difference between wt and *Bsx* mutant sections suggesting that the arcuate neurons of $Bsx^{lacZ/lacZ}$ mice are responsive to leptin.

From the two populations of the arcuate nucleus, it is only NPY/AgRP that expressed Growth-Hormone Secretagogue (*Ghsr*) receptor of the hormone ghrelin. Since ghrelin is acetylated in vivo, GHRP-6 peptide was used, an analogue of the hormone in order to investigate ghrelin responsiveness of the NPY/AgRP expressing neurons. Intra-venous administration of GHRP-6 in wt mice induced Fos immunoreactivity (IR) in the NPY/AgRP neurons (Figure 2.5.1B). Since the increase of the Fos IR is a molecular read-out of electric neuronal activation of these neurons, this is showing that the neurons are activated upon GHRP-6 administration. Double immunostaining with Fos and Bsx antibodies revealed that Bsx neurons are activated by GHRP-6 (Figure 2.5.1B), indicating in addition that it is the same NPY/AgRP population. Conversely to the wt, GHRP-6 failed to induce Fos immunoreactivity in the *Bsx* mutant hypothalamus (Figure 2.5.1C), despite the fact that they do express *Ghsr* at same levels as wt mice (Figure 2.5.1D). These data indicate that loss of *Bsx* in the NPY/AgRP neurons leads to an intrinsic problem in these neurons. This intrinsic defect of the NPY/AgRP neurons is responsible for the impairments of ghrelin intracellular signaling in the NPY/AgRP neurons in *Bsx* mutant mice.

2.6 *Bsx* mutant mice develop Diet Induced Obesity

Data obtained from the in situ hybridization analysis and the hormonal injections of the *Bsx* mutant mice indicate hypo-phagia and leanness of the homozygous mice. Since NPY and AgRP, that are orexigenic peptides, are down-regulated and ghrelin responsiveness, that triggers meal initiation, is impaired the mutant mice were expected to exert decreased food intake and be leaner than wt mice. Body weight measurements though of the mice (Figure 2.6.1A and B) at 12 weeks of age showed no significant difference between *Bsx* mutant and wt mice.

On a high fat Diet chow, though *Bsx* mutant mice are larger than control littermate mice as shown by their physical appearance (Figure 2.6.1 C). Weight curves of both males and females (Figure2.6.1 D and E) traced by weekly monitoring of the weight since the beginning of the high fat diet experiment, indicating that *Bsx* mutant mice gain weight and fat mass faster than wt or heterozygous mice. The effect was more pronounced in the *Bsx* mutant females than males (Figure2.6.1 D-G). The Diet induced obesity phenotype that mutant mice developed seemed paradoxical according to the molecular data we obtained from the in situ hybridization analysis. We next wanted to further analyze the mice physiologically and investigate possible physiological defects that could explain the weight gain despite the strong down-regulation of the orexigenic peptides. To this end we established a collaboration with Petre Wiedmer from Matthias's Tschoep lab in the German Institute of Human Nutrition, Potsdam who performed the following measurements.

Figure 6.1

Figure 6.2

The increased weight gain of the *Bsx* mutant mice on high fat diet could not be explained by any difference in the feeding behavior, since food intake measurements performed over 2 days and averaged (Figure 2.6.2 A) showed a modest reduction in *Bsx* mutant compared to wt littermates control mice. However, they showed a slight increase in their fat mass (Figure 2.6.2 B) as measured by MRI, in spite of decreased caloric intake. In addition, their energy expenditure was nearly unchanged with a slight decrease in the respiratory quotient, consistent with a modest increase in fat deposition (Figures 2.6.2 C-D). Despite the strong down-regulation of the two orexigenic peptides *Npy* and *Agrp* in *Bsx* mutant mice the observed modest changes of physiological parameters are not unexpected as even complete devoid of both, *Npy* and *Agrp* expression do not show a more severe phenotype (Qian et al., 2002). Surprisingly, however, overall locomotor activity of Bsx mutant mice was substantially reduced during the high activity dark as well as the low activity light phase (Figure 2.6.2 E-F). The decrease of spontaneous locomotory activity can be observed in the monitoring of locomotory activity of individual wt and homozygote *Bsx* mutant littermate mice (Figure 2.6.2G and H). Expression pattern analysis of other hypothalamic neuropeptides involved in the regulation of locomotory activity by ^{35}S-in situ hybridization in *Bsx* mutant mice seem to be unchanged compared to wt situation (Figure 2.6.3 A-E). This data revealed that Bsx expressing neurons are new component in the hypothalamic based neuronal circuitry controlling spontaneous locomotory activity including the Melanocortin-Concentrating Hormone and the Orexin expressing neurons. Since, locomotion though is not impaired in *Npy* or *Agrp* deficient mice (Segal-Lieberman et al., 2003b; Wortley et al., 2005), this defect in Bsx mutant animals cannot be explained by down-regulation of *Npy* or *Agrp*. Because arcuate nucleus neurons are implicated in the regulation of locomotory behavior (Coppari et al., 2005), these findings suggest that Bsx function is required for NPY/AgRP neurons for locomotor activity. Furthermore, it raises the possibility that the decrease in locomotor activity may be the cause of the small increase in fat mass of *Bsx* mutant mice and the primary factor responsible for the excessive weight gain that the mutant mice develop under high fat diet conditions.

2.7 Loss of *Bsx* attenuates the obesity syndrome of *ob*/*ob* mice

To further explore the role of *Bsx* in the regulation of locomotor activity we took advantage of the fact that leptin deficient *ob*/*ob* mice display a locomotor activity defect similar to that of *Bsx* mutant mice. In contrast to the *Bsx* mutant mice, the *ob*/*ob* mice display a morbid obesity phenotype due in addition to the impairment of other physiological functions. As already discussed in the introduction leptin being the main component of the fat tissue- hypothalamic negative feedback loop, when is absent then the brain senses constant starvation despite the massive obesity of the body. The obesity phenotype is partially due to the constitutively de-repression of both orexigenic peptides *Npy* and *Agrp*, since loss of *Npy* in the *ob*/*ob* background (Erickson et al., 1996b). Two of the questions we wanted to address were, if loss of Bsx in *ob*/*ob* mutant mice would lead to attenuation of the obesity syndrome and rescue of the locomotory activity defect that mice of this genetic background display mimicking the phenotype observed in double mutant $Npy^{-/-}$*ob*/*ob* mice. To this end heterozygous $Bsx^{lacZ/+}$ were crossed to *OB*/*ob* mice that enabled us to generate compound $Bsx^{lacZ/lacZ}$ *ob*/*ob* mutant mice. Remarkably, mice mutant for both leptin and *Bsx* show an ameliorated physical appearance (Figure 2.7.1 A) leaner than ob/ob mutants but still bigger compared to wt control mice. The weight curves of mice in both females and males confirmed that double $Bsx^{lacZ/lacZ}$ *ob*/*ob* mutants are significantly leaner to *ob*/*ob* mutants but weigh more than wt mice. Attenuation of the obesity was more pronounced in females than males.

In situ hybridization analysis showed that expression of the orexigenic neuropeptides *Npy* and *Agrp* in double homozygous mutant $Bsx^{lacZ/lacZ}$ *ob*/*ob* mice did not exceed the low levels described in *Bsx* mutant mice and did not show the strong increase in expression normally observed in the *ob*/*ob* animals due to de-repression of *Npy* (Figure 2.7.1B). Similarly to *Npy*, *Agrp* is substantially decreased in the double $Bsx^{lacZ/lacZ}$ *ob*/*ob* mutant mice compared to expression levels observed in the control *OB*/*OB* mice and *ob*/*ob* leptin mutant mice (Figure 2.7.1C). No difference was detected though in *Pomc* expression between *ob*/*ob* and $Bsx^{lacZ/lacZ}$ *ob*/*ob* mice, which was lower than in wt controls in both cases (Fifgure 2.7.1D).

Consistent with the observed down-regulation of Npy expression in *Bsx*$^{lacZ/lacZ}$ *ob*/*ob* mice (Erickson et al., 1996b), fat mass was strongly reduced due to the fact that *Bsx*$^{lacZ/lacZ}$ *ob*/*ob* mice show a 20 % increase of food intake compared to control littermates, whereas *ob*/*ob* mice ingested 70 % more (Figures 2.7.2 A-B). This indicates a substantial reduction of hyperphagia. In addition body temperature in *Bsx*$^{lacZ/lacZ}$ *ob*/*ob* mice was elevated compared to ob/ob mice, which reflects enhanced energy expenditure due most probably to the down-regulation of *Agrp* (Figure 2.7.2 C). Fertility of ob/ob female mice was also improved by removal of Bsx, similar to what have been observed for *Npy*$^{-/-}$ *ob*/*ob* mice (Erickson et al., 1996b). The data presented support the initial hypothesis that *Bsx* is required for *Npy* expression since the phenotype of both double mutant mice were similar and *Npy* in the arcuate nucleus of *Bsx*$^{lacZ/lacZ}$ *ob*/*ob* mice was strongly decreased.

In this context it is noteworthy that locomotory activity was not improved in *Bsx*$^{lacZ/lacZ}$ *ob*/*ob* mice compared to *ob*/*ob* mutant mice (Figure 2.7.2 D-E), yet the double mutants showed significant reduction in the body weight. In addition, reduction of hypophagia and of body weight in *Bsx*$^{lacZ/lacZ}$ *ob*/*ob* mice is comparable to the ones observed in *Npy*$^{-/-}$ *ob*/*ob* mice, indicating that in addition to *Npy,* Bsx controls the expression of additional hypothalamic factors influencing locomotory activity. These results demonstrate that locomotor activity can be genetically uncoupled from body weight control in mice.

2.8 *Bsx* regulates *Npy* expression

The low expression of *Npy* in the $Bsx^{lacZ/lacZ}$ *ob/ob* mice, in the absence of the inhibitory leptin signal, suggested that *Bsx might directly regulate Npy*. The rat PC-12 cell line express *Npy* at low levels but do not express endogenous Bsx and since the *Npy* promoter region is not yet defined this cell line is a very good system to study transcriptional regulation of *Npy* (Higuchi et al., 1988). We therefore asked if expression of *Bsx* in PC12 cells could stimulate *Npy* expression. Northern blot analysis for *Npy* on isolated total RNA from *Bsx* transfected cells showed a clear induction of *Npy*, whereas no signal was detected in mock-transfected cells (Figure 2.8.1 A). Quantitative Real-Time PCR enabled us to measure the induction as 50-fold induction compared to mock transfected situation (Figure 2.8.1 B). In order to examine if this induction is specific to *Bsx* or if any other homeobox transcription factor could also induce *Npy* expression in PC12 cells we used one of the closest related homeobox genes *Nkx2.1/ttf-1*, which is co-expressed during development in the hypothalamus (Lazzaro et al., 1991)and *Pit1* another pituitary specific homeobox transcription factor as control (Ingraham et al., 1988). Over-expression of Nkx2.1 or of Pit1 led only to a modest increase in *Npy* RNA of four and two fold respectively (Figure 2.8.1 B).

To evaluate the specificity of Bsx for *Npy* expression further, we performed DNA microarray analysis using the GE/Codelink whole genome rat chip. RNA from VP16::Bsx and mock-transfected cells was isolated. For each microarray, the Codelink software calculates a normalized threshold. Genes with intensities below the threshold of the microarray are considered not to be expressed. For all of the microarrays, the threshold was between 0.275 and 0.338. We were able to define by using the Genespring software, that only if a gene would be above the threshold in all three biological replicates for the VP16::Bsx transfected or all three biological replicates for the mock-transfected cells would be considered expressed in the PC12 cells. By this definition 18819 genes out of the 33911 genes on the microarray were expressed in all three VP16::Bsx and three mock-transfected PC12 cells. The microarray data was subsequently analyzed using Genespring 6.2 (Silicon genetics). The raw intensity values were normalized to the 50^{th} percentile of the array intensity Figure 2.8.2 shows

a scatterplot of the average expression of the three biological replicates for each individual gene in the VP16::Bsx (y axis) vs the mock (x axis) transfected PC12 cells for all 33911 genes expressed in the PC12 cells. Along the diagonal, the two lines indicate two fold above and two fold below identity. It is apparent that most genes fall into these two lines. To identify genes differentially expressed in the VP16::Bsx transfected cells compared to mock-transfected ones, we generated two sets of genes. One set contained genes whose average expression in the VP16::Bsx transfected cells was 2 fold higher than that of mock-transfected cells, and the other set contained genes whose expression was two fold higher in the mock-transfected cells compared to VP16::Bsx transfected ones. 899 genes were up-regulated and 256 genes were down-regulated in VP16::Bsx transfected PC12 cells. In order to eliminate genes, where a single outlying data point led to an unrepresentative average, a student t-test was performed on the three biological replicates and only genes with a P value less than 0.05 were considered before generating the two lists. The condition tree of the three VP16::Bsx and the three mock-transfected biological replicates PC12 cells (Figure 2.8.3 A) shows that the replicates cluster together, since every line represents one genes behavior in the mock and VP16::Bsx-transfected replicates, suggesting that the overall differences are biggest between the mock and VP16::Bsx transfected cells rather than between the replicates themselves and that predominant gene expression changes are due to the over-expression of the VP16::Bsx construct. Biological replicates are between 95.3 and 96.2 percent identical and for samples with different treatments the identity is between 94.5 and 94.8 percent (Figure 2.8.3 B).

Npy transcript was induced 70-fold in VP16::Bsx transfected compared to mock-transfected cells. The activation potential of Bsx on the transcription of *Npy* was that specific that *Npy* was the fourth gene that came up in the list of the higher to lower up-regulated transcripts in Bsx transfected cells. This microarray analysis not only confirmed that Bsx targets *Npy* transcription but that this activation potential is very specific since even in a whole genome analysis it is one of the first up-regulated genes. Few other interesting genes that might have a physiological in vivo importance came up after *Npy* including, the Tissue-type transglutaminase, brain-enriched SH3 domain protein Besh3, Relaxin 3 hormone, Immediate early gene transcription factor

NGFI-B, Kruppel-like factor 4, Neuromedin N precursor, regulator of G-protein signaling protein 2, early growth response 1 (Table 2.8.4).

Npy has been shown to be regulated by cAMP activating drugs in the PC12 cells (Higuchi et al., 1988) at a similar rate to that of Bsx, as measured by qRT-PCR and the microarray experiment. In addition during starvation the transcription factor CREB becomes phosphorylated on Ser133 in the NPY/AgRP neurons (Shimizu-Albergine et al., 2001) and that this is a prerequisite for its full transcriptional activity. I repeated the experiments to find that treatment of the PC12 cells with Phorbol-Myristrate Acid (PMA) and Dibutyryl-cAMP (DibcAMP) in combination induced *Npy* transcripts as detected by Northern blot analysis and by qRT-PCR (Figure 2.8.1 A, B) 50-fold compared to mock-transfected. Surprisingly, when we treated the cells with DibcAMP/PMA in combination with *Bsx* transfection we observed a synergistic effect in the activation of *Npy* transcription since it was measured that *Npy* transcripts were 200 fold up-regulated compared to control. (Figure 2.8.1 A, B).

Interestingly, similar to *Npy*, *Sst* promoter contains a CREB response element (CRE) (Burbach, 2002) and very close to the CRE sequence we could detect several homoebox binding sites (Figure 2.8.5 A). *Sst* was just like *Npy* strongly down-regulated in mutant *Bsx* mice compared to wt control, I therefore decided to address in a cell culture system if Bsx regulates *Sst* expression by directly binding onto the homeodomain binding site of the *Sst* promoter. To this end I cloned the 660bp (Figure 2.8.5 A) flanking the 5 prime of Sst upstream a luciferase cassette and cotransfect this construct with either an IRES::Bsx or a VP16::Bsx construct into the 293-kidney cell line. Luciferase activity was measured by a luminometer in order to measure the activation potential of Bsx on *Sst* promoter. Bsx induces in average 5-fold up-regulation of luciferase activation compared to mock co-transfected cells (Figure 2.8.6 A). The activation is much stronger when Bsx was fused with VP16, a viral transcriptional activator (Figure 2.8.6 B), suggesting that Bsx binds on the Sst promoter and activates its transcription. The differential activation potential of the cmv and VP16 constructs is probably due to the lack of certain co-activators in the 293 necessary for the factor to function as transcriptional activator. An additional result that supports the above hypothesis is that the same experiment performed in cos7 cells results to the same results but higher relative luciferase activity values (Figure 2.8.6 C). The luciferase essay experiments indicate that Bsx directly regulates

Sst transcription, like for *Npy*. Given that both genes are CREB regulated and the synergistic effect observed in the PC12 experiment on Npy expression, we wanted to investigate furthermore if Bsx interacts physically with CREB and when they are both present the transcriptional activation effect is synergistically increased. Thus GST pull-down assays were performed (Figure 2.8.1 D). Bacterially expressed full length GST::Bsx interacted strongly physically with in vitro translated and labeled CREB. The interaction was then confirmed by expressing in bacteria GST::CREB and pulled-down in vitro translated Bsx. In order to define the area of Bsx that binds CREB We cloned 2 Bsx constructs, Bsx-α containing a deletion at the N-terminus and Bsx-β containing a deletion at the C-terminus of the protein. Bsx-α but not Bsx-β was pulled-down by bacterially expressed GST::CREB, indicating that the interaction between CREB and Bsx is mediated via the C-terminus of Bsx (Figure 2.8.1 D).

In *Bsx* mutant mice, the ^{35}S-in situ hybridization analysis revealed down-regulation of *Agrp* transcripts at similar levels as the ones observed for *Npy*. Since Agrp is not annotated in the rat genome, we could not use the list of up-regulated genes that we generated from the microarray experiment to see if it was regulated. To examine if Bsx activates directly in addition to *Npy*, *Agrp* expression, *Agrp* transcription was measured by quantitative real-time PCR on Bsx transfected PC12 cells. 3-fold up-regulation of *Agrp* transcripts was detected upon Bsx transfection compared to mock transfected Bsx cells (Figure 2.8.7 A). In addition it has been shown that activated FoxO1 forkhead protein mediates *Agrp* transcription (Kitamura et al., 2006). We could reproduce 4-fold increase of *Agrp* transcripts in our PC12 cell system when we transfected the constitutively active FoxO1-ADA mutant construct of FoxO1 (Figure 2.8.7 A). Surprisingly, when we co-transfected Bsx and FoxO1-ADA constructs we measured 9-fold up-regulation of *Agrp* transcripts compared to mock transfected cells (Figure 2.8.7 A). We then wondered if the synergistic effect that the two factors have on *Agrp* is due to a physical interaction of Bsx and FoxO1 and reciprocal binding on their respective binding sites on *Agrp* promoter. To test this hypothesis I performed reciprocal GST pull-down assays with bacterially expressed and purified GST::Bsx and GST::FoxO1-ADA and in vitro translated and labeled FoxO1-ADA and Bsx (Figure 2.8.7 B). In both assays we detected a strong binding of the factors, suggesting that these factors interact and bind together on *Agrp* promoter to induce the full effect of *Agrp* expression observed in wt mice.

Starvation induced negative energy balance for the mouse, leads to down-regulation of leptin serum levels and de-repression of *Npy* and *Agrp* transcription in the NPY/AgRP neurons. In order to investigate if Bsx is required for the induction of the two orexigenic peptides upon starvation we examined expression levels of both peptides by ^{35}S-in situ hybridization on wt and Bsx mutant mice normally fed and fasted. Despite the fact that both *Npy* and *Agrp* were strongly induced upon starvation compared to normally fed wt mice, in Bsx mutant mice expression level of the peptides didn't even attaint the one observed in wt normally fed mice (Figure 2.8.8 A-H). This experiment constitutes an additional in vivo indication of the importance of the Bsx - CREB synergy on the *Npy* promoter and of Bsx-FoxO1 on *Agrp* promoter, since upon fasting, induction of *Npy* and *Agrp* transcripts were abolished in the *Bsx* deficient mice compared to the effect observed in the *wt* mice (Figure 2.8.8 D and H). These data provided in vivo proof that although Bsx is required for the induction of *Npy* and *Agrp* it is not an exclusive factor for their expression and induction since expression of CREB and FoxO1 ensure basal expression levels of the peptides even in Bsx absence.

3 Discussion

Food intake has to be tightly controlled to maintain sufficient energy stores, which is indispensable for survival. Over the last decade a large number of animal models containing specific gene deletions have been generated and analyzed in depth. As a result of these studies the knowledge about the hypothalamic neuronal network that regulates energy homeostasis have increased substansially.

Peripheral hormones related to energy storage levels like leptin, insulin or ghrelin act upon the hypothalamic neurons of the brain and utilize the hypothalamic neuropeptide Y, agouti related peptide, melanocortins, orexin and melanin concentrating hormone as mediators. Conversely to the melanocortin circuitry, that has been implicated in promoting satiety, the neuropeptide Y and the AgRP system is activated when hormones from the periphery signal to the brain that the body is starving. Although initial pharmacological studies gave evidence for their implication in the control of feeding, genetic studies haven't been able to confirm this data. However, their importance in promoting feeding in the leptin deficient *ob*/*ob* mutant mice is undisputable since *Npy* has been shown to mediate most of the feeding and metabolic defects of the *ob*/*ob* mice. Recent, ablation studies have also highlighted the fact that NPY/AgRP expressing neurons are indeed required for feeding, since although early ablation has no effect on feeding behavior ablation during adulthood leads to starvation to death; indicating that the hypothalamic circuitry regulating feeding is highly plastic and is able to compensate loss of any of its components early on. The function of the NPY/AgRP neurons has been extensively studied, however, there are still many questions to be addressed. Which are the components regulating transcription of the two peptides? What is the transcriptional circuitry responsible for NPY induction in accordance to peripheral hormonal signals? Are there additional factors in the NPY/AgRP neurons other than the two peptides that regulate energy homeostasis? Is NPY or AgRP involved in the regulation of energy expenditure and physical activity? How are they able to control energy partitioning?

Bsx, a hypothalamic specific transcription factor was identified in an in situ hybridization screen for novel transcriptional regulators in the hypothalamic-pituitary

axis. *Bsx* is exclusively expressed in the NPY/AgRP expressing neuronal population of the arcuate nucleus. The high conservation of the homeodomain sequence that *Bsx* contains and the specific neuronal expression of *Bsx* throughout other species like Drosophila, C.elegans, zebrafish, rat, mouse and human suggest that Bsx is involved in a circuitry that is very highly conserved throughout evolution. The aim of my thesis was to elucidate, by reverse genetics the role of Bsx in the hypothalamus in mouse. To this end we generated and characterized mice lacking Bsx function.

Homozygous Bsx mutant mice were born in Mendelian ratio. *Bsx* mutant mice had no anatomical defects and were both viable and fertile. Analysis of adult mutant mice indicated that Bsx is required for expression of the orexigenic *Npy* and *Agrp* neuropeptides and for grhelin responsiveness in the NPY/AgRP expressing neurons, a potent appetite inducing process. Despite the fact that molecular data suggested that *Bsx* mutant mice should be hypophagic and lean, the mice developed a diet induced obesity phenotype, since they gained more weight than *wt* control littermates when fed with highly caloric diet. The diet induced obesity phenotype could be explained by an imbalance between caloric intake and energy expenditure that would lead to the positive energy balance. Physiological parameters were measured in collaboration with Petra Wiedmer from Matthias Tschoep's lab. This revealed that a defect in the energy expenditure of the mice could explain this phenotype, since the mutant mice display a severe locomotory activity defect. Considering that spontaneous activity constitutes around 45% of the daily energy expenditure for an individual, the 50% decrease of the locomotory activity measured in *Bsx* mutant mice may well account for the diet induced obesity phenotype.

Physical activity is very important component of energy homeostasis and body weight regulation (Bensimhon et al., 2006). In obesity rodent models and human obese patients, locomotory activity is regulated conversely to body weight; overweight individuals display a decrease in physical activity and *vice versa*. One of the open remaining questions in the obesity research fiel is whether the decrease of locomotory activity is the cause or whether it is the consequence of obesity. In order to explore the locomotory activity defect of *Bsx* mutant mice, and to investigate if we could genetically uncouple the obesity phenotype from the physical activity defect we crossed *Bsx* mutant mice into the leptin deficient *ob*/*ob* background mice.

Double mutant *Bsx*$^{lacZ/lacZ}$ *ob*/*ob* mice displayed attenuated obesity compared to the morbid obesity that *ob*/*ob* mice develop and this was due to the strong decrease of *Npy* transcripts and of hyperphagia in the double mutant mice. *Npy* expression in the *ob*/*ob* mice is constitutively de-repressed, since the leptin negative feedback loop from the adipocytes to the brain suppressing the expression of orexigenic peptides is disrupted. In the double *Bsx*$^{lacZ/lacZ}$ *ob*/*ob* mouse this induction doesn't take place indicating that Bsx directly targets *Npy* expression. The phenotype is similar to the one that double *Npy*$^{-/-}$ *ob*/*ob* mutant mice display since they also have decreased food intake and fat mass, increased basic energy expenditure and improved fertility compared to *ob*/*ob* leptin deficient mice (Erickson et al., 1996b). However, in contrast to the double *Npy*$^{-/-}$ *ob*/*ob* mutant mice, the locomotory activity defect of the *ob*/*ob* mice was not rescued in the double *Bsx*$^{lacZ/lacZ}$ *ob*/*ob* mutant mice. These data suggest that *Bsx* targets *Npy* expression in the arcuate nucleus of hypothalamus and that it is also a crucial component of a distinct hypothalamic circuit situated in the arcuate nucleus regulating spontaneous physical activity. In addition, double *Bsx*$^{lacZ/lacZ}$ *ob*/*ob* mutant mice showed decreased caloric intake leading to weight loss, however the locomotory activity defect was not restored in contrast to observations of the double *Npy*$^{-/-}$ *ob*/*ob* mutant mice. Taken together, this suggests that weight and physical activity can be uncoupled genetically.

3.1 *Bsx* directly targets *Npy* and Agrp expression

In situ hybridization analysis of *Bsx* mutant mice in combination with cell culture experiments gave evidence that Bsx regulates *Npy* transcription directly. Despite the fact that *Npy* is expressed in different CNS structures, it was only specifically down-regulated in the arcuate nucleus of hypothalamus in *Bsx*$^{lacZ/lacZ}$ mutant mice. This is the only area of the brain where its expression overlaps with that of *Bsx*. NPY is a potent orexigenic peptide. The importance of *Npy* in regulating feeding, has been demonstrated by both pharmacological and genetic experiments, however, its presence is not necessary for development and feeding regulation in mice (Erickson et al., 1996a). Until recently the role of *Npy* in feeding regulation was not that clear because although loss of *Npy* in the *ob*/*ob* leptin deficient mice results to a

significant decrease of food intake, *Npy* deficiency has a blunt phenotype. Genetic ablation of the NPY/AgRP neurons provided a powerful tool to assess the importance of these neurons in feeding regulation. Deletion of the NPY/AgRP expressing neuronal population in adulthood leads to starvation and death although ablation of the neurons early after birth had no effect in feeding (Luquet et al., 2005). This shows not only that NPY/AgRP expressing neurons are mandatory for feeding regulation, but also that when a defect occurs in the neurons early on during development, compensatory mechanisms can take place to overcome any feeding deregulation. Given that loss of *Bsx* in the NPY/AgRP expressing neurons occurs early on during development, at embryonic day 10.5 as soon as *Bsx* promoter is turned on, hypothalamic compensatory factors or circuitries may be activated at that point. Induction of compensatory mechanisms, the nature of which still remains to be determined, explains the lack of any hypo-phagic defect in the *Bsx* mutant mice despite deregulation of the orexigenic peptides expression and the impairment of ghrelin responsiveness.

These results in combination with the genetic analysis of the compound $Bsx^{lacZ/lacZ}$ *ob*/*ob* mice gave evidence that *Bsx* is required upstream of the orexigenic peptides to induce *Npy* and *Agrp* basal expression and their up-regulation upon serum leptin levels decreased. Up-regulation of leptin, representing increase of the fat mass in the body is responsible for down-regulation of the *Npy* transcripts in the arcuate nucleus (Ahima et al., 2000) and conversely decrease of leptin levels increases *Npy* transcript that is required for food intake in response to the starvation signal. Genetic proof for this have been provided by the generation of the double mutant $Npy^{-/-}$ *ob*/*ob* mice, where lack of *Npy* rescues the morbid obesity phenotype that *ob*/*ob* mice display due to substantial decrease of food intake (Erickson et al., 1996b). Interestingly loss of *Bsx* in the *ob*/*ob* background had the same effect on feeding as that of loss of *Npy*, indicating that both act on the same pathway in order to induce increase of feeding. The impairment of *Npy* and *Agrp* induction upon starvation in *Bsx* mutant mice is a third independent experiment showing that Bsx is required for the expression of the orexigenic peptides by interacting with ghrelin and leptin signaling. The “commitment” of *Bsx* in inducing food intake is suggested in parallel by loss of ghrelin responsiveness in the *Bsx* mutant mice, in contrast to what has been observed in *Npy* mutant mice, that still respond to ghrelin signaling (Tschop et al., 2002).

Ghrelin, controlling meal initiation and the feeling of hunger, is a very potent orexigenic peptide. In this context the difference between the two mutant mice could have two interpretations; the first one being that since AgRP is still expressed in the *Npy* mutant mice they are able to respond to ghrelin. The second is that additionally to *Npy,* other Bsx target-genes are required for mediating ghrelin responsiveness in the NPY/AgRP neurons. The list generated from the microarray experiment performed on VP16::Bsx transfected PC12 cells will be an entry point to investigate the possible role of some of these genes acting downstream of Bsx to in inducing feeding in mice.

Loss of ghrelin responsiveness of the NPY/AgRP neurons in the Bsx mutant mice, directly influences both other neurons of the arcuate nucleus and other additional hypothalamic nuclei where second order neurons are situated. NPY/AgRP neurons project and inhibit POMC neurons in the arcuate nucleus in a tonic manner; lack of this inhibitory tone would lead to a constant activation of the anorexigenic POMC neurons causing loss of weight. The most logic explanation for the fact that *Bsx* mutant mice exert no weight loss is because of the counteracting locomotory activity defect that the mice display preventing them from increasing energy expenditure.

The starvation experiment we undertook provides additional proof for the importance of *Bsx* expression and function in regulating feeding response by controlling *Npy* transcription and up-regulation. Despite the fact that CREB phosphorylation in the nucleus has been correlated with the starvation response (Ahima et al., 1996; Schwartz et al., 1998; Shimizu-Albergine et al., 2001), it is not the only factor necessary for this response to take place. CREB phosphorylation in the nucleus needs to act synergistically with Bsx to activate even more *Npy* transcription as shown by the in vitro experiments. The lack of the *Npy* starvation response in the *Bsx* mutant mice underlined exactly this aspect, since although there is *Npy* expressed at basal levels and this is most probably due to CREB activity. *Bsx* expression is needed in order that the response attaints the one observed in *wt* mice.

Despite the fact that NPY/AgRP neurons have been extensively studied throughout the last decade, Bsx is the first transcription factor discovered specifically expressed in these neurons that regulates the expression of the two orexigenic peptides. Because Bsx not only regulates the expression of the two peptides but also the exclusive responsiveness of the neurons to the orexigenic gut hormone, ghrelin,

we believe that it has the role of molecular integrator in these neurons in order to regulate hyperphagia in physiological and non-physiological situations.

3.2 *Bsx* is involved in the regulating locomotory activity in mice.

The three main components of energy expenditure are basal metabolic rate, thermic effect of food, and activity thermo-genesis. The energetic cost of medication and emotion are small components that contribute to the whole of energy expenditure (Bensimhon et al., 2006; Levine, 2004). Basal metabolic rate is the amount of energy expended while an animal is at rest in a neutrally temperate environment, in the post-absorptive state (meaning that the digestive system is inactive, which requires about twelve hours of fasting in humans). The release of energy in this state is sufficient only for the functioning of the vital organs. In sedentary individuals it represents 60% of total energy expenditure. The thermic effect of food is the energy that is spent in association with digestion, absorption, and caloric storage; this represents the 10-15% of daily total energy expenditure. Furthermore, activity thermogenesis is either related to exercise, that only humans display or to non-exercise activity thermogenesis (NEAT). NEAT, or spontaneous physical activity is the predominant component of activity thermogenesis even for individuals that exercise regularly; it includes leisure, sitting, standing, walking, talking and it is the most variable component of energy expenditure both within and between subjects. NEAT is the only physical activity also displayed by animals and mice, since there is no evidence that animals exercise voluntarily.

NEAT is biologically regulated and influenced by both environmental and genetic factors. The occupation of the individual, the lifestyle and the cultural milieu, or the sedentary urban environment and the high degree of mechanization of our every day life, are major constituent of the variability of NEAT. Nevertheless, it is very difficult to estimate to which extend do these

environmental factors influence and have an impact on the possible range NEAT can have in different individuals.

There is strong evidence about the importance of NEAT in energy homeostasis. Several studies for example have demonstrated that following forcible overfeeding leading to positive energy balance and increase of body weight in humans. This increase of NEAT that occurs (Schoeller, 2001) correlate negatively with body weight increase. This experiment in humans provided the first evidence that NEAT is genetically determined and that it is regulated by the same network involved in the regulation of body weight stability. More evidence for genetic determination of NEAT came mainly from the following experiments. Stimulation of NEAT prevented hyperphagic individuals to gain weight, (Levine et al., 1999), again underlining the importance of spontaneous physical activity in body weight regulation. Moreover, recent works have demonstrated that ambulation or walking about, correlated negatively with fat mass content of individuals. Notably, measurements performed over several days showed that mildly obese individuals were displaying decreased spontaneous physical activity compared to lean ones (Levine et al., 2005). Forced feeding of the lean individuals and diet restriction of the mildly obese ones that in both cases caused changes in their original body weight didn't have any effect in the levels of spontaneous activity (Levine et al., 2005). This adds to the argument for a genetic regulation of NEAT and of the role that NEAT plays in determining body weight. This, moreover, shows that high or low spontaneous activity is not regulated as a consequence of body weight changes but determined independently by different neuronal networks.

Interestingly, leptin treatment in human patients undergoing caloric restriction is successful in maintaining body weight constant due mainly to the increased levels of spontaneous physical activity (Rosenbaum et al., 2005), suggesting that activity is probably regulated by the same hypothalamic neuronal network that responds to leptin. Furthermore, it has been shown that specific reactivation of the leptin receptor in the arcuate nucleus of leptin receptor deficient mutant mice (*db*/*db* strain), remarkably improved both glucose homeostasis and locomotor activity but not body weight (Coppari et al., 2005). This indicates that

distinct neuronal hypothalamic pathways regulate body weight and locomotor activity and that both circuitries are regulated by the leptin signaling pathway in the hypothalamus. This data provides indirect evidence that the effect of leptin on locomotor activity is mediated by neurons of the arcuate nucleus.

The main defect that *Bsx* mutant mice displayed was impaired locomotory activity contributing to a lower overall energy expenditure of the organism. Nevertheless, despite the substantial decrease of the energy expenditure we could measure no effect on body weight of mutant mice when they were provided with normal chow diet. In the opposite, when the mutant mice were challenged by excess of caloric intake as a result of a change in the diet, they developed obesity. This observation points to a contribution of spontaneous activity in body weight regulation. The analysis of this defect that *Bsx* mutant mice display, in combination with a hypothalamic specific expression of the transcription factor, provided strong evidence that locomotory activity is regulated by a neuronal network including the NPY/AgRP neurons of the arcuate nucleus that express Bsx. That locomotory activity and body weight control might use overlapping hypothalamic neuronal networks is supported through analysis of other mutant mice. It is well established that NPY/AgRP neurons send dense projections to Melanin-concentrating hormone (MCH) expressing neurons of the Lateral hypothalamus (Elias et al., 1999). Loss of MCH function in mice has been shown to improve the locomotor activity defect observed in *ob*/*ob* mice and suppressing by this means their obesity syndrome (Segal-Lieberman et al., 2003a). In addition, disruption of the MCH receptor 1 has been reported to lead to hyperactivity (Marsh et al., 2002). Therefore, it is not unlikely that NPY/AgRP neurons may partially act through MCH and modulate the dopaminergic system which is a critical component of the locomotory behavior regulation (Zhou and Palmiter, 1995). Further physiological studies have shown that microcircuits also exist between neurons of the arcuate nucleus and neurons situated in the ventral area of hypothalamus (VMH) (Sternson et al., 2005). In this respect, it is interesting to note that genetic ablation of the VMH by mutations in the gene encoding Steroidogenic factor-1 has revealed an important role of neurons in this nuclei in controlling locomotor activity (Majdic et al., 2002). Another system showing divergent roles in regulating feeding and activity are the orexin expressing neurons (Willie et al., 2001). Orexins (A and B) are a pair of peptides that are expressed in the lateral hypothalamic area of the brain. They have

been involved in the regulation of caloric intake, since when they are injected intracereborventricularly they increase caloric intake, metabolic rate and arousal (Hagan et al., 1999; Lubkin and Stricker-Krongrad, 1998; Sakurai et al., 1998; Willie et al., 2001). And although, *Bsx* expressing neurons do not overlap with Orexin expressing ones, the existence of high connectivity between these neurons and the NPY/AgRP neurons of the arcuate nucleus has been shown (Horvath et al., 1999a; Horvath et al., 1999b). An electrophysiological defect in the innervations between NPY/AgRP and Orexin or MCH expressing neurons in the lateral hypothalamus could explain the locomotory activity defect of the *Bsx* mutant mice. Given the connectivity of these neurons, the similarity of the locomotory defects in the *MCH, orexin* and *Bsx* deficient mice and the proof of a physiological defect already shown by the impairment of ghrelin responsiveness in the *Bsx* mutant mice, it is very likely that the locomotory defect is due to a connectivity failing between these neurons. In addition, intracerebroventricular administration of orexin A has been shown to increase NEAT in rats (Kiwaki et al., 2004; Kotz et al., 2002), suggesting that Orexin expressing neurons might function in the same circuit as *Bsx* expressing neurons do, in order to regulate spontaneous activity.

Y2R is one of 5 NPY receptors expressed in the NPY/AgRP neurons of the arcuate nucleus. *Y2R* deficiency in mice had no effect in feeding, but similar to the case of *Bsx* deficiency, a locomotory activity defect was observed. In addtition, double $Y2^{-/-}$ *ob*/*ob* mutant mice showed attenuated obesity compared to *ob*/*ob* mice (Sainsbury et al., 2002a; Sainsbury et al., 2002b), similar to the double $Npy^{-/-}$ *ob*/*ob* mutant mice. The difference between $Npy^{-/-}$ *ob*/*ob* and $Bsx^{lacZ/lacZ}$ *ob*/*ob* mice is that in the first ones loss of *Npy* restores the locomotory activity defect that *ob*/*ob* mice display but loss of Bsx doesn't restore this defect. One possible explanation is that Bsx except of *Npy* and *Agrp*, targets additional, until now unknown factors that are involved in specifically regulating locomotor activity and by its loss these factors are unable to be expressed. Another explanation for the difference between the two compound mutant mice is that since Y2R signaling in the NPY/AgRP neurons. Y2R is the only NPY binding receptor expressed in the NPY/AgRP and loss of function experiments in mice have shown that it is the only component of the NPY system involved in, an until now, unknown way in regulating spontaneous locomotory activity. This observation together with our finding, that *Bsx* deficiency in the *ob*/*ob*

background does not rescue the locomotory activity defect like *Npy* does, suggests an auto-regulatory negative feedback loop involving NPY and Bsx in the control of locomotor activity downstream the Y2R.

Phenotypic analysis of other mouse mutants have shown that locomotory activity and body weight control might use overlapping hypothalamic neuronal. Bsx is the first hypothalamic transcription factor involved in the regulation of energy homeostasis in two opposing ways, by regulating hyper-phagia via targeting expression of the orexigenic *Npy* and *Agrp* and by controlling spontaneous locomotory activity, one of the main energy expenditure components. That explains in parallel the different phenotypes of *Bsx* deficient mice depending on the context. *Bsx* deficient mice developed obesity when excess calories were supplied, since down-regulation of the orexigenic *Npy* and *Agrp* was developmentally compensated and the locomotory activity defect that contributes to lower levels of energy expenditure takes over. In contrast locomotion is already impaired in *ob*/*ob* background to a similar extend as in *Bsx* mutant mice and no change in locomotor activity is observed in the double mutant. Therefore suppression of hyper-phagia in this case due to the impaired expression of *Npy* and *Agrp* in *ob*/*ob* mice leads to a reduction in body weight and partial rescue of the obesity syndrome.

The homeobox sequence of Bsx is very highly conserved throughout various species, raising the possibility of *Bsx* constituting a necessary component circuitry of energy homeostasis regulation. During my PhD we discovered that Bsx has a role in two processes that are regulating body weight: feeding, by targeting *Npy* and *Agrp* expression, and spontaneous locomotory activity, a main component of energy expenditure. Should a system exist regulating food acquisition, Bsx is one of the main candidates for functioning within this system. Feelings of hunger and the ability to move in order to search for the food are crucial for acquiring food. It is well documented, for example, that starvation leads to an increase of physical activity, possibly modulated by ghrelin, as animals have to move to find food even though this will lead to energy consumption (Castaneda et al., 2005; Finger, 1951; Novak et al., 2005; Wald and Jackson, 1944). However, once the food is secured, then short-term satiety signals like the gut hormones CCK, GLP, PYY, act on the NPY/AgRP neurons of the arcuate nucleus in order to induce the feeling of satiety and to decrease physical

activity towards the end of saving energy. And despite the fact that *Bsx* mutant mice have a blunt phenotype in respect to food intake, due most likely to the high plasticity of the hypothalamic area responsible for the overcoming of any deficiency in the feeding system, our work has demonstrated that it is necessary to mediate the hyperphagia and the obesity phenotype of the *ob*/*ob* leptin mutant mice. Although the weight of the double mutant *Bsx*$^{-/-}$ *ob*/*ob* mice is partially rescued, the locomotory activity is not. The uncoupling of the locomotion from feeding behavior in the *Bsx*$^{-/-}$ *ob*/*ob* mice provided the first genetic prove of the existence of a distinct hypothalamic circuit (including NPY/AgRP neurons) which is implicated in the food acquisition process. In addition, the uncoupling of feeding from physical activity is the first indication that locomotion is not something that is regulated as a consequence of being over- or under- weight. It is rather a separate function that contributes to overall body weight. Dissociation between locomotory activity and body weight regulation and the identification of a genetic circuitry that regulates locomotory activity in hypothalamus, are the most critical findings that involved elucidating the role of Bsx in energy homeostasis. It will be interesting to see if by over-expressing *Bsx* it will also be possible to generate mice that have higher activity levels and that will eventually be leaner. Spontaneous locomotory activity contributes to energy expenditure and has a significant effect on body weight as observed by the analysis of Bsx mutant mice. Our findings in combination with latest studies performed in humans suggesting that physical activity may be biologically rather than environmentally determined support the hypothesis that Bsx levels and or activity are one important determinant of such locomotor activity. With this in-depth in vivo functional characterization of Bsx function, we provide a novel molecular target as well as a new genetic model showing that decreased physical activity in the presence of normophagia can increase *per se*, rather than being a response to it. Thus, human BSX if mutated may qualify as a perfect candidate for the postulated “lazy” gene contributing to human obesity. Development of pharmacological ways to target Bsx or Bsx effectors to modulate spontaneous locomotory activity may provide a new way to fight obesity in the future.

Future studies on the regulation of Bsx activity and of the transcriptional network underlying the physiology of NPY/AgRP neurons will provide new insights

into the mechanisms that are specifically stimulating and modulating spontaneous physical activity and that might open new avenues for controlling obesity.

4 Materials and Methods

4.1 Materials

4.1.1 Chemicals

Acrylamide	Biorad
L-Adenine	Sigma
Agar, Bacto	Becton-Dickinson
Agarose	Invitrogen
Ampicillin	Sigma
Ammonium Chloride	Merck
Ammonium-Persulfate (APS)	Biorad
Bovine Serum Albumin, Fraction V (BSA)	Sigma
Bromophenol blue	Sigma
Calcium Chloride	Merck
Carrier DNA (Herring testis)	Clontech
Chloramphenicol	Sigma
Colchicine	Sigma
Dextran Sulfate	Amersham Pharmacia
Dextrose	Merck
Dithiothreitol (DTT)	Biomol, Germany
DMSO (Dimethylsulfoxide)	Sigma
DPX	Agar Scientific
EDTA	Merck
Ethanol	Merck
Ethidium Bromide	Sigma
Fetal Calf Serum	Invitrogen

N,N-Dimethylformamide	Sigma
Formalin	Electron Microscopy Sciences
L-Glutamine	Invitrogen
Glycine	Merck
HEPES	Invitrogen
Isopropanol	Merck
Kanamycin	Sigma
Lithium Acetate	Sigma
Lithium Chloride	Merck
Lipofectamine 2000	Invitrogen
Magnesium Chloride	Merck
Malate acid	Sigma
MEM Non-essential amino acids	Invitrogen
Mercaptoethanol	Sigma
Methanol	Merck
Mowiol Reagent	Calbiochem
P^{32}-dCTP	Amersham
Paraformaldehyde (PFA)	Sigma
Penicillin/Streptomycin	Invitrogen
Peptone	Difco
PEG4000	Sigma
Potassium Chloride	Merck
Protease Inhibitors Complete	Roche
^{35}S-Methionine	Amersham Bioscience
^{35}S-UTP	Amersham Bioscience
Sodium Acetate	Merck
Sodium Hydroxide	Merck
Sodium Pyruvate	Invitrogen
SYBR green PCR master mix	ABI Applied Biosciences
TEMED	Biorad
Triethanolamine	Sigma
Triton X-100	Sigma
Trypsin	Invitrogen

Tween20	Gerbu
L-Uracil	Sigma
Xylene	Sigma

4.1.2 Equipment, plastic ware and other materials

Acid washed beads (0,5 mm)	Sigma
Agilent Bioanalyser	Agilent
Aquamount, Aqueous Mountant	LERNER Laboratories
Bacterial Petri dishes	Greiner Bio-One
High-Density mouse BAC membranes	Research Genetics
Cell counter chamber	(Neubauer improved) BRAND
Cell culture dishes	NalgeNUNC International
Cell incubator Hera cell	KendroLaboratoryProducts
Centricon YM-10	Amicon
Centrifuge 5417C	Eppendorf
Centrifuge RC5C	Sorvall, Instruments
Centrifuge RC-3B	Sorvall, Instruments
Cryotome CM 3050S	Leica Microsystems
Codelink 40K rat	Bioarray Amersham
Coverslips (24x60 mm)	Superior Marienfeld
Electrophoresis chambers	PeqLab
Electroporation system Gene Pulser II	BIO RAD
Electro-SeparationSystem S&S BIOTRAP	Schleicher & Schuell Bioscience
Filtration bottles STERICUP	MILLIPORE
Fine forceps and scissors	ROBOZ
Gene Pulser , Electroporation cuvettes	BIO RAD
Hybridizer incubator Techne HB-1D	TECHNE
Hybridization bottles	TECHNE
Hybridization Transfer Membrane NEN	Life Science Products

Microlance hypodermic needles	Becton Dickinson
Microscope Slides Super Frost ,Plus 25x75mm	ROTH
Microscope Axiovert 25	Zeiss
Mini Protean 3 system	Bio-Rad
Mini Trans-Blot Cell	Bio-Rad
Nitrocellulose Membranes PROTRAN	Schleicher & Schuell
Nylon Membranes Biotrans	ICN Biomedicals Inc.
Nylon positively charged membranes	Genescreen plus, NEN Life science
OCT Coumpound Embedding Medium	Tissue-Tek,
Optical Microscope	Zeiss
Paraffin Microtome RM2165	Leica Microsystems
PCR thermal cycler PTC-200	Biozym
PCR thermal reaction tubes	ABgene
PCR quantitative thermal cycler	ABI Applied Biosciences
Plastic tubes (50 ml and 15 ml)	FALCON
Power supply Power Pac 300	BioRad
Reaction tubes (1.5 ml)	ROTH
Serological Pipets (25 ml; 10 ml; 5 ml; 2 ml)	FALCON
Spectrophotometer Ultraspec 3000	Pharmacia Biotech
Vibrotome VI 1000S	Leica Microsystems
Ultracentrifuge L8-M	BECKMAN

4.1.3 Enzymes

Proteinase K	MERCK
Hot Star Taq DNA Polymerase	QIAGEN
Restriction endonucleases	New England BIOLABS; Roche,
Pwo DNA polymerase	Roche
Expand High Fidelity system	Roche

Klenow	New England Biolabs
T7, T3, SP6 RNA polymerase	Roche
RNase A	Roche
Proteinase K	Roche

4.1.4 Molecular weight markers

1kb DNA ladder	Invitrogen
Broad Range protein ladder	Biorad

4.1.5 Oligonucleotides

Mouse Genotyping

Bsx 3 (b-gal 3'):	5'- GAT GGG CGC ATC GTA ACC GTG CAT CTG CC-3'
Bsx 4 (wt 5')	5'- GAG AGA TGG GTT CCA GGA GCT TTG GAG C-3'
Bsx 6 (wt 3')	5'- GAA GAG CAG GAC GCA GAA TCC GGG GCA TCC-3'
OBM-1	5'- ATG ACC TGG AGA ATC TCT - 3'
OBW-1	5'- ATG ACC TGG AGA ATC TCC - 3'
OBW-2	5'- CCA TCC AGG CTC TCT GGC - 3'

Southern Blot Probes

Bsx 5' probe 5'	5'- GGA CTA CAC GGG CAC TGT ACA GTT C - 3'
Bsx 5' probe 3'	5'- GGA TTC TTG ATC TTC CCA AAC TCT GG - 3'

In Situ probes

Agrp forward	5'-GCTCTAGAA TGC TGA CTG CAA GGT TGC TGA G-3'
Agrp reverse	5'- CGG AAT TCT GCG ACT ACA GAG GTT CGT GG-3'
Cart forward	5'- GCT CTA GAT GCT ACC TTT GCT GGG TGC - 3'
Cart reverse	5'- GGG GTA CCT CAC ACA GCT TCC CGA TCC - 3'
Ghsr forward	5'- GCT CTA GAG CAA CAT GTG GAA CGC GA - 3'
Ghsr reverse	5'- CCG GTA CCA AGC AGA TGG CGA AGT AGC G - 3'
Npy forward	5'-CGGGAT CCT GCT AGG TAA CAA GCG AAT GGG-3'
Npy reverse	5'- CGG AAT TCA GTC CAG CCT AGT GGT GGC A - 3'
Obrb sense	5'- GCT CTA GAT CCC AGC AGC TAT GGT CTC C - 3'
Obrb antisense	5'- CCG GTA CCG ATT CCT GCC TCA CCA GTC AA - 3'
Pomc1 sense	5'- GCT CTA GAA CTT TCA GCT TCC AAG TCC ATA - 3'
Pomc1 antisense	5'- GGG GTA CCG CGG ACC AGC AGG TAT CAG AC - 3'
Sst sense	5'- GCT CTA GAA AGG AGA CGC TAC CGA AGC C - 3'
Sst antisense	5'-GGGGTA CCG GGC CAG GAG TTA AGG AAG AGA-3'
Trh sense	5'- CGG GAT CCT GCG ACT CCA AGA TGC AGG - 3'
Trh antisense	5'- CCG GTA CCG GCA TTA AGC CAC CCT CCT CT - 3'

Real Time quantitative PCR

Npy forward	5'- TCT CAT CTC ATC CTG TGA AAC CAG TCT GC - 3'
Npy reverse	5'- AAG GGA AAT GGG TCG GAA TCC AGC CTG G - 3'
TBP forward	5'- GCA CAG GAG CCA AGA GTG A - 3'
TBP reverse	5'- AGC TCC CCA CCA TGT TCT G – 3'
Actin forward	5'- GGC CCA GAG CAA GAG AGG TAT CC - 3'
Actin reverse	5'- ACG CAC GAT TTC CCT CTC AGC - 3'

4.1.6 Antibodies

Primary antibodies

AgRP	rabbit	Alpha Diagnostic International
βEndorphin	rabbit	Parlow
Fos	rabbit	Oncogene research products
βgalactosidase	rabbit	Cappel
GFP	rabbit	Torey Pines
α-MSH	sheep	Chemicon International
NeuN	mouse	Chemicon
NPY	rabbit	Peninsula Laboratories Inc
Phospho-STAT3	rabbit	Cell signaling technology

Bsx antibodies

Two antibodies against Bsx were generated. One by administrating in a rabbit a fused protein GST::Bsx expressed and purified in E.coli bacteria (Rossetta strain) using Ribi adjuvant to induce antibody production against the epitope. In a final

bleeding after the 6th boost, 70 ml of serum were obtained. Dilution series showed that the signal to background ratio is best in a 1:200 dilution for immunohistochemical application. The second antibody was produced in rat after administration of a fused protein 6xHis::Carboxy-terminusBsx using Ribi adjuvant to induce antibody production against Bsx. Carboxy-terminus of *Bsx* was obtained by digesting and isolating a PvuII and EcoRI 250 bp fragment from the full length cDNA of *Bsx* Dilution series of the serum obtained after the 6th boost of rats revealed good immunoreactivity against Bsx when diluted 1;100 in PBS.

Secondary antibodies

HRP-coupled αRabbit (western)	Goat	Chemicon
HRP-coupled αRat (western)	Goat	Chemicon

All fluorophore labeled antibodies were raised in Donkey and purchased from Jackson ImmunoResearch Laboratories.

4.1.7 Plasmid Vectors

Bacterial vectors

PBluescript SK+	Stratagene
PSP73	Promega
pET41-a-c	Novagen
pET30a-c	Novagen
pSP73 Vector	Promega

Mammalian vectors

pGL3 L Luciferase reporter vectors	Promega

pIRES-DsRed Vector	BD Biosciences
pIRES-eGFP Vector	BD Biosciences
p3XFLAG-CMV-10	Sigma

4.1.8 Commercial Kits

ABC kit	Vectastain
Codelink Expression Assay Reagent	Amersham Bioscience
DIG RNA labeling kit	Roche
Geneclean Spin kit	Q-BIO gene
Large construct kit	Qiagen
Maxiprep	Qiagen
Riboprobe combination system	Promega
Rneasy mini kit	Qiagen
Superscript first strand synthesis system for RT-PCR	Invitrogen
TNT-T7 coupled reticulocyte lysate system	Promega
TSA –Avidin Texas-Red	Perkin Elmer
QIAquick Gel Extraction kit	Qiagen

4.1.9 Generally Used Solutions

BAC Church	7 % SDS, 25 mM Na_2HPO_4 pH 7.2, 1 % BSA, 1 mM EDTA
BAC Wash	1 % SDS, 20mM Na_2HPO_4, 1mM EDTA
Gel-loading Buffer	0.25 % bromophenol blue, 15 % Ficoll, in water
PBS	137 mM NaCl, 2.7 mM KCl, 6.5 mM Na_2HPO_4, 1.5 mM KH_2PO_4
20xSSC	3M NaCl, 0.3M Na_3citrate•2H2O (pH to 7.0 with 1M HCl)
50xTAE	0.04 M Tris-Acetate, 0.001 M EDTA
LB	1% Bacto-tryptone, 0.5% Bacto-yeast extract, 0.5% NaCl

Tail Buffer	0.1 M EDTA, 0.1 M NaCl, 1 % SDS, 0.05 M Tris-Hcl, pH7.6, Proteinase K, 0.5mg/ml
5xTBE	45 mM Tris-borate, 1 mM EDTA
TBF1	30 mM Potassium acetate, 100 mM RbCl, 10 mM $CaCl_2$, 50 mM $MnCl_2$, Glycerol to 15 % (v/v), pH 5.8 with acetic acid
TBF2	10 mM MOPS, 75 mM $CaCl_2$, 10 mM RbCl, Glycerol 15 % (v/v), PH 6.5 with KOH
TBS	100 mM Tris-Hcl pH 7.5, 150mM NaCl
TE	10 mM Tris-Hcl (pH 8.0), 1 mM EDTA (pH 8.0)

4.1.10 Cell lines

Bacterial strains

E.coli XL-10 strain:Tetr, D(mcrA)183, D(mcrCB-hsdSMR-mrr)173, endA1, supE44, thi-1, recA1, gyrA96, relA1, lac Hte (F' proAB, lacIqZ DM15 Tn10 (Tetr) Amy Camr)a BL21 DE3

ES cells

ES cells used for gene targeting were from IB10. The IB10 is a mycoplasma-free ES cell line rederived at the EMBL Transgenic Service from the E14,1 ES cell line, therefore containing a 129/OLA genetic background.

Mammalian cell lines

The PC-12 cell line is a rat cell line adrenal gland derived that expresses neuronal markers. Cos-7 and HEK 293 cell lines used for transient transfections and luciferase essays are both mammalian immortal kidney cell lines.

4.2 Methods

4.2.1 DNA - Plasmids

Preparation of plasmid DNA from bacteria

Mini preparation of plasmid DNA was performed according the following procedure: 1.5 ml of an overnight (O/N) bacterial culture was centrifuged in an eppendorf tube for 1 minute at 14000 rpm and room temperature (RT), the pellet was ressuspended in 300 μl of ressuspension buffer (50 mM Tris-Cl, pH 8.0, 10 mM EDTA, 100 mg/ml RNAse A), 300 μl of lysis buffer (200 mM NaOH, 1 % SDS) were added, mixed by inversion and incubated at RT for 1 minute, the lysate was mixed with 300 μl of cold neutralization buffer (3.0 M Potassium Acetate, pH 5.5), incubated on ice for 10 minutes and centrifuged for 10 minutes at 14000 rpm at RT, 800 μl of the supernatant were transferred to a new tube and the DNA was precipitated with 500 μl isopropanol, centrifuged for 5 minutes at 14000 rpm and washed with 1 ml of 70% ethanol. The DNA was air dried and resuspended in 50 μl TE. For large-scale preparation of plasmid DNA, the QIAGEN Plasmid Maxi Kit was used according to the manufacturer's instructions.

Purification of supercoiled DNA by CsCl gradient centrifugation

For purification of supercoiled plasmids, 4 g Cesium Chloride were dissolved in 3.8 ml of TE containing the DNA to be purified. 0.2 ml of Ethidium Bromide solution (10 mg/ml in water) were added and the mixture was transferred to a 4 ml

centrifuge tube (Beckman) for centrifugation in a Beckman vertical Vti65 rotor. After sealing, the tubes were spun O/N at 60000 rpm and 25°C. One visible band at the center of the gradient was collected into a glass tube using a hypodermic needle. Ethidium Bromide was extracted from the DNA by a series of equal volumes of 1-Butanol extractions until no pink color was detected. The DNA was centrifuged in a centricon filter device at 4000 rpm (SS34 - Sorvall) and 25°C and washed 3 times with TE to remove CsCl.

Spectrophotometric determination of DNA and RNA concentration

Spectrophotometric measurements of DNA solutions were done at wavelengths of 260 nm. An OD=1 at 260 nm corresponds to a concentration of 50 μg/ml for double-stranded DNA and 33 μg/ml for single-stranded oligonucleotides and 40 μg/ml for RNA.

DNA restriction and Klenow treatment

To a solution of DNA the appropriate 10xbuffer and restriction enzyme were added according to the manufacturer's recommendations, mixed in a reaction tube and typically incubated O/N at the appropriate temperature. Klenow treatment was done in accordance with the NEB protocol.

Electrophoresis of DNA

Analysis and preparation of DNA were performed using agarose gels containing 0.5 μg/ml Ethidium Bromide. 1xTAE-buffer was used as gel and electrophoresis buffer. DNA samples were loaded into the gels in 1xDNA loading buffer and run at 5 V/cm of gel. The DNA samples were generally run in parallel to a DNA molecular weight marker (1kb ladder).

Isolation and purification of DNA from preparative agarose gels

DNA was isolated from agarose using two different commercial kits according to the fragment size. For fragments up to 6 kb, the QIAquick® Gel extraction Kit (Qiagen) was used according to the manufacturers instructions. For fragments bigger than 6 kb, the Gene Clean Spin Kit was used according to the manufacturers instructions. For
purification of large amounts of DNA from agarose gels, the S&S BIOTRAP Electro-Separation-System for elution and purification of charged molecules was used according to the manufacturer's instructions.

DNA ligation

For ligation of purified DNA fragments into linearized plasmid vectors, an appropriate amount of each DNA species was incubated O/N in a total volume of 10 μl with 1 μl of 10xbuffer and 1U DNA ligase. Ligation reactions were incubated O/N at 16°C.

Cloning of the *Bsx*^{lacZ} and the *Bsx*^{H2BeGFP} alleles.

Bsx^{lacZ} allele was generated using standard mouse embryonic stem cell technology. A 129BAC was isolated and a 8kb BamHI-fragment was subcloned containing the *Bsx* genomic locus. The flanking arms of the *Bsx*^{lacZ} targeting vector were generated by PCR using the 8kb genomic BamHI fragment in pBluescript SK (Stratagene) and the following primers:
5'arm: 5'-TGAAGCTTGGTGGCAGATTGAGTTCAAGAC-3' (forward)
and 5'- GCGGATCCCGGTGCGGGAACAGCGCCGGGACCGG-3' (reverse)
3'arm: 5'-GCGGATCCGGATTCTGCGTCCTGCTCTTCC–3' (forward)
and 5'-ATGCGGCCGCATAGCCCCAGACACTTGGTTCC–3' (reverse).

The 5' arm was fused in frame with a lacZ-Neo cassette and a DTA cassette was added to the 3' arm for negative selection. Unfortunately, the lacZ expression did shut down after the second generation.

Bsx^{lacZ} allele was genotyped using the following primers:

Bsx4 + Bsx6 = 500bp wild type band; Bsx4 + Bsx3 = 700bp mutant band

Bsx3 (b-gal 3'): 5'- GAT GGG CGC ATC GTA ACC GTG CAT CTG CC –3'

Bsx4 (wt 5'): 5'- GAG AGA TGG GTT CCA GGA GCT TTG GAG C –3'

Bsx6 (wt 3'): 5'- GAA GAG CAG GAC GCA GAA TCC GGG GCA TCC –3'

Primers for Southern probe generation:

Bsx 5' probe 5': 5'- GGA CTA CAC GGG CAC TGT ACA GTT C –3'

Bsx 5' probe 3': 5'- GGA TTC TTG ATC TTC CCA AAC TCT GG –3'

The flanking arms of the *Bsx*^{H2BeGFP} targeting vector were generated by PCR using the 8 Kb genomic BamHI fragment in BSSK and the following primers:

5' arm 5' – CCAAGCTTGCAGAGCGCCTGTCACAGG – 3' and T7 primer

3' arm 5' – CCTTAATTAACTCCTCACCCCTCACGCTC – 3' and T3 primer.

The 5' arm was fused to the ATG in frame with a Histone2BeGFP-Neo cassette and a DTA cassette was added to the 3' arm for negative selection.

Bsx^{H2BeGFP} allele was genotyped using the following primers:

BsxHisWT5': 5' – GCAGCTGCAGGCTCTTGAGTAGGC – 3'

BsxHISWT3': 5' – CTCTGAGAAGATGCTGGATGAAGAGG – 3'

BsxHisMut3': 5' – GGAAGCCTCACCTGCGATGCGCTCG – 3'

Preparation of chemocompetent Escherichia coli XL-10 cells

5 ml of LB medium (+tetracycline) were inoculated with a single colony of E.coli XL-10 and incubated with shaking (300 rpm) O/N at 37°C. 250 ml of LB medium were inoculated with 3-4 ml of the overnight culture and incubated with shaking at 37°C until an OD600 of 0.5 to 0.6. The cell suspension was incubated on ice for 5 minutes, poured into 50 ml Falcon tubes and centrifuged at 3000 rpm (GSA - Sorvall) and 4°C for 10 minutes. The supernatant was discarded and the bacterial pellet was resuspended in 20 ml of TBF1 buffer (2/5 volume) and incubated on ice for 5 minutes. The cell suspension was centrifuged at 3000 rpm (RC-3B) and 4°C for 5

minutes, the supernatant was discarded and the bacterial pellet was resuspended in 2 ml TBF2 buffer (1/25 initial volume). After 15 minutes of incubation on ice 200 μl aliquots were frozen in liquid nitrogen and stored at -80°C.

Transformation of chemocompetent Escherichia coli XL-10 cells

100μl of competent E.coli XL-10 cells were added to DNA in an eppendorf tube and incubated on ice for 30 minutes, the mixture was then heat shocked for 90 seconds at 42°C, followed by a 3 minutes incubation on ice. 1 ml of LB medium was added and the cell suspension was incubated for 30 minutes at 37°C. The transformation was then plated on the appropriate selective media and incubated at 37°C overnight.

Preparation and transformation of electrocompetent E.coli XL-10 cells

5 ml of LB medium was inoculated with one colony of XL-10 and grown O/N at 37°C. 500 ml of LB was inoculated from the overnight culture and grown to an OD600 of 0.6. The bacteria were chilled on ice for 10 minutes and spun down at 4000 rpm (GSA) at 4°C for 20 minutes. The supernatant was aspired and the pellet resuspended in 500 ml of ice-cold water and spun as above. This procedure was repeated. After two washes, the bacteria were resuspended in one volume of ice-cold water. Up to 0.5 μg plasmid DNA in 1 μl H_2O was mixed with 100-300 μl of competent bacteria and placed in a pre-chilled cuvette. The electroporation apparatus was set at 2.5 kV, 25 mF and 200 ohms and the transformation was subjected to one pulse. The transformation was transferred to 1ml of LB and incubated on a wheel for 30 minutes at 37°C. Finally the bacteria was plated on the appropriate selective plates (LB-ampicillin in the case of pGAD vector recovery).

4.2.2 DNA - Genomic

Preparation of genomic DNA

For genomic DNA preparation from mouse-tails, each tail was incubated O/N in 800 µl of tail buffer at 56°C. The following day, 300 µl of 6M NaCl was added, mixed by shaking and centrifuged for 10 minutes at 14000 rpm (Eppendorf) at RT to pellet the tail debris. 800 µl of the supernatant were transferred into a new reaction tube, mixed with 500 µl isopropanol and centrifuged at 14000 rpm for 5 minutes to pellet the genomic DNA. Supernatant was aspirated and the recovered DNA was washed in 70 % ethanol and dissolved in 100 µl TE. For preparation of genomic DNA from ES-cells, a confluent well from a 24 well plate was washed twice in PBS, incubated O/N at 37°C with 600 µl ES-cell lysis buffer (10 mM Tris- HCl pH 8.0, 5 mM EDTA, 100 mM NaCl, 1 % SDS and 0.5 mg/ml Proteinase K). The next day DNA was precipitated in an eppendorf tube by addition of 500 µl isopropanol followed by mixing by shaking. The precipitated DNA was transferred to a new tube with a tip and washed O/N with 70% ethanol. After spinning down the DNA was resuspended in 100 µl TE O/N at 37°C

Polymerase Chain Reaction (PCR)

For mouse genotyping, the standard genomic PCR reaction was performed with a hot start protocol that employs the HotStarTaq DNA polymerase. One reaction contained:

17 µl H2 O
2 µl 10xPCR buffer (QIAGEN)
0.5 µl dNTP solution (10 mM each dATP, dCTP, dGTP, dTTP)
0.2 µl each primer 50 mmol)
0.5-1U HotStarTaq DNA polymerase
5 ng DNA

The PCR reaction was initially denatured for 15 minutes at 94°C to activate the HotStarTaq DNA polymerase. PCR was typically performed with 36 cycles, each cycle consisting of 40 seconds denaturation at 95°C; 40 seconds annealing at the appropriate temperature for the oligonucleotides; 45 seconds of elongation at 72°C. The amplification products were assayed by gel electrophoresis.

For cloning purposes either the Pwo polymerase or the High Fidelity Expand was used, essentially as described above with the omission of the 15 minutes hot start.

Southern blot analysis

Detection and localization of specific sequences within genomic or plasmid DNA was performed using the Southern blot technique. Typically the DNA (20mg of mouse genomic DNA or 1mg of plasmid DNA) was treated with one or more restriction enzymes. The resulting fragments were separated according to size by agarose gel electrophoresis (0.6 % gel cast in 0.5xTBE containing 0.5 μg/ml Ethidium Bromide was used for genomic DNA samples). After electrophoresis was completed, the gel was photographed with a fluorescent ruler for subsequent assessment of band sizes. The DNA was denatured by incubating the gel in 0.5 N NaOH, 1.5 M NaCl for 30 minutes with agitation. The gel was then briefly rinsed in deionized water before the DNA was transferred to a nylon membrane by capillarity under neutral conditions (20XSSC). The membrane was incubated for two hours at 80°C to immobilize the attached DNA, followed by a pre-hybridization (2 hours minimum) in Church hybridization solution at 65°C. The membrane was then probed O/N at 65°C with a radioactive labeled probe in 30 ml of Church buffer. After hybridization, the membranes were washed in the following series of increasingly a stringent washing buffers: 2xSSC, 1 % SDS; 0.5xSSC, 1 %S DS; 0.1xSSC, 1 % SDS for 30 minutes each. Autoradiography was used to locate the positions of the bands complementary to the probe.

Radioactive labeling of DNA probes for southern blot analysis

Labeling of DNA probes for southern blot analysis was performed PCR. Using a previously amplified sequence (in general with a size of 300 bp) as a template in the following reaction, radioactive dCTP-P32 was incorporated of into the probe:

8 μl H2O

2 μl 10xPCR buffer

3 μl dNTP solution (0.5 mM each dATP, dGTP, dTTP)

5 μl P^{32}-dCTP (50 μCi)

0.5 μl each primer

2.5 U HotStarTaq DNA polymerase (QIAGEN)

5 ng Template DNA

The PCR reaction was initially denatured for 15 minutes at 94°C to activate the HotStarTaq DNA polymerase. PCR was usually performed with 30 cycles, each cycle consisting of 20 seconds denaturation at 95°C, 30 seconds annealing at 50°C, and 30 seconds of extension at 72°C. A final cycle of 5 minutes at 95°C was performed to denature the labeled probe. The probe was incubated on ice for 4-5 minutes and then added into the hybridization solution.

DNA constructs for in situ probes

All probes were generated by cloning a DNA fragment containing either the complete cDNA or relevant parts of the cDNA of the gene to be probed into the pBluescript + vector. For all probe the fragment were generated by PCR from a hypothalamic cDNA library.

4.2.3 RNA

RNA isolation from PC-12 cells

RNA isolation has been performed on 10 cm diameter confluent PC-12 cell culture dishes for further analysis by either Northern blotting, quantitative Real Time polymerase chain reaction or expression profiling by hybridizing it on microarrays. The plates were washed with PBS and lysed by addition of 600 ml of RLT lysis buffer (Qiagen) after addition of β-Mercaptoethanol, according to the manufacturer's protocol. The lysed cells were collected in an eppendorf tube by using a cell scrapper and were sheared with a 21-gauge syringe. RNA was then prepared by using the RNeasy Qiagen kit according to the manufacturer's instructions.

RNA precipitation

RNA was precipitated by addition of 3.4 µl LiCl 8 M and of 160 µl 100 % Ethanol, followed by an incubation of 2 hours at – 20^0C. Later the precipitated RNA was centrifuged at 14000 rpm for 15 minutes and washed with 1 ml 70 % ethanol. The RNA was air-dried for 5 min and resuspended in 6 µl of RNase free water.

Northern blot analysis

Detection and localization of specific RNA sequences expressed in the PC-12 cells was performed by using the Northern blot analysis technique. Typically 15-20 µg RNA / lane were load and separated in a denaturing formaldehyde agarose gel (1 % agarose, 20 mM MOPS, 0.75 % formaldehyde, 0.5 µg/ml Ethidium bromide, Running buffer:20 mM MOPS). After electrophoresis was completed, the gel was photographed with a fluorescent ruler for subsequent assessment of band sizes and visualization of the two rRNA subunits, the 18SrRNA and 28SrRNA. The gel was next blotted onto positively charged nylon membranes (Genescreen Plus) and the RNA was transferred on the membrane by capillarity under neutral conditions (10xSSC) over night. The membrane was baked at 80 ^{0}C in vacuum for 2 hours in order to immobilize the RNA on and blocked for 2 hours at 65 ^{0}C in Church buffer with salmon sperm. Hybridizations with radioactively ^{32}P labeled probes (prepared in similar way as probes for the southern analysis) for the NPY RNA were carried out

over night at 65 ^{0}C in 30ml Church buffer. Following hybridization the membranes were washed four times for about 20 minutes at 65 ^{0}C in 40 mM Na-phosphate buffer, pH 7, 1 % SDS and 1 mM EDTA.

Quantification of NPY expression in the PC-12 cells

Quantitative Real Time PCR (qPCR) was performed on cDNA produced from the total RNA isolated, using oligodT oligos and the first strand synthesis system for RT-PCR (Invitrogen), according to the manufacturer's protocol. One reaction of q-PCR contained:

1.25 µl primers from a 1.25 µM mixed stock

12.5 µl Syber-green PCR master mix (ABI)

8 µl dH_2O

2 µl template cDNA

For every sample, two copies were measured and the quantity of RNA was calculated as an average of the two values in order to avoid miscalculations due to pipeting mistakes. The data were normalized by quantifying the expression of housekeeping genes like actin that is highly expressed and TBP (TATA Binding Protein) that is expressed in lower levels. The reactions were performed and calculated by SDS ABI Applied Biosystems cycler (Genecore Facility/ EMBL).

All values were reported as mean ± SEM. Data analysis was performed by one way ANOVA followed by a *post-hoc* or t-test. Statistically significant threshold was accepted as $P < 0.05$.

Microarray analysis of Bsx transiently transfected PC-12 cells expression pattern

To proceed with the expression profiling of PC-12 cells RNA was quantified by spectrophotometry and the quality of the RNA was analyzed by denaturing gel electrophoresis (Gel: 1 % Agarose, 20 mM MOPS, 0.75 % formaldehyde, 0.5 μg/ml Ethidium Bromide. Running buffer: 20 mM MOPS.) on 2 μg of RNA. 1.8 μg of total RNA from each transfected plate was labeled with biotin using the Codelink

Expression Assay Reagent kit according to the protocol. The labeled mRNA was assayed by use of the Agilent Bioanalyser and quantified by spectrophotometry. 10 μg of labeled mRNA were fragmented and loaded on the 40K rat Bioarray as describe in the protocol and hybridized O/N at 37°C. The Bioarrays were then washed and bound biotin labeled probe detected with Cy5- streptavidin. The arrays were scanned in a GenePix Array scanner at 635 nm as described and analyzed by Codelink Expression Analysis software. Microarray results were analyzed using the software Genespring from Silicon Genetics.

4.2.4 Cell Culture and Transfection Methods

Culture conditions

Mouse embryonic stem (ES) cells were cultured in ES medium: glucose-rich (4500 mg/liter) DMEM medium supplemented with 15 % Fetal Calf Serum (FCS), 1 % MEM nonessential amino acids, 1 % Penicillin-Streptomycin, 1 % Glutamine, 1 % Sodium Pyruvat and Leukaemia Inhibitory Factor (LIF). The ES cells were grown on a layer of mouse embryo fibroblasts (MEFs) at 37°C with 5 % CO2. Selection of ES cell clones that had integrated the replacement vectors was done by adding the antibiotic G418 (250 mg/ml) to the medium. Ongoing cultures of MEFs and ES cells were typically grown in 10-cm tissue culture dishes with 10 ml of medium. All ES-cell mediums were changed daily.

PC-12 cells were cultured in medium glucose-rich (4500 mg/L) DMEM medium supplemented with 10 % Horse Serum heat inactivated, 5 % FCS, 1 % glutamine and 1 % Penicillin-Streptomycin. The cell culture dishes were coated with Poly-L-Lysine (10 µg/ml) before plating of the cells since they don't attach on the plastic like fibroblast cells.

The cos7 and HEK293 cells were cultures in medium DMEM medium supplemented with 10 % Fetal Bovine Serum (FBS), 1 % glutamine and 1 % Penicillin-Streptomycin. All three cell lines where growing in an incubator at 37 ^{0}C with 5 % CO_2.

Trypsinisation of cells

PC-12, cos7 and HK cells when they were at sub-confluent density they were passed into new tissue culture dishes at lower density. The medium was aspirated and the cells were washed once with PBS. The cells were subsequently covered with 0.5 % (w/v) trypsin and incubated at 37 ^{0}C until they were visibly detached from the dish. The trypsinisation reaction was stopped by addition of FCS containing medium. Cells were collected in a 50 ml tube, centrifuged (1500 rpm, 3 minutes) and the pellet was resuspended in new medium. The cells were plated next with the following dilution : for the PC-12 1:4, cos7 and HEK 293 1:6 or 1 :8 depending on the cell amount in the pellet.

ES cells and fibroblasts at sub-confluent density were passed into new tissue culture dishes at lower density. The medium was aspirated and the cells were washed once with PBS. The cells were subsequently covered with 0.5 % (w/v) trypsin and incubated at room temperature until they were visibly detached from the dish. The trypsinisation reaction was stopped by addition of FCS containing medium. Cells were collected in a 50 ml tube, centrifuged (1500 rpm, 3 minutes) and the pellet was resuspended in new medium. The cells were counted using a Neubauer chamber and plated at appropriate numbers on new tissue culture dishes.

Transfection of PC-12 cells

PC-12 cells in 90 % confluency were trypsinised and distributed to new Poly-L-lysin coated plates in a 1:4 dilution one day before transfection. For a 10 cm diameter plate 12 μg of total DNA plasmid were transfected in cells by using Lipofectamin 2000 reagent (Invitrogen) according to the manufacturer's protocol.

Cos-7 and HEK293 transfection

Cos-7 and HEK293 cells were calcium phosphate transfected. One day before the transfection a 95 % confluent plate was trypsinised and diluted 1:6 on new plates. For a 10 cm diameter plate 5 – 10 μg of total DNA plasmid were used and mixed in an eppendorf tube with H_2O to 450 μl volume. 50 μl $CaCl_2$ 2.5 M were added next in the DNA dropwise. The DNA was then added dropwise in a 15 ml falcon tube that contained already 500 μl of 2x HBS (280 mM NaCl, 50 mM Hepes, 1.5 mM Na_2HPO_4 x 2 H_2O, pH 7.1 ± 0.05 with NaOH) while air was continuously bubbled into the solution. DNA precipitates were formed 20 minutes later, and the slightly turbid $Ca_3(PO_4)_2$/DNA solution was added dropwise on the cells and left over night in the cell incubator. Next morning the medium was changed and the cells were harvested 36 hours later to check for luciferase expression.

Mitomycin C treatment of Mouse Embryo Fibroblasts

To mitotically inactivate feeder cells, confluent layers of MEFs in tissue culture dishes were treated with medium containing 10 mg/ml of Mitomycin C for 3 hours at 37°C with 5 % CO2. The dishes were washed three times with PBS and the cells collected by trypsinisation. After centrifugation, the cells were resuspended in feeder medium (glucose-rich (4500mg/liter) DMEM medium supplemented with 15 FCS, 1 % MEM nonessential amino acids, 1% penicillin-streptomycin, 1% glutamine), counted and the appropriate number was transferred to tissues culture dishes to ensure the production of a uniform confluent mono layer of cells.

Freezing and thawing cells

Cells were trypsinised, counted and centrifuged for 3 minutes at 1500 rpm. The supernatant was discarded and the pellet was resuspended in new medium at a

density of 2.5x106 cells/ml. Aliquots of 1x106 cells were transferred into individual cryo-vials and an equal volume of medium containing 20% DMSO was added to each vial (10% DMSO final concentration). The cell suspension was frozen, by storing the vials at -80°C. For long-term storage, vials were transferred into liquid nitrogen. For thawing, cells the vials were rapidly warmed at 37°C and the cell suspension was transferred into a centrifuge tube containing medium. The cells were centrifuged at 1500 rpm for 3minutes, resuspended in new medium and transferred to tissue culture dishes. ES cells were transferred to tissue culture dishes containing a confluent layer of mitotically inactive MEFs.

Electroporation of ES cells

An exponentially growing culture of ES cells at passage #4 was prepared for electroporation by changing medium approximately 3 hours before harvesting the cells. The cells were trypsinised and medium added to stop the trypsinisation reaction. Cells were centrifuged for 4 minutes at 3000 rpm and RT, washed once and resuspended in PBS as a single cell suspension. The ES cell suspension was counted, and the cell suspension was centrifuged once more, washed and resuspended at a density of 1.5x107 cells/ml in Ca_2+ /Mg_2+ free PBS. For each electroporation, 0.8 ml (1.5x107 cells) of cell suspension was placed in a sterile cuvette and 25 μg of linearised DNA were added and mixed well. This mixture was left at room temperature for 5 minutes and a single pulse of 240 V, 500 mF was applied to the cuvette. After electroporation, the cells were incubated on ice for 5 minutes and plated onto 10-cm tissue culture dishes of neo-resistant MEF feeder cells. Each 0.8 ml sample from the electroporation was divided and equally distributed on eight tissue culture dishes. The cells were allowed to recover for 48 hours in non-selective medium. The G418 selection of ES clones that had integrated the replacement vectors started 48 hours after electroporation.

Isolation of individual ES cell colonies

Selected individual ES cell colonies were isolated 9-10 days after electroporation. Sets of 96- well tissue culture dishes containing confluent mono-layers of MEFs in fresh medium were prepared in advance. Culture medium was replaced by PBS. The tip of a 10 μl micropippete was used to dissociate individual colonies to small aggregates of only a few cells. The dissociated colonies were transferred into the 96-well dishes and incubated at 37°C with 5 % CO_2. 48 hours after isolation, the individual clones were trypsinised and further cultured in the same well to give rise to an exponentially growing set of evenly distributed ES cell colonies. The growth of all ES cell clones was monitored daily and when considered appropriate (~50%confluency for the highest number of clones) all clones in one dish were trypsinised and divided in the following way: Half of the ES cells of each clone were transferred to a new 96- well dish containing mitomycin C treated MEFs and these cells were subsequently frozen; the remaining cells from each clone were transferred to gelatin coated 24-well dishes for later preparation of genomic DNA. Homologous recombination was verified by southern blot.

ES cell injection into blastocysts and chimera production

Blastocyst injection was performed at the EMBL Transgenic Service. IB10 targeted ES cells with a 129/OLA genetic background were injected into E4.5 mouse blastocysts of the C57/Black6 strain produced by natural matings. Always approximately 12 cells are injected with an eppendorf microinjection apparatus in an inverted microscope under phase contrast. Two hours after injection, living blastocysts were implanted into pseudopregnant CD1 females (7-8 per oviduct arm) 2.5 days after mating to a sterile male to induce pseudopregnacy.

4.2.5 Tissue sectioning

Tissue preparation and fixation

Fixation of mouse tissues, organs and whole embryos was performed differently depending on whether the samples would be used for histology, immunohistochemistry or in situ hybridization.

For histological analysis of tissues using vibrotome sections, brains were isolated from mice perfused in 2 % PFA and fixed over night at 4°C in 4 % PFA. The brains were
subsequently washed in PBS for 10 minutes at 4°C and stored indefinitely in 0.5 % paraformaldehyde at 4°C.

For analysis of gene expression by in situ hybridization, brains from mice perfused in 10 % formalin were properly dissected and stored indefinitely in 10% formalin.

Cryosectioning

After fixation, organs were incubated O/N at 4°C in RNAse-free 20 % Sucrose/PBS (w/v) solution over night or until the tissue sank. OCT medium was placed in embedding molds and the tissue sample was introduced in the medium. The molds were placed in dry ice-cold ethanol to freeze the medium. Typically, 18 μm sections were cut on a Leica Cryotome with a chamber temperature of -20°C. Tissue sections were transferred onto glass slides, air dried for a minimum of 2 hours and stored at -20°C for later processing.

Paraffin embedding and mounting

Mouse organs preserved in 70% ethanol were dehydrated in a series of 85%, 96% and three times 100% ethanol at least for 1 hour for each step at room temperature. The samples were cleared in two changes of xylene for 30 minutes each and incubated O/N in xylene at room temperature. The organs were carried through a series of four changes in paraffin 1hour each at 60°C and embedded in the proper

orientation in embedding molds. The molds were stored at 4°C until sectioning. The microtome was set to cut 7 μm sections.

Vibrotome sectioning

Brains from mice perfused in 2 % PFA were fixed in 2 % PFA over night at 4 °C. On the next day brains were washed in PBS and embedded in 2 % Agarose in PBS. The agarose block was mounted on the vibrotome, and 50 μm section were cut. The agarose was removed when possible with a brush, the tissue sections were stored in 0.5 % PFA in PBS at 4°C for later processing.

4.2.6 Histochemistry and Immunohistochemistry

Hematoxylene and Eosin staining

For hematoxylene and eosin staining of the fat pad tissue paraffin sections, slides were incubated twice for 10 minutes in xylene followed by rehydration in a series of 100%, 96% and 70% ethanol. After rinsing in distilled H_2O, sections were stained in hematoxylene solution (Sigma) for 10 minutes and washed in water for 10 minutes. Sections were subsequently stained in eosin solution (Sigma) for approximately 30 seconds, rinsed in distilled water, dehydrated in an ascending ethanol series, cleared in xylene and mounted.

Immunofluorescence

Imunofluorescence stainings were performed on 50 μm free-floating vibrotome sections prepared as described. Sections were rinsed for 10 minutes in

PBS. For blocking, the tissue sections were incubated for 2 hours with 5 % (v/v) secondary antibody species serum in TBS/0.4 % Triton X-100 at room temperature. Sections were washed twice with TBS/0.4% triton X-100 and incubated with the primary antibody at the appropriate dilution in TBS/0.4% triton X-100 O/N at 4°C. The slides were rinsed twice with TBS/0.4% triton X-100 and incubated with fluorescent-coupled secondary antibody in TBS/0.4 % Triton X-100 for 1 hour at room temperature in the dark. The slides were washed twice in 1xTBS/0.4% triton X-100 and mounted with 30 μl of Mowiol reagent, according to the manufacturer's indications. Slides were stored at 4°C in the dark until analyzed by confocal microscopy.

Pretreatment of the sections for Phospho-STAT3 immunostaining

Animals were deeply anesthetized, the heart was uncovered, and the circulation was flushed with 30 ml PBS via the left ventricle, followed by 30 ml 2 % PFA. After that, the brain was carefully removed, postfixed for 12–15 h in PBS containing 2 % PFA solution. For the immunohistochemistry free-floating tissue sections were used. For P-STAT3 immunostaining, the tissue needed to be pretreated with 1% NaOH and 1% H_2O_2 in H_2O for 20 min, 0.3% glycine for 10 min, and 0.03% sodium dodecyl sulfate for 10 min. After that, sections were blocked for 1 h with 3% normal goat serum in PBS/0.25% Triton X-100/0.2% sodium azide, P-STAT3 antibody was added (rabbit anti-P-STAT3, 1:3000 in blocking solution), and finally incubated overnight at 4 C. On the next day, The Tyramide Signal Amplification kit (TSA kit, Perkin Elmer) was used in combination with Avidin Texas- Red coupled, to intensify the immunostaining (Munzberg et al., 2003).

4.2.7 In situ hybridization

Generation of radioactively labeled in situ probes by in vitro transcription

The radioactive labeling of RNA probes was performed using the Riboprobe® Combination System-SP6/T7. An in vitro transcription labeling reaction was set up and incubated for 1 hour at 37°C:

5xtranscription buffer	4 μl
100 mM DTT	2 μl
Rnasin	0.6 μl
A/G/C mix (2.5mM each nucleotide)	4 μl
linearised template	1 μg
Nuclease free H_2O	to 14 μl
^{35}S-UTP (100 μCi)	5 μl
RNA polymerase	1 μl

The labeling reaction was followed by a treatment with DNaseI at 37°C for 15 minutes. This reaction was stopped by addition of 30 μl nuclease-free water and the labelled RNA was recovered using ProbeQuant™ G-50 Micro Columns according to the manufacturer's protocol. A probe concentration of $5x10^6$ cpm/ml or of $10x10^6$ was routinely used on the different tissue sections. The calculated amount of ^{35}S-labeled probe for 1 ml Hybridization solution was initially mixed with 50 μl tRNA, 10 μl 1M DTT and nuclease-free H_2O to 200 μl. This mixture was incubated at 65°C for 5 minutes to denature annealed strands in the labeled probe and added to 800 μl Hybridization solution (50 ml l Hybridization solution: 25 ml formamide, 10 ml 50 % dextran sulphate, 3 ml 5 M NaCl, 1 ml 1xDenhardt's solution, 0.5 ml 1 M Tris-HCl pH 8.0, 0.1 ml 0.5 M EDTA pH 8.0, 0.4 ml nuclease free H_2O). The hybridization mixture was stored at -20°C until the hybridization step for a maximum of 1 week.

Radioactive In Situ Hybridization

18 μm frozen cryostat sections were used for in situ hybridization. The tissue sections were initially treated with Proteinase K (10 mg/ml) in proteinase digestion buffer (0.1 M Tris-HCl pH 8.0, 50 mM EDTA pH 8.0) at 37°C for 30 minutes. Slides

were rinsed briefly in dH_20 and incubated in 0.1 M triethanolamine (TEA) pH 8.0 for 3 minutes at room temperature, and then acetylated in acetylation buffer (625 μl acetic anhydrid, 250 ml 0.1 M TEA) for 10 minutes at room temperature. Slides were then incubated in 2xSSC for 5 minutes and dehydrated through an ethanol series of 50%, 70%, 90% and 2 times 100% ethanol for 3 minutes each step. The slides were drained for 5 minutes and dried under vacuum in an exsiccator for a minimum of 2 hours until hybridization.

To hybridize the tissue sections with the a ^{35}S-labelled probe, an aliquot of the hybridization mixture was placed at 65°C for 10 minutes and then centrifuged for 10 minutes at 3000 rpm to eliminate any dextran sulfate precipitates that may have formed. 65 μl of hybridization mixture was applied to each slide (50x22 mm) and the tissue sections were then covered with a coverslip and sealed with the application of a bead of liquid DPX mounting medium. For hybridization, the slides were incubated O/N on 60°C slide-warming tray.

The next day, after hybridization, the slides were cooled and incubated four times 15 minutes with 4xSSC. The slides were subsequently treated with RNaseA in RNase buffer (RNaseA 20 μg/ml, 25 ml 5 M NaCl, 2.5 ml 1 M Tris-HCl pH 8.0, 500 μl 0.5 M EDTA pH 8.0, dH2O to 250 ml) for 37 minutes at 37°C. This was followed by a washing and gradual de-salting series of the following solutions: 2xSSC, 1 mM DTT for 5 minutes at RT; 1xSSC, 1 mM DTT for 5 minutes at RT; 0.5xSSC, 1mM DTT for 5 minutes at RT; 0.1xSSC, 1mM DTT for 37 minutes at 65°C; 0.1xSSC, 1mM DTT for 3 minutes at RT. Slides were then dehydrated through an ethanol series of 50 % ethanol (with 0.08xSSC, 1mM DTT), 70 % ethanol (with 0.08xSSC, 1mM DTT), 95 % ethanol and 100% ethanol each step for 3 min. The slides were finally drained for 5 minutes and dried under vacuum in an exsiccator for a minimum of 2 hours.

Generation of Digoxigenin (DIG) labeled in situ probes by in vitro transcription

DIG labeling of RNA probes was performed using the Digoxigenin labeling kit from Roche. An in vitro transcription labeling reaction was set up and incubated for 2 hour at 37°C:

1 µg purified template DNA in 13 µl DEPC-water	
10x NTP labeling mixture (10 mM)	2 *µl*
10x transcription buffer	2 *µl*
RNase inhibitor (20U/µl)	1 *µl*
RNA polymerase (Sp6, T7, T3)	2 *µl*

The labeling reaction was followed by a treatment with DNaseI at 37°C for 15 minutes. This reaction was stopped by addition of 0.8 *µl* of 0.5 M EDTA (pH8.0), followed by precipitation of the labeled RNA generated as described and resuspension of the RNA in 20 *µl* 100mM DTT.

DIG- Non-radioactive In situ hybridization

Tissue cryosections before hybridization were digested with 0.001 % proteinase K in proteinase digestion buffer (0.1 M Tris-HCl pH 8.0, 50 mM EDTA pH 8.0) at 37°C for 30 minutes when proceeded for in situ only and for 15-20 minutes when proceeded for combined in situ and immunohistochemistry. Next, slides were rinsed briefly in dH_20 and incubated in 0.1 M triethanolamine (TEA) pH 8.0 for 3 minutes at room temperature, and then acetylated in acetylation buffer (625 *µl* acetic anhydrid, 250 ml 0.1 M TEA) for 10 minutes at room temperature. Slides were then incubated in 2xSSC for 5 minutes and permeabilized for 30 minutes with 1 % Triton X-100 in PBS and washed 3 times with PBS when the slides are going to be processed for in situ hybridization and immunohistochemistry simultaneously followed by an incubation in hybridization buffer (50 ml l Hybridization solution: 25 ml formamide, 10 ml 50 % dextran sulphate, 3 ml 5 M NaCl, 1 ml 1xDenhardt's solution, 0.5 ml 1 M Tris-HCl pH 8.0, 0.1 ml 0.5 M EDTA pH 8.0, 0.4 ml nuclease free H_2O) for 1 hour at room temperature.

To hybridize the tissue sections with the DIG labeled probe, 1 *µl* of the labeled probe was mixed in 1 ml of hybridization solution and was placed at 65°C for 10

minutes and then centrifuged for 10 minutes at 3000 rpm to eliminate any dextran sulfate precipitates that may have formed. 65 μl of hybridization mixture was applied to each slide (50x22 mm) and the tissue sections were then covered with a coverslip and sealed with the application of a bead of liquid DPX mounting medium. For hybridization, the slides were incubated O/N on 60°C slide-warming tray.

The next day, after hybridization, the slides were cooled and incubated for 5 minutes in 5x SSC at 65 ^{o}C, next transferred in 0.2x SSC for 1 hour at 65 ^{0}C and balanced for 5 minutes in B1 buffer (for 1 L of a 5x buffer, 58g malate, 44g NaCl, 35g NaOH pellets, pH 7.5). The slides were next blocked for 1 hour with 2 % Blocking Reagent (Roche) in B1 buffer, followed by incubation with antibodies, an anti-DIG antibody (1:2000 dilution Roche) and an anti-GFP antibody (1:500 Torey Pines) for 3 hours at room temperature in a humidified tray. The slides where then rinsed 3 times with B1 buffer and equilibrated with B3 buffer (100 mM NaCl, 50 mM $MgCl_2$, 100 mM Tris pH 8.5 or 9.5 depending on the alkaline phosphatase substrate, 0.1 % Tween 20), followed by development with the Fast Red Tablets according to manufacturer's protocol.

Visualization of the immunostaining was performed by incubation with a secondary antibody fluorescent coupled (anti-rabbit FITC, 1:400, Molecular Probes). Slides when next washed in PBS 0.5 % Triton X-100 and mounted on Mowiol for further microscopical analysis.

4.2.8 Mouse methods

Mice were housed in a specific pathogen free environment (SPF) and under controlled light, (12 hour light/dark cycle), temperature, (21°C) and humidity (50 % relative humidity) conditions. Water and food were provided as needed ad libidum. Animals were fed with regular chow diet (Harlan Winkelmann, Teklad, TD2018S) or with high fat diet (Harlan Winkelmann, Teklad, TD97070) where indicated. Mice were routinely weaned from their parents at the age of 3 weeks with males and

females being housed separately. Mice were tagged using six-digit number eartags and tail biopsies were taken for genotyping. The procedures for performing animal experiments were in accordance with the principles and guidelines of the LAR/EMBL. The *Bsx*^{lacZ} allele was backcrossed for at least 10 generations to C57/BL6J before the physiological measurements and interbreeding with *Leptin*^{ob} mice were performed. Mice carrying the spontaneous *Leptin*^{ob} mutation were obtained from Jackson Laboratories/Maine, USA.

Colchicine injection

For the colocalization immunohistochemical detection of Bsx in combination with various hypothalamic specific neuropeptides, wt mice were treated with colchicine (Sigma). Colchicine arrests axonal transfer, thus brains from treated mice show enhanced cell body neuropeptide immunoreactivity and enables us to identify if they colocalize with Bsx. 60 μg of colchicine (10 mg/ml in 0.9 % saline) was administrated in the third ventricle of the mice by usage of a stereotaxical table.

GHRP-6 – Leptin injections

GHRP-6 was administrated in 8-10 weeks old wt and *Bsx*$^{-/-}$ mice for detection of Fos immunoreactivity in the Arc nucleus. They were given intravenous injection of 0.5 μg GHRP-6 / gr of body weight (GHRP-6 synthetic peptide, Bachem). Mice were sacrificed as described above 90 minutes after the injection and brains were removed and postfixed as mentioned.

48 hours starved wt and *Bsx*$^{-/-}$ mice were injected intravenously with 2 $\mu g$of leptin / gr of body weight (Parlow). Mice were anesthetized 45 minutes after the injection and perfused transcardially with 2 % paraformaldehyde. Brains were next removed and postfixed over night at 4 ºC in 2 % paraformaldehyde and processed as described for phospho-STAT3 immunostaining.

4.2.9 Proteins

Cell-extracts

All extracts from cell-culture and mouse tissues were done in RIPA buffer (50mM Tris-HCl pH 7.5, 150 mM NaCl, 1 % NP-40, 0.1 % SDS, 0.5 % Sodium deoxycholate, 0.05 % •- mercaptoethanol, protease and phosphatase inhibitors). Mouse hypothalamus were removed after perfusion with PBS, snap frozen in liquid nitrogen and lysed in RIPA buffer in an eppendorf tube with a pestel. The extracts were sheared with a pipette tip and insoluble debris spun down at 14000 rpm.

Protein concentration measurements

Protein concentrations were determined by Bio-Rad Bradford protein assay according to the manufactures protocol. In all assays, BSA was used as a standard.

SDS-PAGE

All SDS-PAGE gels were run on the Mini Protean 3 system and the gels were prepared as follows:

Separation gel: 0.375 M Tris-HCl pH 8.8, 8-18 % acrylamide, 0.1 % SDS, 0.05 % APS and TEMED (3 μl in 5 ml)

Stacking gel: 0.125 M Tris-HCl pH 6.8, 3.9 % acrylamide, 0.1 % SDS, 0.05 % APS and TEMED (5 μl in 5 ml)

Extracts were heated to 90°C for 4 min. in Laemmli buffer (5xLeammli buffer: 0.15 M Tris- HCl pH 6.8, 5 % SDS, 25 % glycerol, and 0.050 % Bromidephenolblue) with 3 % •- mercapto-ethanol added freshly just before heating. The heated samples were spun at 14000 rpm for 2 minutes before loading on the gels. Gels were run at 100-200V in running buffer (25 mM Tris, 192 mM Glycine)

Western blotting

All blots were done using the Mini Trans-Blot Cell. I all cases nitrocellulose membranes were used. The mini-gels were blotted in a buffer containing 20 % Methanol (analytic grade), 0.1 % SDS, 8.3 mM Tris, and 64 mM Glycine at 80 volts for 60-90 minutes at 4°C.

Probing

Membranes were blocked in PBS, 0.075% Tween20 + 5 % milk for an hour at room temperature or overnight at 4°C. All primary antibodies were used in 1:1000 times dilution in PBS, 0.075% + 1-5 % milk unless otherwise indicated in the figure legends. In all cases incubations were for 2 hours at RT or overnight at 4°C. All washes were done in PBS, 0.075% Tween20. All secondary antibodies were used in 1:5000 times dilution in PBS, 0.075% Tween20 (washing buffer) + 1-5 % milk for 1 hour at RT. Western blot were developed using ECL from Promega

Purification of GST-Bsx

Bacteria transformed with pET-41a-*Bsx* were grown in 10 ml LB, 30 μg/ml Kanamycin O/N. The culture was diluted to 4000 ml in LB, 30 μg/ml Kanamycin and grown to an OD600 of 0.6. 1mM IPTG were added and the bacteria grown for four additional hours. The bacteria were spun down (4000 rpm, GSA) and resuspended in 50 ml PBS, 0,5 mM DTT + protease inhibitors. The bacteria were sonicated 8-10 times 30 seconds and Triton X-100 was added to 1% followed by mixing for 30 minutes at 4°C. The bacterial lysates were spun at 10000 rpm (SS34) for 10 minutes at 4°C to pellet insoluble aggregates. Glutathion-Sepharose was washed three times in cold PBS, added to the cleared bacterial lysate and incubated for 2 hours 4°C on a wheel. The beads were spun down at low speed (1000g) and washed 4 times with PBS- Triton X-100. GST-Bsx was eluted in 2x1 ml of 20 mM reduced glutathione, 50

mM Tris-HCl, pH 8.0. Eluates were concentrated and the buffer changed to PBS using Centricon filter devises.

Purification of 6xHis tagged Bsx

Bacteria transformed with pET-30a-*Bsx* were grown in 10 ml LB, 30 μg/ml Kanamycin O/N. The culture was diluted to 4000 ml in LB, 30 μg/ml Kanamycin and grown to an OD600 of 0.6. 1mM IPTG were added and the bacteria grown for four additional hours. Bacteria were spun down (4000 rpm, GSA) and resuspended in 40 ml of a 5 mM DTT in 6 M Guanidine-HCl solution. The bacteria were sonicated 8-10 times for 30 seconds, the bacterial lysates were next spun at 9000 rpm (SS34) for 10 minutes at 4 ºC to pellet the insoluble aggregates. The lysates were next incubated for 2 hours at 4°C on a wheel, with Ni-NTA resins (8.0 mg/ml protein binding capacity) and washed subsequently with, 1 column 5 mM DTT Guanidine- HCl pH 8.0, 1 column Guanidine-HCl pH 5.9 and 5 mM DTT, 1 column 2:1 ratio of Guanidine-HCl pH 8.0: Dialysis buffer (50 mM $NaPO_4$, 0.1 M KCl, 20 % glycerol, 0.2 % NP-40, 1 mM DTT, protease inhibitors, complete), 1 column 1:2 ratio of Guanidine-HCl pH 8.0: Dialysis buffer, and 1 column Dialysis buffer only. Elution of the 6xHis tagged protein was performed by adding sequentially 1 column of Dialysis Buffer with 10 mM imidazol pH 8.0 and 3 columns of Dialysis buffer with 200 mM imidazol pH 8.0.

GST- Pull-down essay

After purification of the fusion proteins with glutathione sepharose beads GST and GST fusion proteins were loaded on an SDS-acrylamide gel for quantification. 2 μg of the protein coupled with the matrix were used in each sample in 1 ml of PBS 0.1 % Tween (w/w), where in vitro translated and ^{35}S-Methionine labeled protein prepared by using the TNT coupled in vitro translation kit (Promega) according to the manufacturer's protocol were added. The reaction was allowed to proceed for 2 hours at 4 ºC. The samples where next rinsed 3 times for 5-10 minutes in the reaction buffer (PBS 0.5 % Tween). The beads were finally resuspended in 1x Laemli buffer and

separted by SDS-PAGE acrylamide gel as described. The gel was dried and analyzed by autoradiography (MR-1 Kodak films).

References

Ahima, R. S., *et al.* (1996). Role of leptin in the neuroendocrine response to fasting. Nature *382*, 250-252.

Ahima, R. S., *et al.* (2000). Leptin regulation of neuroendocrine systems. Front Neuroendocrinol *21*, 263-307.

Asakawa, A., *et al.* (2001). Ghrelin is an appetite-stimulatory signal from stomach with structural resemblance to motilin. Gastroenterology *120*, 337-345.

Auernhammer, C. J., *et al.* (1999). Autoregulation of pituitary corticotroph SOCS-3 expression: characterization of the murine SOCS-3 promoter. Proc Natl Acad Sci U S A *96*, 6964-6969.

Bagnol, D., *et al.* (1999). Anatomy of an endogenous antagonist: relationship between Agouti-related protein and proopiomelanocortin in brain. J Neurosci *19*, RC26.

Banks, A. S., *et al.* (2000). Activation of downstream signals by the long form of the leptin receptor. J Biol Chem *275*, 14563-14572.

Banks, W. A., *et al.* (1996). Leptin enters the brain by a saturable system independent of insulin. Peptides *17*, 305-311.

Bannon, A. W., *et al.* (2000). Behavioral characterization of neuropeptide Y knockout mice. Brain Res *868*, 79-87.

Baskin, D. G., *et al.* (1999). Leptin receptor mRNA identifies a subpopulation of neuropeptide Y neurons activated by fasting in rat hypothalamus. Diabetes *48*, 828-833.

Batterham, R. L., *et al.* (2002). Gut hormone PYY(3-36) physiologically inhibits food intake. Nature *418*, 650-654.

Bensimhon, D. R., *et al.* (2006). Obesity and physical activity: a review. Am Heart J *151*, 598-603.

Bittencourt, J. C., *et al.* (1992). The melanin-concentrating hormone system of the rat brain: an immuno- and hybridization histochemical characterization. J Comp Neurol *319*, 218-245.

Bjorbaek, C., *et al.* (2001). Divergent roles of SHP-2 in ERK activation by leptin receptors. J Biol Chem *276*, 4747-4755.

Bjorbaek, C., *et al.* (1998a). Identification of SOCS-3 as a potential mediator of central leptin resistance. Mol Cell *1*, 619-625.

Bjorbaek, C., *et al.* (1998b). Expression of leptin receptor isoforms in rat brain microvessels. Endocrinology *139*, 3485-3491.

Bjorbaek, C., *et al.* (1997). Divergent signaling capacities of the long and short isoforms of the leptin receptor. J Biol Chem *272*, 32686-32695.

Blomqvist, A. G., and Herzog, H. (1997). Y-receptor subtypes--how many more? Trends Neurosci *20*, 294-298.

Boden, G., *et al.* (1996). Effect of fasting on serum leptin in normal human subjects. J Clin Endocrinol Metab *81*, 3419-3423.

Burbach, J. P. (2002). Regulation of gene promoters of hypothalamic peptides. Front Neuroendocrinol *23*, 342-369.

Butler, A. A., *et al.* (2000). A unique metabolic syndrome causes obesity in the melanocortin-3 receptor-deficient mouse. Endocrinology *141*, 3518-3521.

Castaneda, T. R., *et al.* (2005). Obesity and the neuroendocrine control of energy homeostasis: the role of spontaneous locomotor activity. J Nutr *135*, 1314-1319.

Challis, B. G., *et al.* (2004). Mice lacking pro-opiomelanocortin are sensitive to high-fat feeding but respond normally to the acute anorectic effects of peptide-YY(3-36). Proc Natl Acad Sci U S A *101*, 4695-4700.

Chen, H., *et al.* (1996). Evidence that the diabetes gene encodes the leptin receptor: identification of a mutation in the leptin receptor gene in db/db mice. Cell *84*, 491-495.

Chen, P., *et al.* (1999). Altered expression of agouti-related protein and its colocalization with neuropeptide Y in the arcuate nucleus of the hypothalamus during lactation. Endocrinology *140*, 2645-2650.

Cheng, A., *et al.* (2002). Attenuation of leptin action and regulation of obesity by protein tyrosine phosphatase 1B. Dev Cell *2*, 497-503.

Cheung, C. C., *et al.* (1997). Proopiomelanocortin neurons are direct targets for leptin in the hypothalamus. Endocrinology *138*, 4489-4492.

Clark, J. T., *et al.* (1984). Neuropeptide Y and human pancreatic polypeptide stimulate feeding behavior in rats. Endocrinology *115*, 427-429.

Cone, R. D. (2005). Anatomy and regulation of the central melanocortin system. Nat Neurosci *8*, 571-578.

Considine, R. V., *et al.* (1996a). The hypothalamic leptin receptor in humans: identification of incidental sequence polymorphisms and absence of the db/db mouse and fa/fa rat mutations. Diabetes *45*, 992-994.

Considine, R. V., *et al.* (1996b). Serum immunoreactive-leptin concentrations in normal-weight and obese humans. N Engl J Med *334*, 292-295.

Coppari, R., *et al.* (2005). The hypothalamic arcuate nucleus: a key site for mediating leptin's effects on glucose homeostasis and locomotor activity. Cell Metab *1*, 63-72.

Cowley, M. A., *et al.* (2001). Leptin activates anorexigenic POMC neurons through a neural network in the arcuate nucleus. Nature *411*, 480-484.

Cummings, D. E., *et al.* (2001). A preprandial rise in plasma ghrelin levels suggests a role in meal initiation in humans. Diabetes *50*, 1714-1719.

Dickson, S. L., *et al.* (1993). Systemic administration of growth hormone-releasing peptide activates hypothalamic arcuate neurons. Neuroscience *53*, 303-306.

Dickson, S. L., and Luckman, S. M. (1997). Induction of c-fos messenger ribonucleic acid in neuropeptide Y and growth hormone (GH)-releasing factor neurons in the rat arcuate nucleus following systemic injection of the GH secretagogue, GH-releasing peptide-6. Endocrinology *138*, 771-777.

Elchebly, M., *et al.* (1999). Increased insulin sensitivity and obesity resistance in mice lacking the protein tyrosine phosphatase-1B gene. Science *283*, 1544-1548.

Elias, C. F., *et al.* (1999). Leptin differentially regulates NPY and POMC neurons projecting to the lateral hypothalamic area. Neuron *23*, 775-786.

Elias, C. F., *et al.* (2000). Chemical characterization of leptin-activated neurons in the rat brain. J Comp Neurol *423*, 261-281.

Elias, C. F., *et al.* (1998). Leptin activates hypothalamic CART neurons projecting to the spinal cord. Neuron *21*, 1375-1385.

Elmquist, J. K., *et al.* (1998a). Leptin activates distinct projections from the dorsomedial and ventromedial hypothalamic nuclei. Proc Natl Acad Sci U S A *95*, 741-746.

Elmquist, J. K., *et al.* (1997). Leptin activates neurons in ventrobasal hypothalamus and brainstem. Endocrinology *138*, 839-842.

Elmquist, J. K., *et al.* (1998b). Distributions of leptin receptor mRNA isoforms in the rat brain. J Comp Neurol *395*, 535-547.

Elmquist, J. K., *et al.* (1999). From lesions to leptin: hypothalamic control of food intake and body weight. Neuron *22*, 221-232.

Erickson, J. C., *et al.* (1996a). Sensitivity to leptin and susceptibility to seizures of mice lacking neuropeptide Y. Nature *381*, 415-421.

Erickson, J. C., *et al.* (1996b). Attenuation of the obesity syndrome of ob/ob mice by the loss of neuropeptide Y. Science *274*, 1704-1707.

Fan, W., *et al.* (2004). Cholecystokinin-mediated suppression of feeding involves the brainstem melanocortin system. Nat Neurosci *7*, 335-336.

Farooqi, I. S., *et al.* (1999). Effects of recombinant leptin therapy in a child with congenital leptin deficiency. N Engl J Med *341*, 879-884.

Faust, I. M., *et al.* (1977). Adipose tissue regeneration following lipectomy. Science *197*, 391-393.

Finger, F. W. (1951). The effect of food deprivation and subsequent satiation upon general activity in the rat. J Comp Physiol Psychol *44*, 557-564.

Frederich, R. C., *et al.* (1995). Leptin levels reflect body lipid content in mice: evidence for diet-induced resistance to leptin action. Nat Med *1*, 1311-1314.

Ghilardi, N., and Skoda, R. C. (1997). The leptin receptor activates janus kinase 2 and signals for proliferation in a factor-dependent cell line. Mol Endocrinol *11*, 393-399.

Gong, D. W., *et al.* (1996). Genomic structure and promoter analysis of the human obese gene. J Biol Chem *271*, 3971-3974.

Gropp, E., *et al.* (2005). Agouti-related peptide-expressing neurons are mandatory for feeding. Nat Neurosci *8*, 1289-1291.

Hagan, J. J., *et al.* (1999). Orexin A activates locus coeruleus cell firing and increases arousal in the rat. Proc Natl Acad Sci U S A *96*, 10911-10916.

Hahn, T. M., *et al.* (1998). Coexpression of Agrp and NPY in fasting-activated hypothalamic neurons. Nat Neurosci *1*, 271-272.

Halaas, J. L., *et al.* (1995). Weight-reducing effects of the plasma protein encoded by the obese gene. Science *269*, 543-546.

Harris, R. B. (1990). Role of set-point theory in regulation of body weight. Faseb J *4*, 3310-3318.

Harris, R. B., *et al.* (1986). Dynamics of recovery of body composition after overfeeding, food restriction or starvation of mature female rats. J Nutr *116*, 2536-2546.

Haskell-Luevano, C., *et al.* (1999). Characterization of the neuroanatomical distribution of agouti-related protein immunoreactivity in the rhesus monkey and the rat. Endocrinology *140*, 1408-1415.

Hazelwood, R. L. (1993). The pancreatic polypeptide (PP-fold) family: gastrointestinal, vascular, and feeding behavioral implications. Proc Soc Exp Biol Med *202*, 44-63.

Hewson, A. K., and Dickson, S. L. (2000). Systemic administration of ghrelin induces Fos and Egr-1 proteins in the hypothalamic arcuate nucleus of fasted and fed rats. J Neuroendocrinol *12*, 1047-1049.

Higuchi, H., *et al.* (1988). Rat neuropeptide Y precursor gene expression. mRNA structure, tissue distribution, and regulation by glucocorticoids, cyclic AMP, and phorbol ester. J Biol Chem *263*, 6288-6295.

Hokfelt, T., *et al.* (1998). Neuropeptide Y: some viewpoints on a multifaceted peptide in the normal and diseased nervous system. Brain Res Brain Res Rev *26*, 154-166.

Hollopeter, G., *et al.* (1998). Role of neuropeptide Y in diet-, chemical- and genetic-induced obesity of mice. Int J Obes Relat Metab Disord *22*, 506-512.

Horvath, T. L., *et al.* (1999a). Synaptic interaction between hypocretin (orexin) and neuropeptide Y cells in the rodent and primate hypothalamus: a novel circuit implicated in metabolic and endocrine regulations. J Neurosci *19*, 1072-1087.

Horvath, T. L., *et al.* (1999b). Hypocretin (orexin) activation and synaptic innervation of the locus coeruleus noradrenergic system. J Comp Neurol *415*, 145-159.

Hosoda, H., *et al.* (2000). Purification and characterization of rat des-Gln14-Ghrelin, a second endogenous ligand for the growth hormone secretagogue receptor. J Biol Chem *275*, 21995-22000.

Hosoi, T., *et al.* (2002). Brain stem is a direct target for leptin's action in the central nervous system. Endocrinology *143*, 3498-3504.

Hubschle, T., *et al.* (2001). Leptin-induced nuclear translocation of STAT3 immunoreactivity in hypothalamic nuclei involved in body weight regulation. J Neurosci *21*, 2413-2424.

Huszar, D., *et al.* (1997). Targeted disruption of the melanocortin-4 receptor results in obesity in mice. Cell *88*, 131-141.

Ingalls, A. M., *et al.* (1950). Obese, a new mutation in the house mouse. J Hered *41*, 317-318.

Ingraham, H. A., *et al.* (1988). A tissue-specific transcription factor containing a homeodomain specifies a pituitary phenotype. Cell *55*, 519-529.

Kaga, T., *et al.* (2001). Modest overexpression of neuropeptide Y in the brain leads to obesity after high-sucrose feeding. Diabetes *50*, 1206-1210.

Kanatani, A., *et al.* (2000). Role of the Y1 receptor in the regulation of neuropeptide Y-mediated feeding: comparison of wild-type, Y1 receptor-deficient, and Y5 receptor-deficient mice. Endocrinology *141*, 1011-1016.

Katsuura, G., *et al.* (2002). Roles of pancreatic polypeptide in regulation of food intake. Peptides *23*, 323-329.

Kelly, A. B., and Watts, A. G. (1996). Mediation of dehydration-induced peptidergic gene expression in the rat lateral hypothalamic area by forebrain afferent projections. J Comp Neurol *370*, 231-246.

Kelly, A. B., and Watts, A. G. (1998). The region of the pontine parabrachial nucleus is a major target of dehydration-sensitive CRH neurons in the rat lateral hypothalamic area. J Comp Neurol *394*, 48-63.

Kennedy, G. C. (1953). The role of depot fat in the hypothalamic control of food intake in the rat. Proc R Soc Lond B Biol Sci *140*, 578-596.

Kitamura, T., *et al.* (2006). Forkhead protein FoxO1 mediates Agrp-dependent effects of leptin on food intake. Nat Med *12*, 534-540.

Kiwaki, K., *et al.* (2004). Orexin A (hypocretin 1) injected into hypothalamic paraventricular nucleus and spontaneous physical activity in rats. Am J Physiol Endocrinol Metab *286*, E551-559.

Klaman, L. D., *et al.* (2000). Increased energy expenditure, decreased adiposity, and tissue-specific insulin sensitivity in protein-tyrosine phosphatase 1B-deficient mice. Mol Cell Biol *20*, 5479-5489.

Kojima, M., *et al.* (1999). Ghrelin is a growth-hormone-releasing acylated peptide from stomach. Nature *402*, 656-660.

Kojima, M., *et al.* (2001). Ghrelin: discovery of the natural endogenous ligand for the growth hormone secretagogue receptor. Trends Endocrinol Metab *12*, 118-122.

Korner, J., *et al.* (1999). Regulation of hypothalamic proopiomelanocortin by leptin in lean and obese rats. Neuroendocrinology *70*, 377-383.

Kotz, C. M., *et al.* (2002). Feeding and activity induced by orexin A in the lateral hypothalamus in rats. Regul Pept *104*, 27-32.

Kristensen, P., *et al.* (1998). Hypothalamic CART is a new anorectic peptide regulated by leptin. Nature *393*, 72-76.

Krude, H., *et al.* (1998). Severe early-onset obesity, adrenal insufficiency and red hair pigmentation caused by POMC mutations in humans. Nat Genet *19*, 155-157.

Kushi, A., *et al.* (1998). Obesity and mild hyperinsulinemia found in neuropeptide Y-Y1 receptor-deficient mice. Proc Natl Acad Sci U S A *95*, 15659-15664.

Lazzaro, D., *et al.* (1991). The transcription factor TTF-1 is expressed at the onset of thyroid and lung morphogenesis and in restricted regions of the foetal brain. Development *113*, 1093-1104.

Lee, G. H., *et al*. (1996). Abnormal splicing of the leptin receptor in diabetic mice. Nature *379*, 632-635.

Levine, J. A. (2004). Nonexercise activity thermogenesis (NEAT): environment and biology. Am J Physiol Endocrinol Metab *286*, E675-685.

Levine, J. A., *et al*. (1999). Role of nonexercise activity thermogenesis in resistance to fat gain in humans. Science *283*, 212-214.

Levine, J. A., *et al*. (2005). Interindividual variation in posture allocation: possible role in human obesity. Science *307*, 584-586.

Low, M. J., *et al*. (2001). Somatostatin is required for masculinization of growth hormone-regulated hepatic gene expression but not of somatic growth. J Clin Invest *107*, 1571-1580.

Lubkin, M., and Stricker-Krongrad, A. (1998). Independent feeding and metabolic actions of orexins in mice. Biochem Biophys Res Commun *253*, 241-245.

Luquet, S., *et al*. (2005). NPY/AgRP neurons are essential for feeding in adult mice but can be ablated in neonates. Science *310*, 683-685.

Maffei, M., *et al*. (1995). Leptin levels in human and rodent: measurement of plasma leptin and ob RNA in obese and weight-reduced subjects. Nat Med *1*, 1155-1161.

Majdic, G., *et al*. (2002). Knockout mice lacking steroidogenic factor 1 are a novel genetic model of hypothalamic obesity. Endocrinology *143*, 607-614.

Marsh, D. J., *et al*. (1998). Role of the Y5 neuropeptide Y receptor in feeding and obesity. Nat Med *4*, 718-721.

Marsh, D. J., *et al*. (1999). Effects of neuropeptide Y deficiency on hypothalamic agouti-related protein expression and responsiveness to melanocortin analogues. Brain Res *848*, 66-77.

Marsh, D. J., *et al*. (2002). Melanin-concentrating hormone 1 receptor-deficient mice are lean, hyperactive, and hyperphagic and have altered metabolism. Proc Natl Acad Sci U S A *99*, 3240-3245.

Mercer, J. G., *et al*. (1996a). Coexpression of leptin receptor and preproneuropeptide Y mRNA in arcuate nucleus of mouse hypothalamus. J Neuroendocrinol *8*, 733-735.

Mercer, J. G., *et al*. (1996b). Localization of leptin receptor mRNA and the long form splice variant (Ob-Rb) in mouse hypothalamus and adjacent brain regions by in situ hybridization. FEBS Lett *387*, 113-116.

Miki, T., *et al*. (2001). ATP-sensitive K+ channels in the hypothalamus are essential for the maintenance of glucose homeostasis. Nat Neurosci *4*, 507-512.

Moran, T. H. (2000). Cholecystokinin and satiety: current perspectives. Nutrition *16*, 858-865.

Munzberg, H., *et al*. (2003). Role of signal transducer and activator of transcription 3 in regulation of hypothalamic proopiomelanocortin gene expression by leptin. Endocrinology *144*, 2121-2131.

Nakazato, M., *et al*. (2001). A role for ghrelin in the central regulation of feeding. Nature *409*, 194-198.

Naveilhan, P., *et al*. (2001). Neuropeptide Y alters sedation through a hypothalamic Y1-mediated mechanism. Eur J Neurosci *13*, 2241-2246.

Naveilhan, P., *et al*. (1999). Normal feeding behavior, body weight and leptin response require the neuropeptide Y Y2 receptor. Nat Med *5*, 1188-1193.

Naveilhan, P., *et al*. (1998). Complementary and overlapping expression of Y1, Y2 and Y5 receptors in the developing and adult mouse nervous system. Neuroscience *87*, 289-302.

Neel, J. V. (1999). The "thrifty genotype" in 1998. Nutr Rev *57*, S2-9.

Niswender, K. D., *et al*. (2001). Intracellular signalling. Key enzyme in leptin-induced anorexia. Nature *413*, 794-795.

Novak, C. M., *et al*. (2005). Caloric restriction and physical activity in zebrafish (Danio rerio). Neurosci Lett *383*, 99-104.

Okada, K., *et al*. (1996). Intracerebroventricular administration of the growth hormone-releasing peptide KP-102 increases food intake in free-feeding rats. Endocrinology *137*, 5155-5158.

Ollmann, M. M., *et al*. (1997). Antagonism of central melanocortin receptors in vitro and in vivo by agouti-related protein. Science *278*, 135-138.

Pedrazzini, T. (2004). Importance of NPY Y1 receptor-mediated pathways: assessment using NPY Y1 receptor knockouts. Neuropeptides *38*, 267-275.

Qian, S., *et al*. (2002). Neither agouti-related protein nor neuropeptide Y is critically required for the regulation of energy homeostasis in mice. Mol Cell Biol *22*, 5027-5035.

Qu, D., *et al*. (1996). A role for melanin-concentrating hormone in the central regulation of feeding behaviour. Nature *380*, 243-247.

Rizk, N. M., *et al*. (1998). Hypothalamic expression of neuropeptide-Y in the New Zealand obese mouse. Int J Obes Relat Metab Disord *22*, 1172-1177.

Roseberry, A. G., *et al.* (2004). Neuropeptide Y-mediated inhibition of proopiomelanocortin neurons in the arcuate nucleus shows enhanced desensitization in ob/ob mice. Neuron *41*, 711-722.

Rosenbaum, M., *et al.* (2005). Low-dose leptin reverses skeletal muscle, autonomic, and neuroendocrine adaptations to maintenance of reduced weight. J Clin Invest *115*, 3579-3586.

Sainsbury, A., *et al.* (2003). Synergistic effects of Y2 and Y4 receptors on adiposity and bone mass revealed in double knockout mice. Mol Cell Biol *23*, 5225-5233.

Sainsbury, A., *et al.* (2002a). Important role of hypothalamic Y2 receptors in body weight regulation revealed in conditional knockout mice. Proc Natl Acad Sci U S A *99*, 8938-8943.

Sainsbury, A., *et al.* (2002b). Y2 receptor deletion attenuates the type 2 diabetic syndrome of ob/ob mice. Diabetes *51*, 3420-3427.

Sainsbury, A., *et al.* (2002c). Y4 receptor knockout rescues fertility in ob/ob mice. Genes Dev *16*, 1077-1088.

Sakurai, T., *et al.* (1998). Orexins and orexin receptors: a family of hypothalamic neuropeptides and G protein-coupled receptors that regulate feeding behavior. Cell *92*, 1 page following 696.

Saladin, R., *et al.* (1995). Transient increase in obese gene expression after food intake or insulin administration. Nature *377*, 527-529.

Saper, C. B., *et al.* (1976). Direct hypothalamo-autonomic connections. Brain Res *117*, 305-312.

Sawchenko, P. E. (1998). Toward a new neurobiology of energy balance, appetite, and obesity: the anatomists weigh in. J Comp Neurol *402*, 435-441.

Schoeller, D. A. (2001). The importance of clinical research: the role of thermogenesis in human obesity. Am J Clin Nutr *73*, 511-516.

Schwartz, M. W., *et al.* (1998). Effect of fasting and leptin deficiency on hypothalamic neuropeptide Y gene transcription in vivo revealed by expression of a lacZ reporter gene. Endocrinology *139*, 2629-2635.

Schwartz, M. W., and Morton, G. J. (2002). Obesity: keeping hunger at bay. Nature *418*, 595-597.

Schwartz, M. W., *et al.* (1996). Identification of targets of leptin action in rat hypothalamus. J Clin Invest *98*, 1101-1106.

Segal-Lieberman, G., *et al.* (2003a). Melanin-concentrating hormone is a critical mediator of the leptin-deficient phenotype. Proc Natl Acad Sci U S A *100*, 10085-10090.

Segal-Lieberman, G., *et al.* (2003b). NPY ablation in C57BL/6 mice leads to mild obesity and to an impaired refeeding response to fasting. Am J Physiol Endocrinol Metab *284*, E1131-1139.

Shimada, M., *et al.* (1998). Mice lacking melanin-concentrating hormone are hypophagic and lean. Nature *396*, 670-674.

Shimizu-Albergine, M., *et al.* (2001). Downregulation of fasting-induced cAMP response element-mediated gene induction by leptin in neuropeptide Y neurons of the arcuate nucleus. J Neurosci *21*, 1238-1246.

Sternson, S. M., *et al.* (2005). Topographic mapping of VMH --> arcuate nucleus microcircuits and their reorganization by fasting. Nat Neurosci *8*, 1356-1363.

Swanson, L. W., and Kuypers, H. G. (1980). The paraventricular nucleus of the hypothalamus: cytoarchitectonic subdivisions and organization of projections to the pituitary, dorsal vagal complex, and spinal cord as demonstrated by retrograde fluorescence double-labeling methods. J Comp Neurol *194*, 555-570.

Tannenbaum, G. S., *et al*. (2003). Interrelationship between the novel peptide ghrelin and somatostatin/growth hormone-releasing hormone in regulation of pulsatile growth hormone secretion. Endocrinology *144*, 967-974.

Tannenbaum, G. S., *et al*. (1998). Expression of growth hormone secretagogue-receptors by growth hormone-releasing hormone neurons in the mediobasal hypothalamus. Endocrinology *139*, 4420-4423.

Tartaglia, L. A. (1997). The leptin receptor. J Biol Chem *272*, 6093-6096.

Tartaglia, L. A., *et al*. (1995). Identification and expression cloning of a leptin receptor, OB-R. Cell *83*, 1263-1271.

Torsello, A., *et al*. (1998). Novel hexarelin analogs stimulate feeding in the rat through a mechanism not involving growth hormone release. Eur J Pharmacol *360*, 123-129.

Treier, M., and Rosenfeld, M. G. (1996). The hypothalamic-pituitary axis: co-development of two organs. Curr Opin Cell Biol *8*, 833-843.

Tschop, M., *et al*. (2000). Ghrelin induces adiposity in rodents. Nature *407*, 908-913.

Tschop, M., *et al*. (2002). GH-releasing peptide-2 increases fat mass in mice lacking NPY: indication for a crucial mediating role of hypothalamic agouti-related protein. Endocrinology *143*, 558-568.

Vaisse, C., *et al*. (1998). A frameshift mutation in human MC4R is associated with a dominant form of obesity. Nat Genet *20*, 113-114.

Vaisse, C., *et al.* (1996). Leptin activation of Stat3 in the hypothalamus of wild-type and ob/ob mice but not db/db mice. Nat Genet *14*, 95-97.

Vrang, N., *et al.* (1999). Neurochemical characterization of hypothalamic cocaine-amphetamine-regulated transcript neurons. J Neurosci *19*, RC5.

Wald, G., and Jackson, B. (1944). Activity and Nutritional Deprivation. Proc Natl Acad Sci U S A *30*, 255-263.

Weigle, D. S. (1994). Appetite and the regulation of body composition. Faseb J *8*, 302-310.

Wilding, J. P., *et al.* (1993). Increased neuropeptide-Y messenger ribonucleic acid (mRNA) and decreased neurotensin mRNA in the hypothalamus of the obese (ob/ob) mouse. Endocrinology *132*, 1939-1944.

Willesen, M. G., *et al.* (1999). Co-localization of growth hormone secretagogue receptor and NPY mRNA in the arcuate nucleus of the rat. Neuroendocrinology *70*, 306-316.

Willie, J. T., *et al.* (2001). To eat or to sleep? Orexin in the regulation of feeding and wakefulness. Annu Rev Neurosci *24*, 429-458.

Woods, S. C., *et al.* (1998). Signals that regulate food intake and energy homeostasis. Science *280*, 1378-1383.

Wortley, K. E., *et al.* (2005). Agouti-related protein-deficient mice display an age-related lean phenotype. Cell Metab *2*, 421-427.

Yamamoto, H., *et al.* (2002). Glucagon-like peptide-1 receptor stimulation increases blood pressure and heart rate and activates autonomic regulatory neurons. J Clin Invest *110*, 43-52.

Yaswen, L., *et al*. (1999). Obesity in the mouse model of pro-opiomelanocortin deficiency responds to peripheral melanocortin. Nat Med *5*, 1066-1070.

Yen, T. T., *et al*. (1994). Obesity, diabetes, and neoplasia in yellow A(vy)/- mice: ectopic expression of the agouti gene. Faseb J *8*, 479-488.

Zabolotny, J. M., *et al*. (2002). PTP1B regulates leptin signal transduction in vivo. Dev Cell *2*, 489-495.

Zeyda, T., *et al*. (2001). Impairment in motor learning of somatostatin null mutant mice. Brain Res *906*, 107-114.

Zhang, Y., *et al*. (1994). Positional cloning of the mouse obese gene and its human homologue. Nature *372*, 425-432.

Zhao, A. Z., *et al*. (2002). A phosphatidylinositol 3-kinase phosphodiesterase 3B-cyclic AMP pathway in hypothalamic action of leptin on feeding. Nat Neurosci *5*, 727-728.

Zhou, Q. Y., and Palmiter, R. D. (1995). Dopamine-deficient mice are severely hypoactive, adipsic, and aphagic. Cell *83*, 1197-1209.

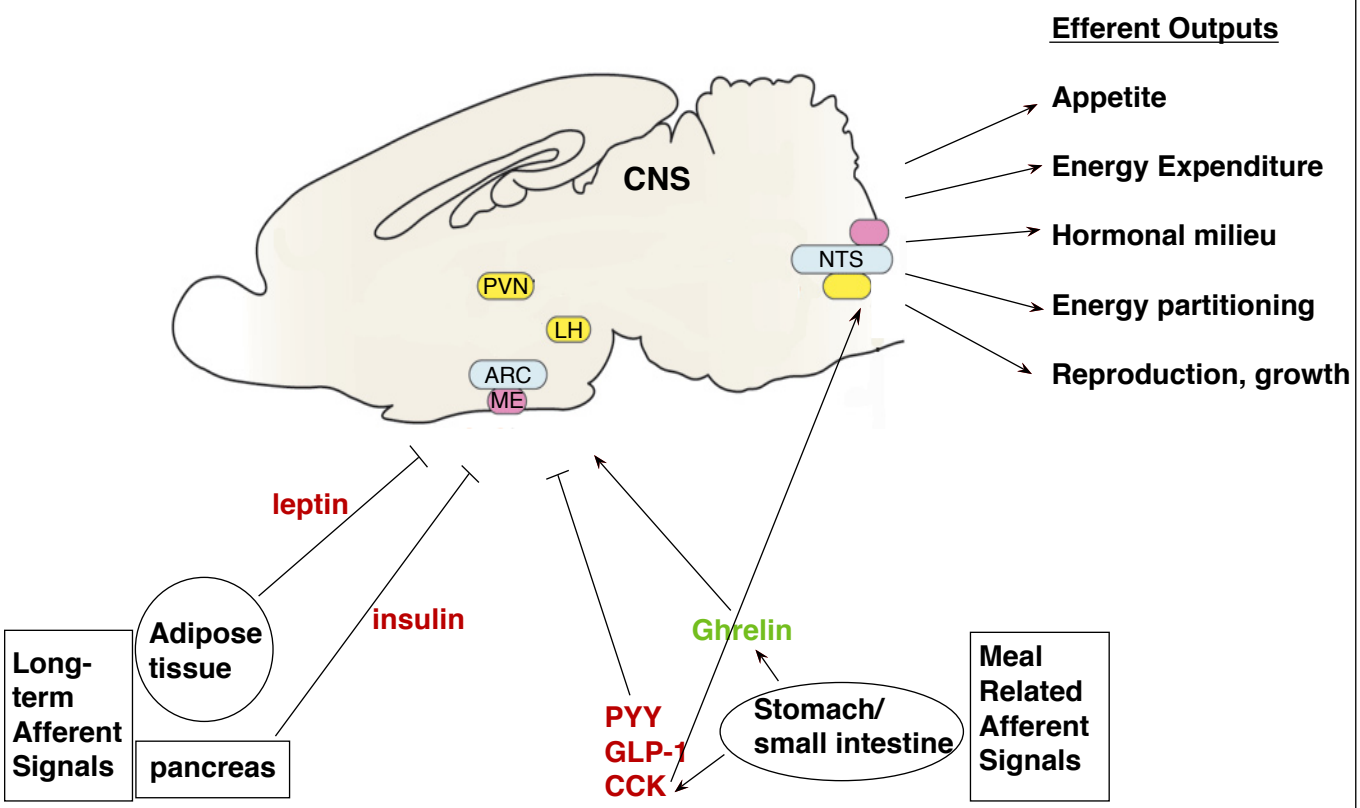

Figure 1.1 Schematic representation of the main components that regulate energy balance. The afferent system involves long-term signals responsible for maintaining fat stores and body weight in long intervals. These signals include leptin and insulin secreted from the adipose tissue and the pancreas respectively. Meal related short -term signals involved in meal initiation and satiety induction. Meal related signals include ghrelin, a feeding stimulator secreted from cells of the gastrointestinal tract and peptide YY (PYY), cholecystokinin (CCK), glucagon like peptide (GLP)-1 secreted postprandially from the intestin and promote satiety. Hypothalamus primarily and other brain structures in a second order integrate these inputs from the periphery and regulate accordingly to the energy stores of the body, appetite, energy expenditure, hormonal milieu, energy partitioning and reproduction, growth. (Adapted by Flier,JS, Cell, 2004)

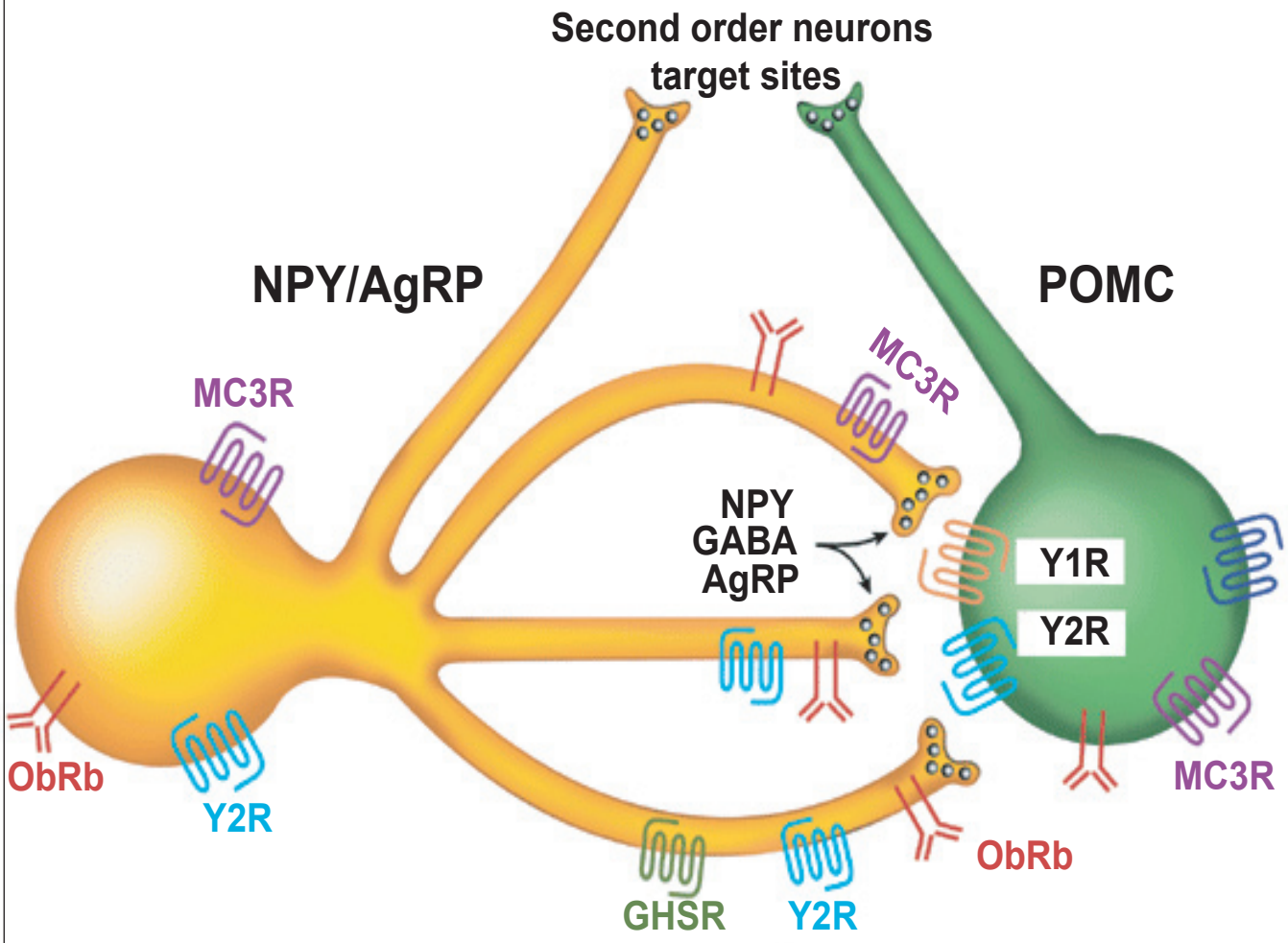

Figure 1.2 Neuronal circuitry in the arcuate nucleus of hypothlamus. Orexigenic NPY/AgRP neurons and anorexigenic POMC express a large number of receptors in order to sense hormones and peptides from the periphery known to modulate the network activity and gene expression. The two neuronal populations coordinate their opposites activities since dense inhibitory NPY/AgRP fibers containing the neurotransmitter GABA project to POMC cell body. The receptors indicated are, ObRb, leptin receptor; Y2R, type 2 NPY receptor; Y1R, type 1 NPY receptor; MC3R, melanocortin 3 receptor. (Figure adapted by Cone RD;2005)

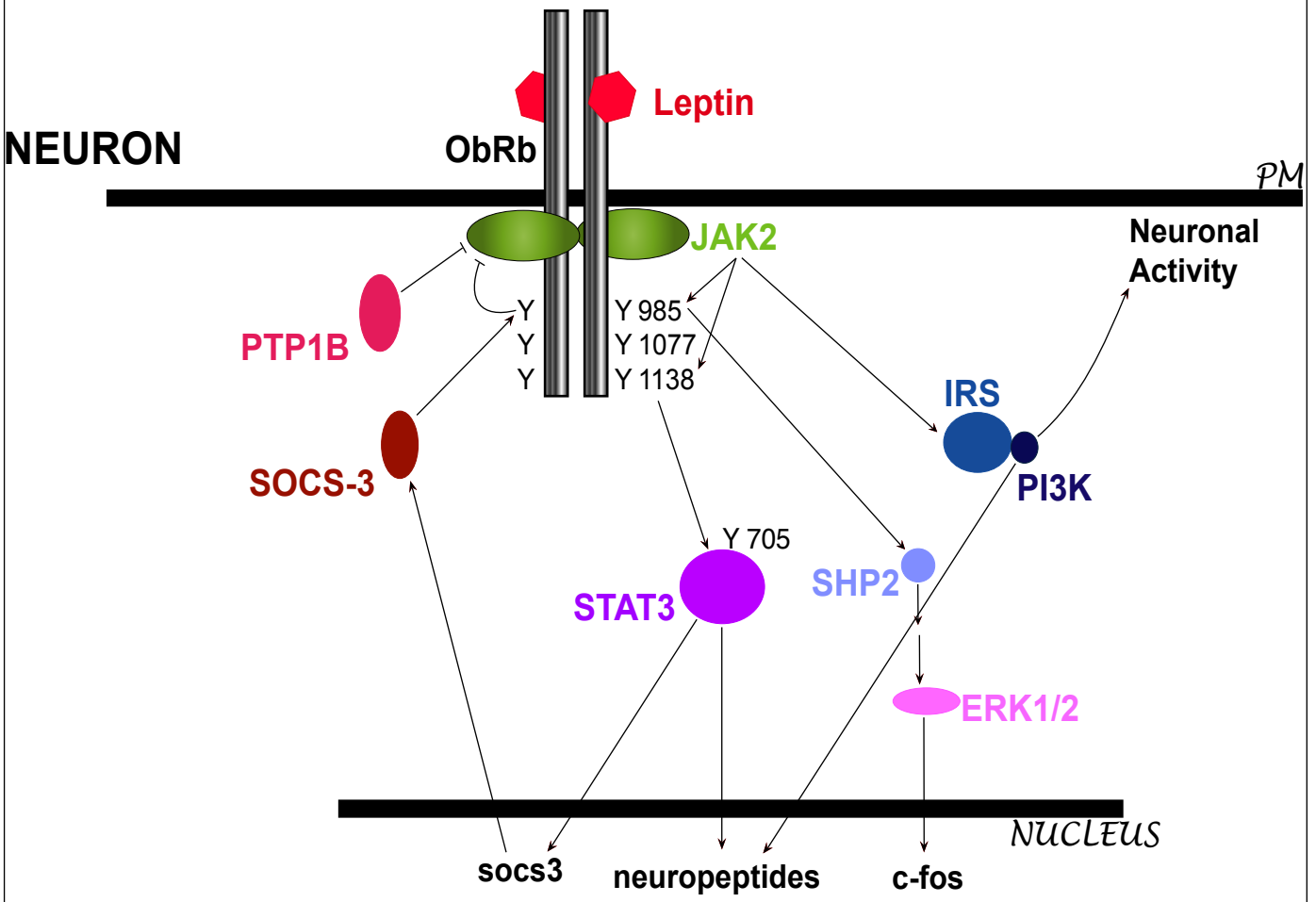

Figure 1.3 ObRb signaling. Leptin binding on the ObRb isoform activates ObRb associated Janus activating Kinase 2 (JAK2) tyrosine kinase, leading to autophosphorylation of tyrosine residues on JAK2 and the phosphorylation of Y 985 and Y 1138 on the intracellular tail of the ObRb. Although signaling by phosphorylation sites on JAK2 remains to be identified, JAK2 activate insulin receptor substrate-phosphoinositol 3 kinase (IRS-PI3K) signaling pathway. Phosphorylation of Y 1138 mediates the phosphorylation and activation of the transcription factor STAT3 which dimerize in the cytoplasm and translocate in the nucleus where it activates transcription. Among other targets, activated STAT3 induces suppressor of cytokine signaling (socs3). Y 985 provides a binding site for both SHP2 and SOCS3 which can also bind with lower affinity on JAK2. SOCS3 by binding on the ObRb-JAK2 complex suppresses ObRb signaling. Protein tyrosine phosphatase (PTP) 1B is a second negativeregulator of ObRb signaling via interaction with JAK2. SH2 domain phosphotyrosine phosphatase (SHP2) is activated via binding on the Y 985 and is an important component for activating extracellular signal-regulated kinase (ERK1/2) and c-fosinduction in the neuron.

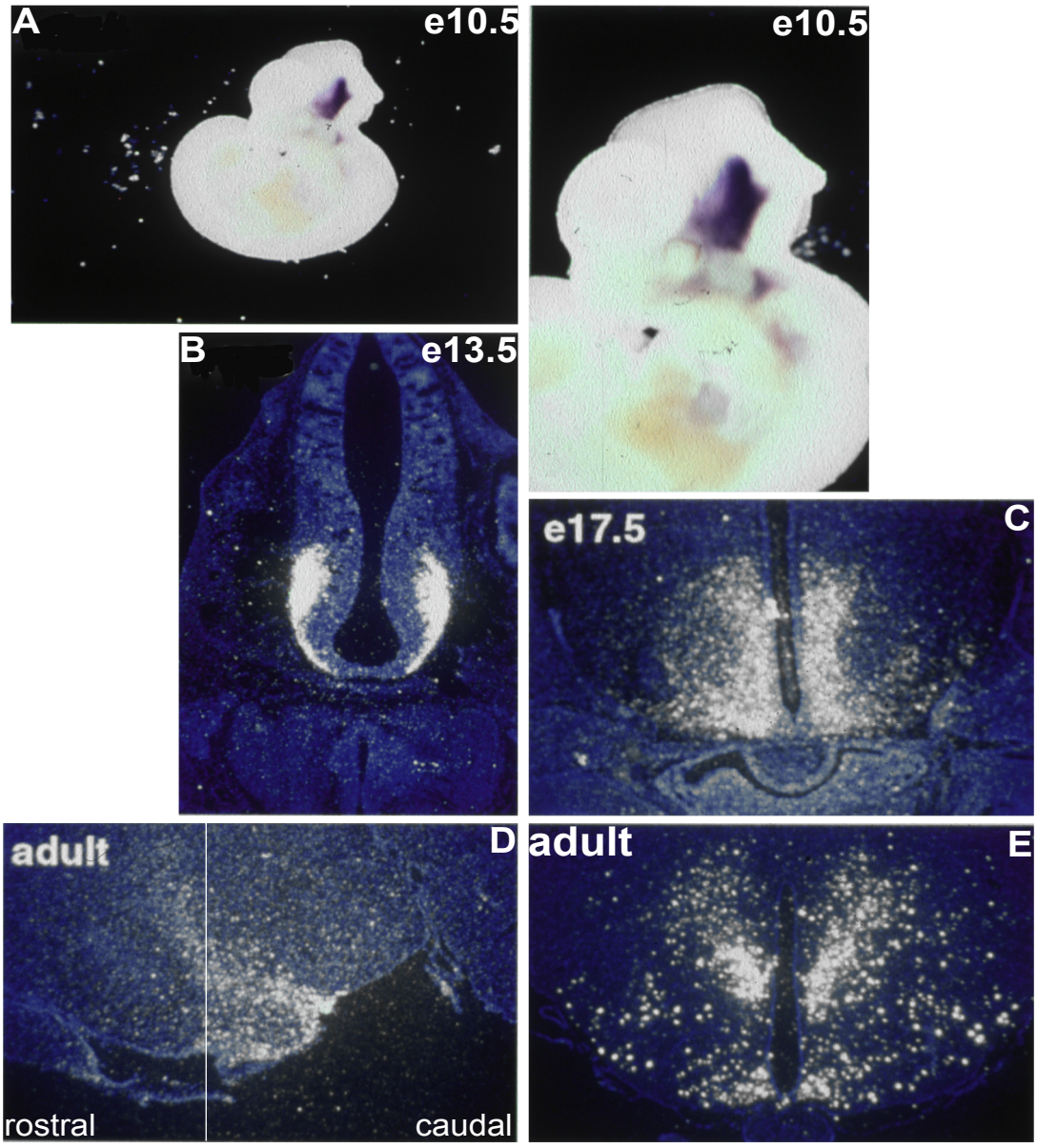

Figure 2.1.1 *Bsx* expression pattern throughout development and adultood in mouse. Whole mount In situ hybridization for *Bsx* on mouse at embyonic day e10.5 (A). ^{35}S-in situ hybridization for Bsx on transversal section from mouse at e13.5 (B) and on coronal brain section from mouse at e17.5 (C). ^{35}S-in situ hybridization on sagittal (D) and coronal (E) brain sections of adult mouse. The coronal section of the panel E is at the level depicted by the white level in the panel D.

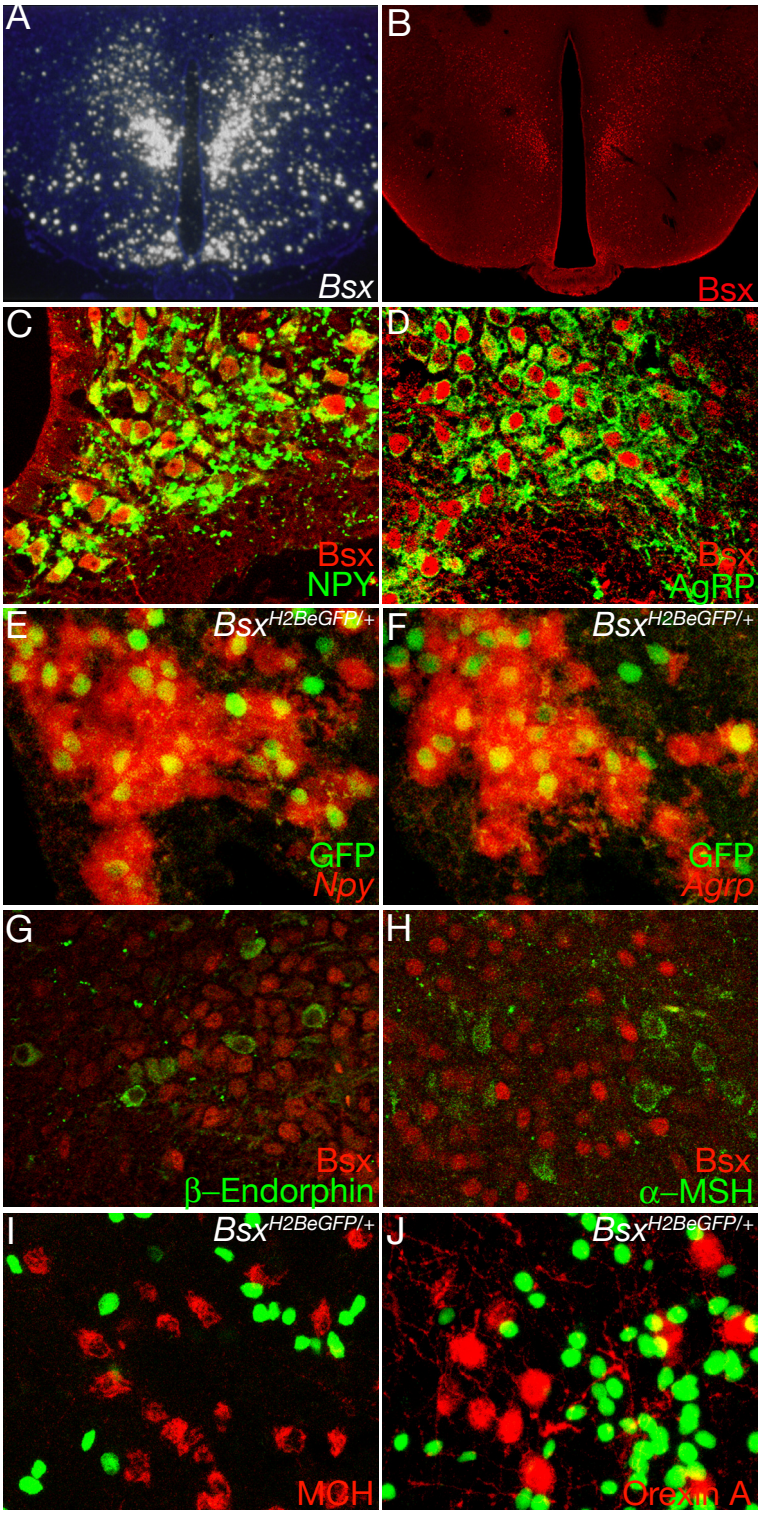

Figure 2.2.1 Bsx is colocalized within the NPY/AgRP but not the POMC expressing neurons Bsx expression in the arcuate nucleus in the adult mouse brain visualized by (A) ^{35}S-in situ hybridization with a *Bsx* probe and (B) immunohistochemistry with a rabbit Bsx antibody. Single layer confocal images of double immunofluorescence stainings on coronal brain sections from colchicine treated 9 weeks old wild type mice with (C) Bsx and NPY, (D) Bsx anf AgRP, (G) Bsx and β–endorphin, (H) Bsx and α–MSH antibodies detects Bsx expression in NPY/AgRP neurons in the arcuate nucleus. Confocal projections of double in situ/immuofluorescence analysis of (E) *Npy* mRNA or (F) *Agrp* mRNA and GFP protein on coronal brain sections from 9 week old heterozygote *Bsx*$^{H2BeGFP/+}$ mice. Confocal projections of immunofluorescence staining with (I) MCH and (J) Orexin antibodies on coronal brain sections from 9 weeks old heterozygote *Bsx*$^{H2BeGFP/+}$ mice.

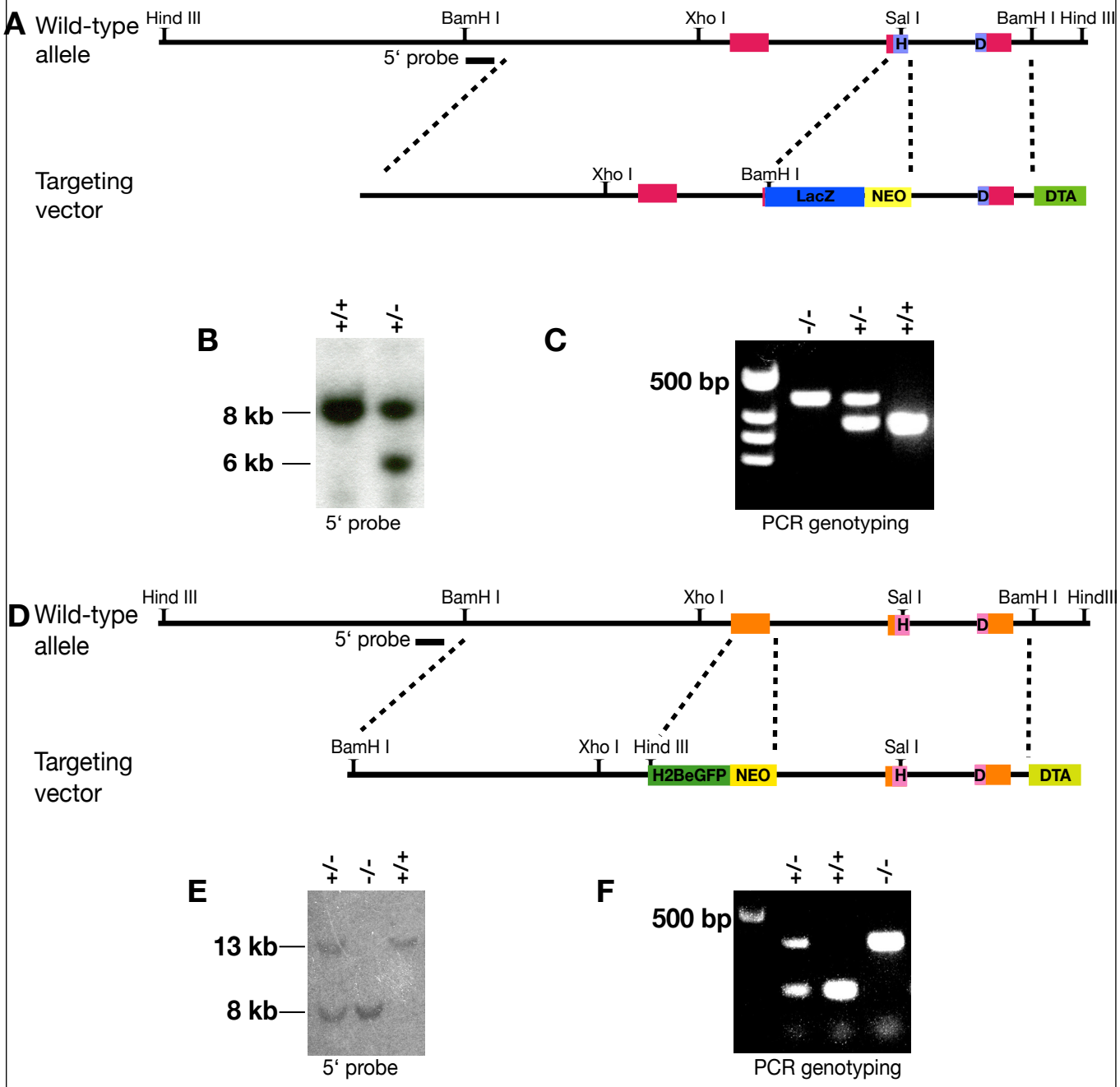

Figure 2.2.2 Generation of *Bsx*^{lacZ} allele (A) *Bsx*^{lacZ} allele was generated by fusing the *lacZ* coding sequence in frame with the *Bsx* ORF and replacing the second exon of *Bsx* that encodes the helix 1 and 2 of the homeodomain. (B) Genomic DNA from targeted ES cells was digested with BamHI and probed with a 5' outside probe to detect homologous recmbination. (C) Genotyping was performed by PCR analysis using 3 primers one of them designed in the *lacZ* coding sequence in order to distinguish between a *wt* and a *lacZ* containing alleles. (D) *Bsx*^{H2BeGFP} allele was generated replacing exon 1 of *Bsx* starting at the ATG with a sequence coding for Histone2BeGFP. (E) Southern blot analysis of tail DNA digested with HindIII and probed with a 5' outside probe to detect homologous recombination. (F) PCR analysis was subsequently used for genotyping.

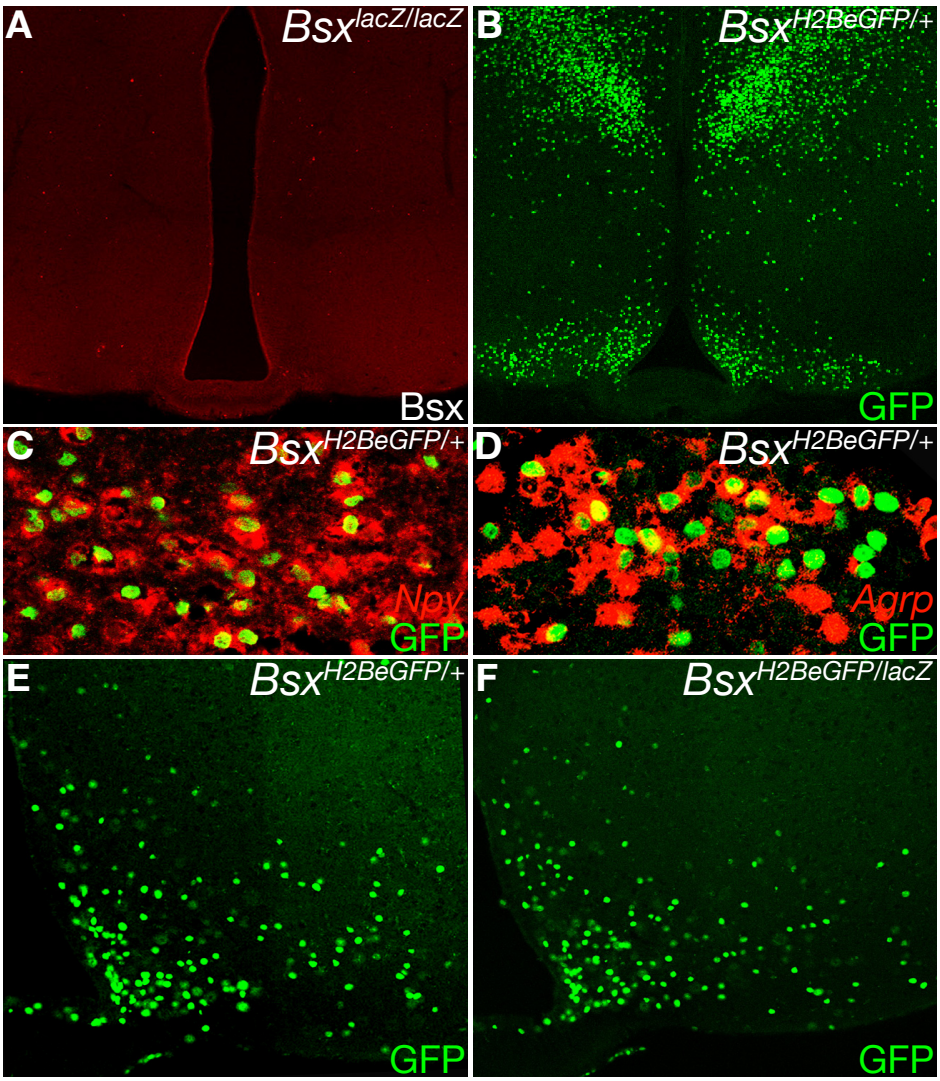

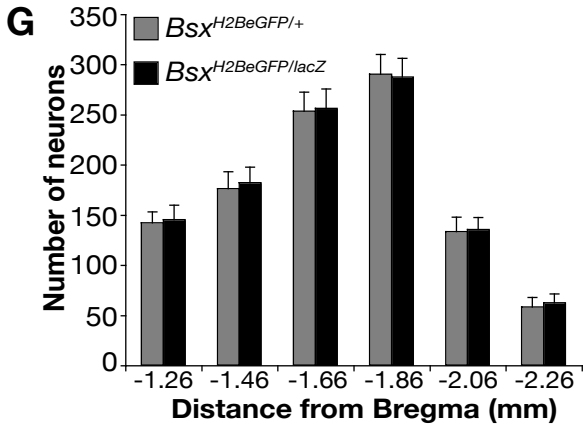

Figure 2.2.3 Bsx Knock out. The *Bsx*^{lacZ} allele is a null allele for Bsx since no staining could be detected with (A) Immunostaining with Bsx specific antibody raised against the C-terminus of the protein, on coronal mouse brain. (B) GFP emission from an heterozygote *Bsx*$^{H2BeGFP/+}$ on coronal brain section. Double in situ hybridization, immunohistochemistry for colocalization of (C) *Npy* and GFP and (D) *Agrp* and GFP. Comparison of GFP positive neurons between (E) *Bsx*$^{H2BeGFP/+}$ and (F) *Bsx*$^{H2BeGFP/H2BeGFP}$ coronal brain sections. Number of GFP positives neurons on coronal sections from *Bsx*$^{H2BeGFP/+}$ and *Bsx*$^{H2BeGFP/H2BeGFP}$ mice from rostral to caudal in the arcuate nucleus (G).

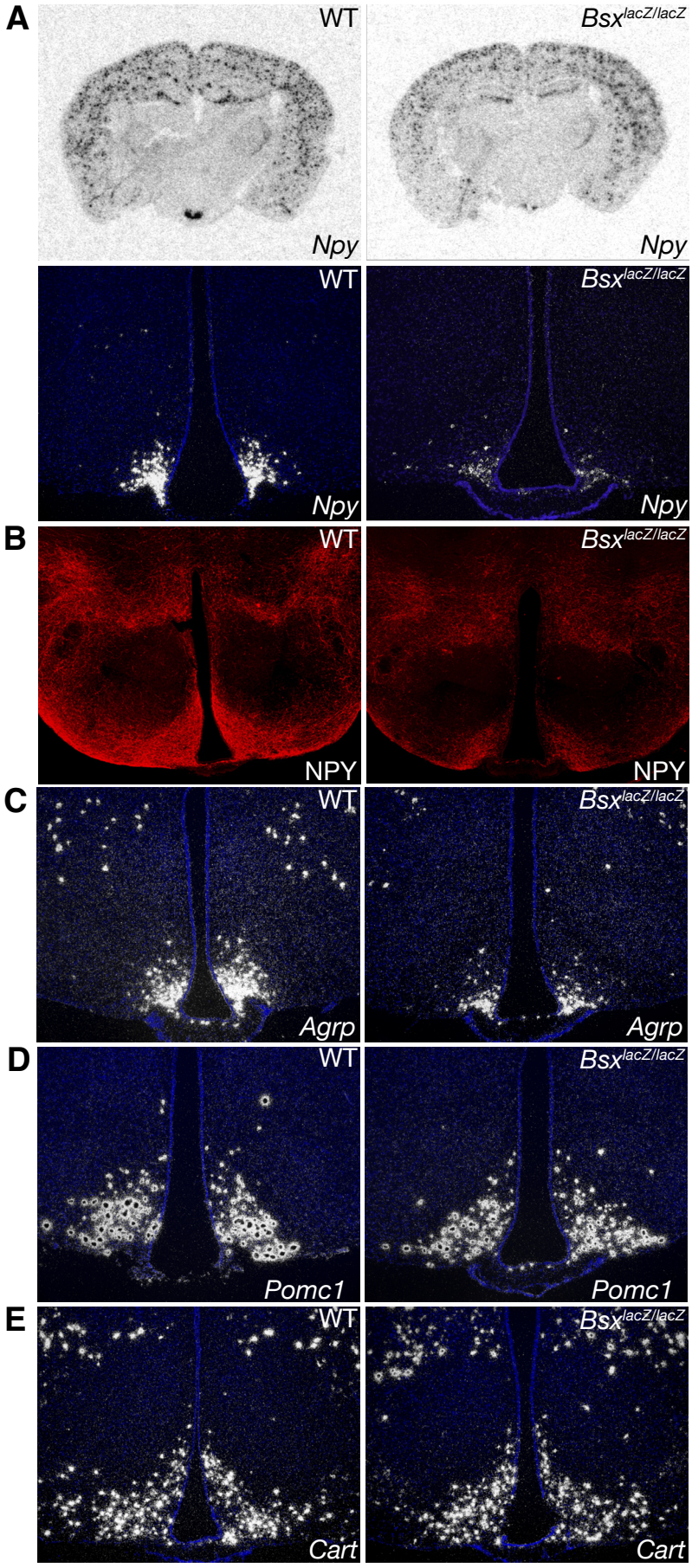

Figure 2.3.1 Bsx display strong down-regulation of *Npy* and *Agrp* expression levels in the Arc nucleus. Comparison of (A) *Npy* mRNA and (B) NPY protein expression detected by ^{35}S-in situ hybridization and immunohistochemistry analysis respectively, (C) *Agrp* mRNA (D) *Pomc1* mRNA and (E) *Cart* mRNA by ^{35}S-in situ hybridization between *Bsx*$^{lacZ/lacZ}$ and *wt* coronal brain sections from 9 weeks old mice.

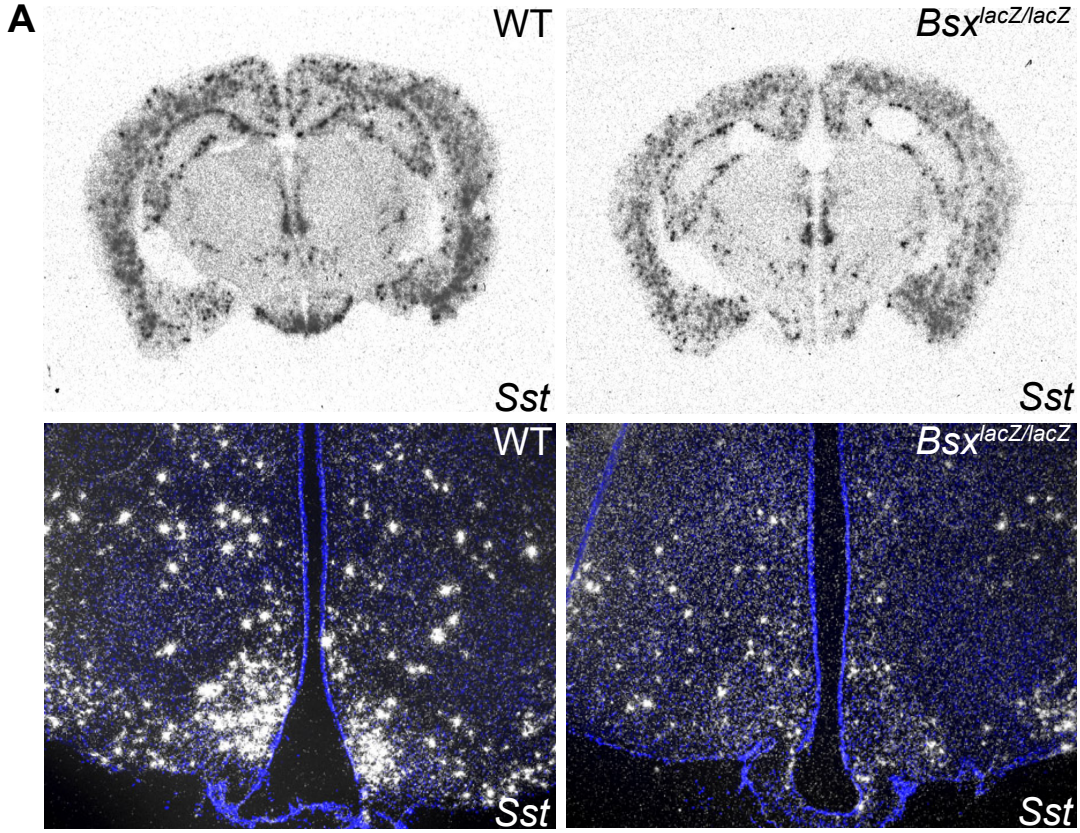

Figure 2.4.1 Bsx is required for Somatostatin expression. Quantitative ^{35}S-in situ hybridization for *Somatostatin* (*Sst*) on coronal wt and mutant brain sections from 9 weeks old wild type (wt) and *Bsx* mutant (*Bsx*$^{lacZ/lacZ}$) mice. (B). The upper panel is a scan of the film and the lower panel is a microscopic picture of the dipped slides.

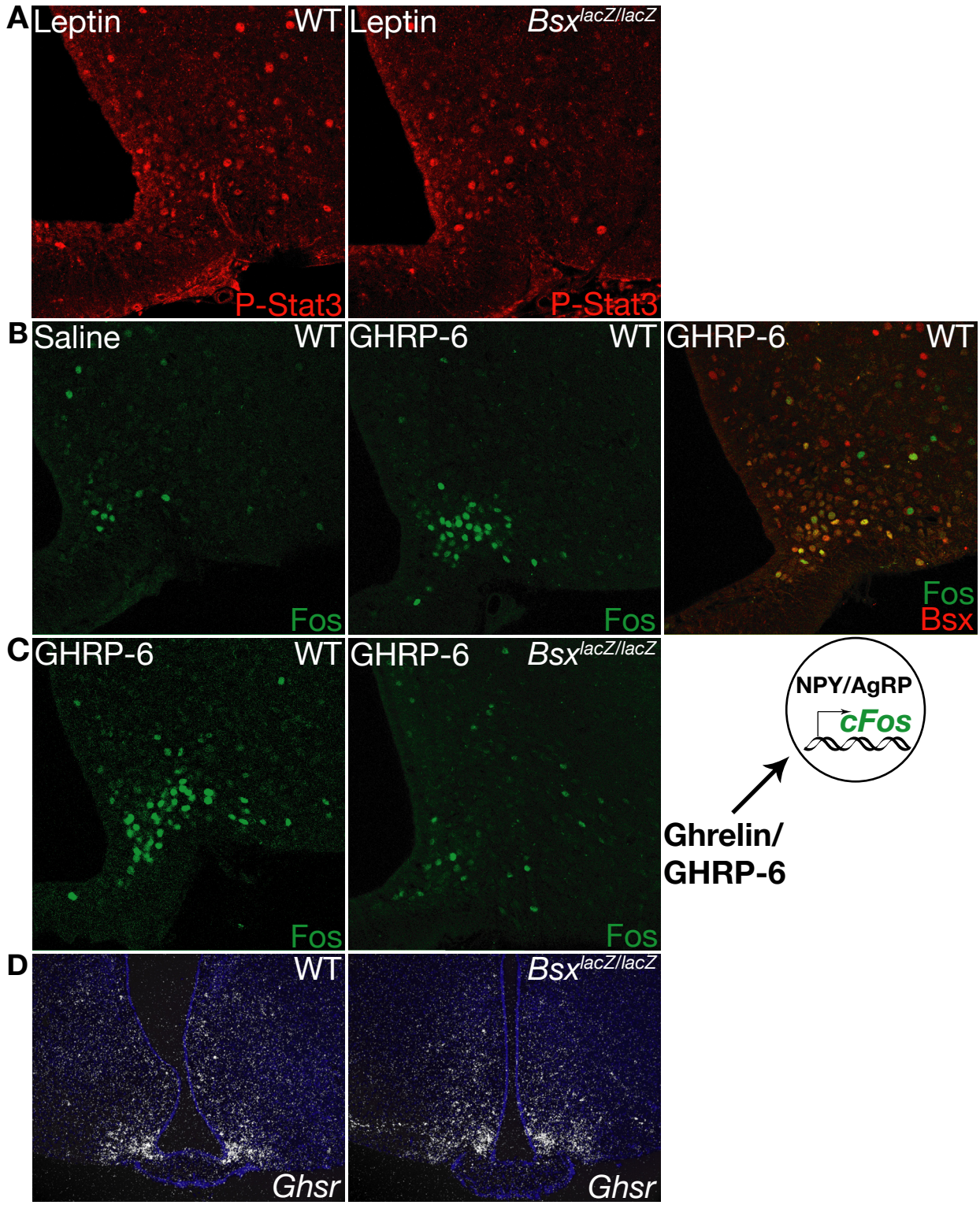

Figure 2.5.1 Leptin response in the arcuate nucleus of *Bsx*$^{lacZ/lacZ}$ mice is intact, whereas ghrelin reponse is abrogated. (A) P-STAT3 immunostaining on leptin administrated wt and *Bsx*$^{lacZ/lacZ}$ coronal brain sections from 9 weeks old mice. (B) Comparison of Fos immunostaining on brain coronal sections between saline and GHRP-6 administrated mice, and double immunostaining with Bsx and Fos antibodies on GHRP-6 administrated mice. (C) Comparison of Fos immunostaining between GHRP-6 administrated wt and *Bsx*$^{lacZ/lacZ}$ coronal brain sections. (D) ^{35}S-in situ hybridization on wt and *Bsx*$^{lacZ/lacZ}$ coronal brain sections from 9 weeks old mice for Ghrelin receptor *Ghsr* mRNA.

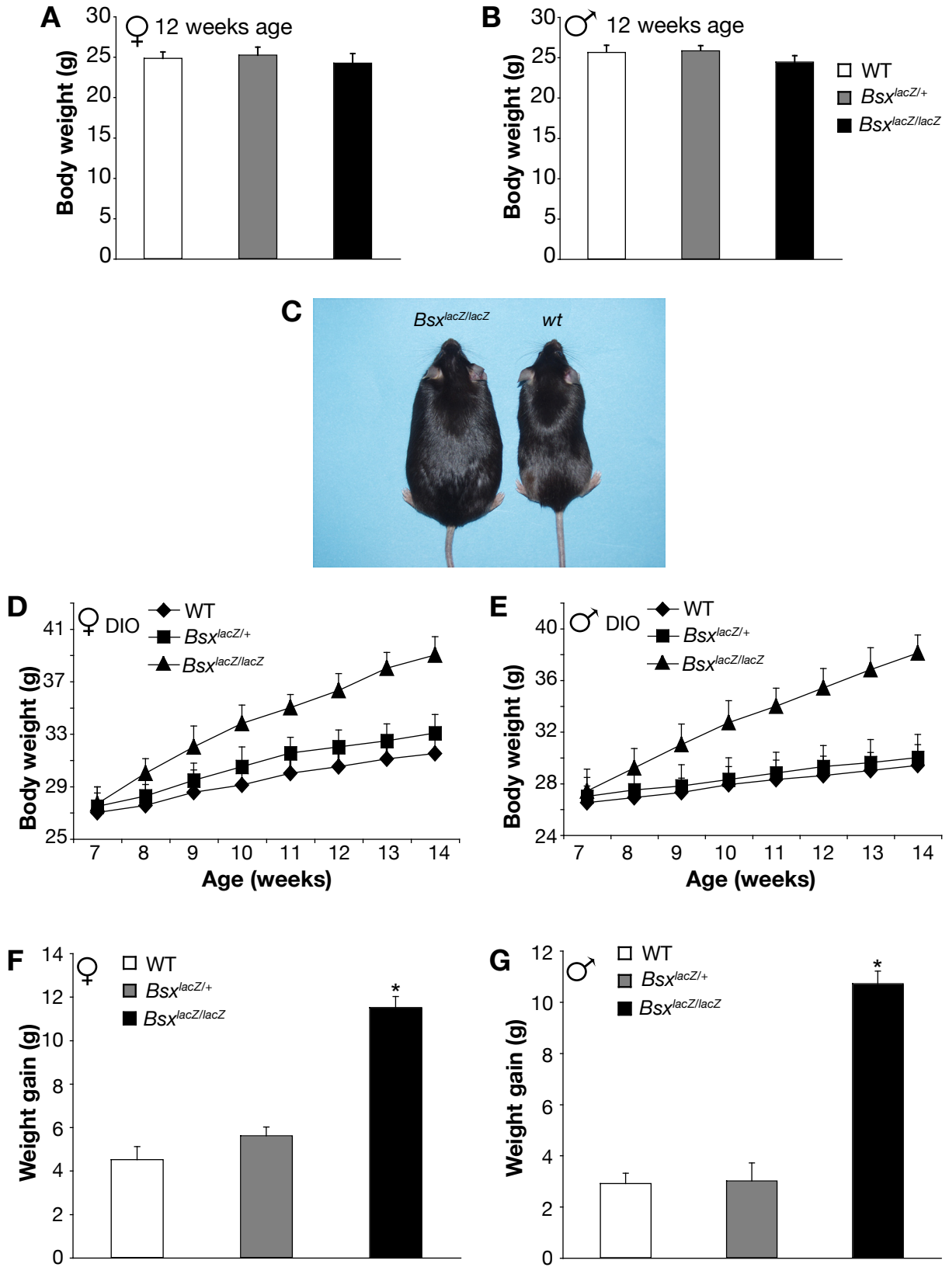

Figure 2.6.1 *Bsx*$^{lacZ/lacZ}$ mice develop Diet Induced obesity (DIO). Average body weight of females (A) and males (B) at 12 weeks of age. Physical appearance of two littermate mice *Bsx*$^{lacZ/lacZ}$ and wt after 14 weeks of highly fat diet(C). Weight curves traced by weekly monitoring of the body weight of mice fed with high fat diet from the age of 7 to 14 weeks old for both (D) females and (E) males. (F) Weight gain histograms in females and (G) males in the period of 7 weeks of high fat diet; n>20 for each genotype in both sexes, values represent mean ± SEM; *P<0.01.

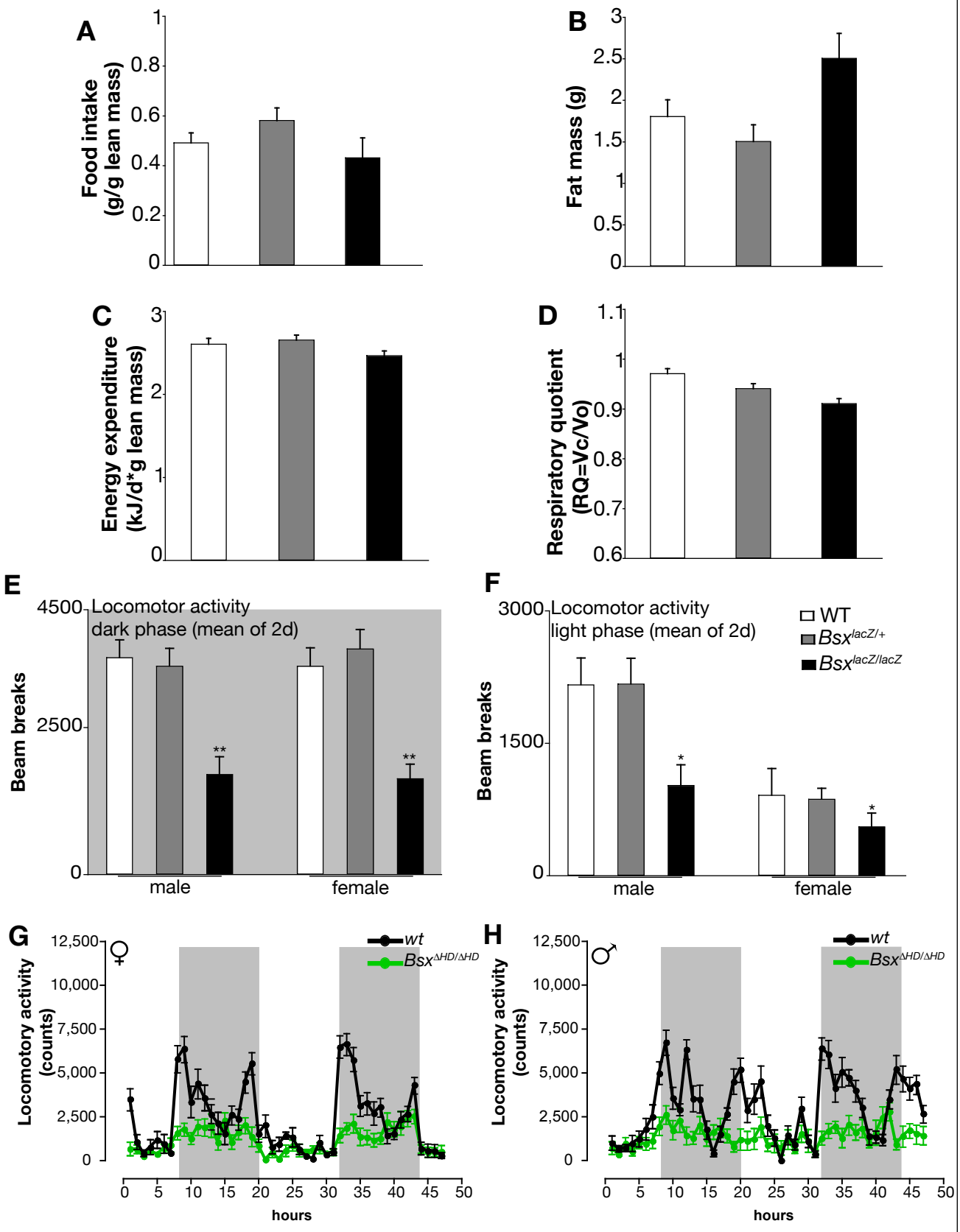

Figure 2.6.2 Physiological measurements and comparison between wt, BsxlacZ/+ and BsxlacZ/lacZ. (A) Food intake measured as the average of 2 days intake in g/g of lean mass in mice of al 3 genotypes in both sexes. (B) Fat mass measured by NMR analysis in mice of all 3 genotypes and sexes. (C and D) Energy expenditure and respiratory quotient measured for all three genotypes. (E-H) Locomotor activity measured as number of beam breaks in both males and females in the dark and light phase as average of 2 days measurements (E,F) or graphs with variations over these two days (G,H). For all the measurements n>15 for each genotype in both sexes, all the values are the mean ± SEM; *P<0.01, **P<0.001.

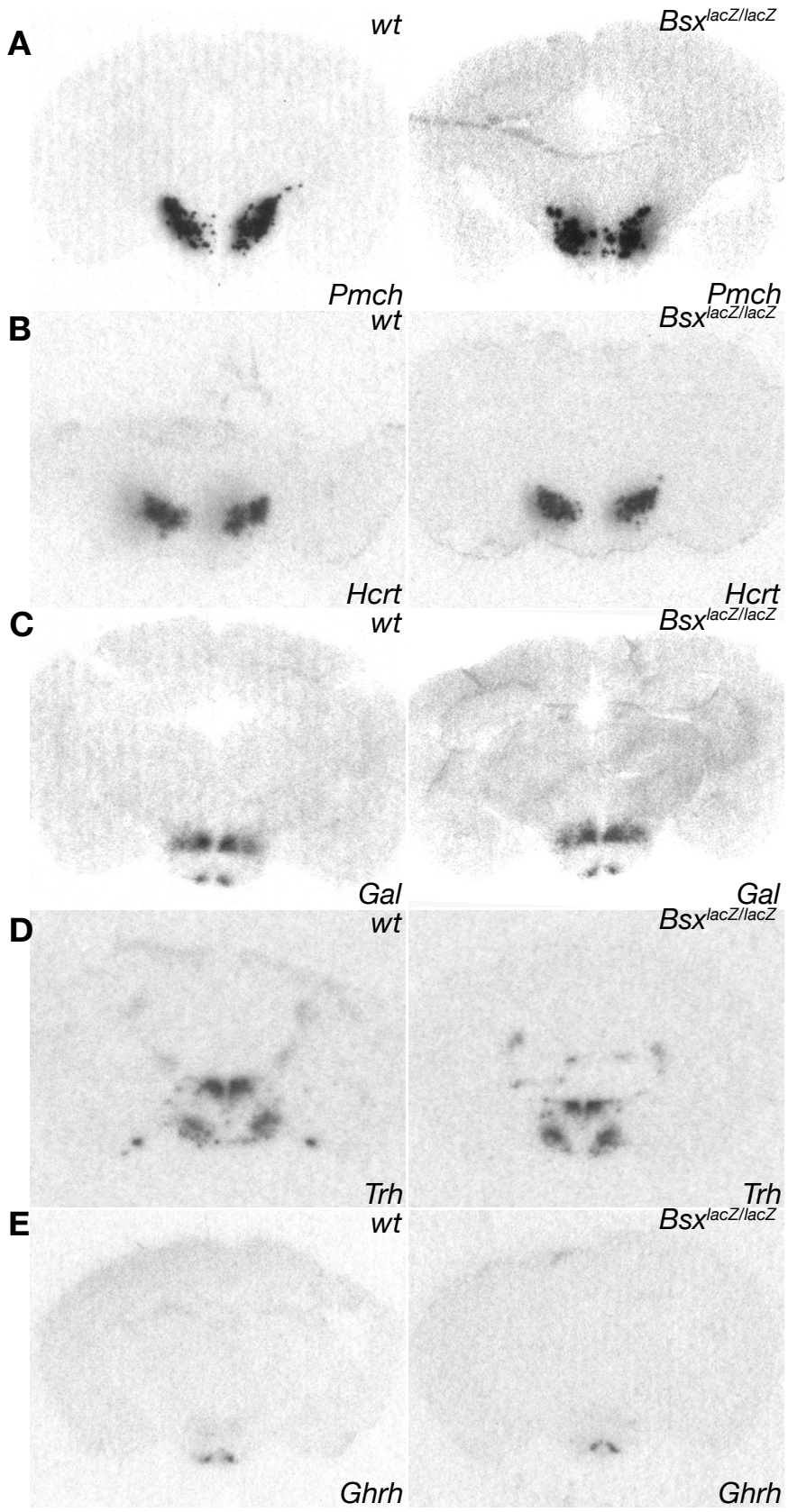

Figure 2.6.3 Expression patterns of neuropeptides expressed in the hypothalamus involved in the control of energy homeostasis. Expression levels of (A) melanocortin concentrating hormone, *Pmch* (B) hypocretin or orexin, *Hcrt* (C) galanin, *Gal* (D) thyrotropin-releasing hormone, *Trh* and (E) growth hormone-releasing hormone, *Ghrh*, are unchanged between wild type (wt) and *Bsx* mutant mice ($Bsx^{lacZ/lacZ}$) also demonstrating that the architecture of the hypothalamus in *Bsx* mutant mice is not affected.

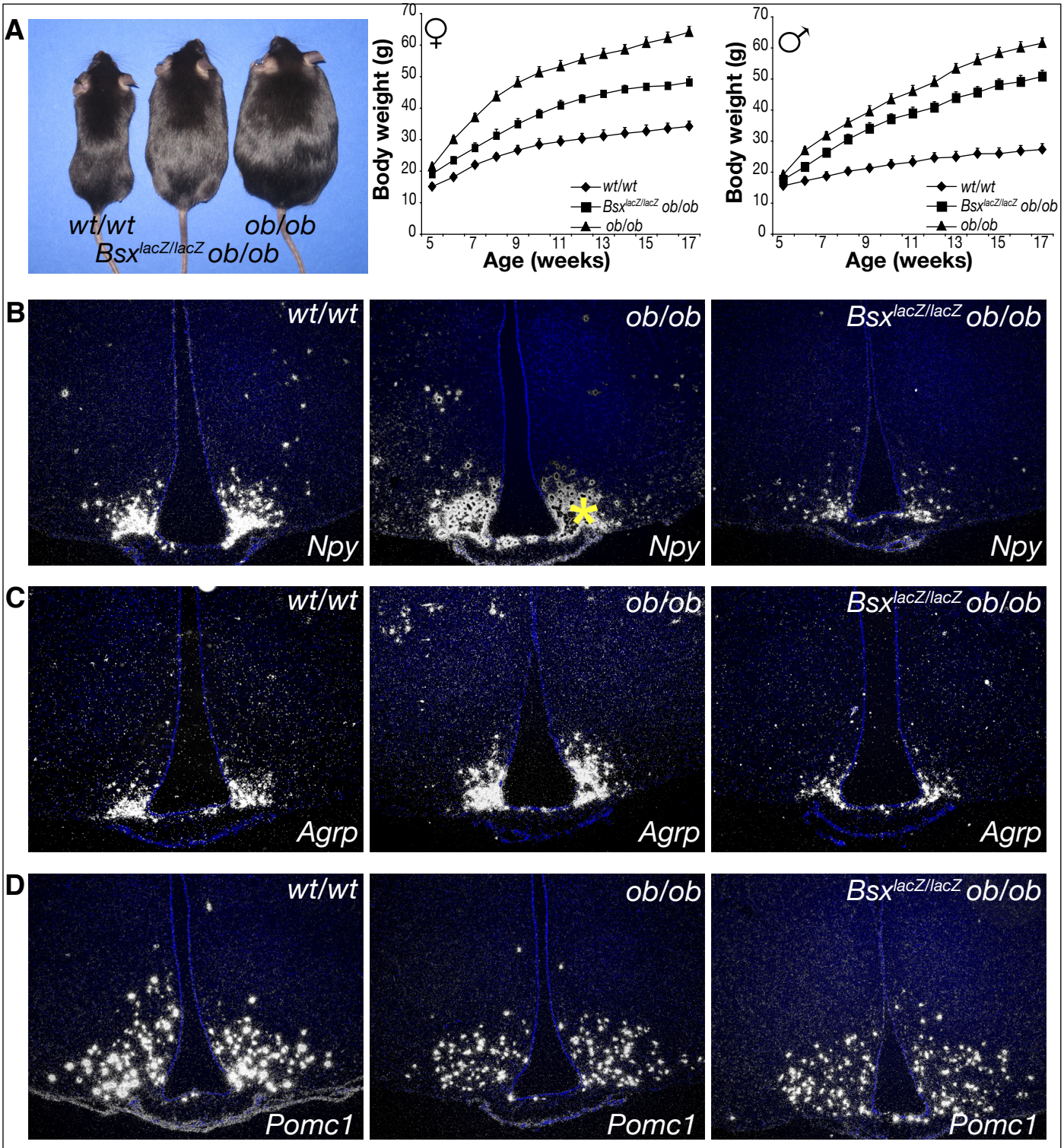

Figure 2.7.1 Compound mutant *Bsx*$^{lacZ/lacZ}$ *ob/ob* mice display attenuated obesity compared to *ob/ob* mice. (A) Physical appearance of wt mice, *ob/ob* mutant and double *Bsx*$^{lacZ/lacZ}$ *ob/ob* mice and weight curves of female and mice mice of the three genotypes traced by weekly monitoring of their body weight; n>15 for each genotype and in both females and males, values represent mean ±SEM. ^{35}S-in situ hybridization for (B) *Npy*, (C) *Agrp* and (D) *Pomc1* on coronal brain sections from 9 weeks old mice of all three genotypes. Slides probed with *Npy* and *Pomc1* probes were exposed for 21 days, *Agrp* incubated slides were exposed for 7 days in the developping emulsion. The asterix (*) in (B) marks the overexposed and hence black region due to high level *Npy* expression.

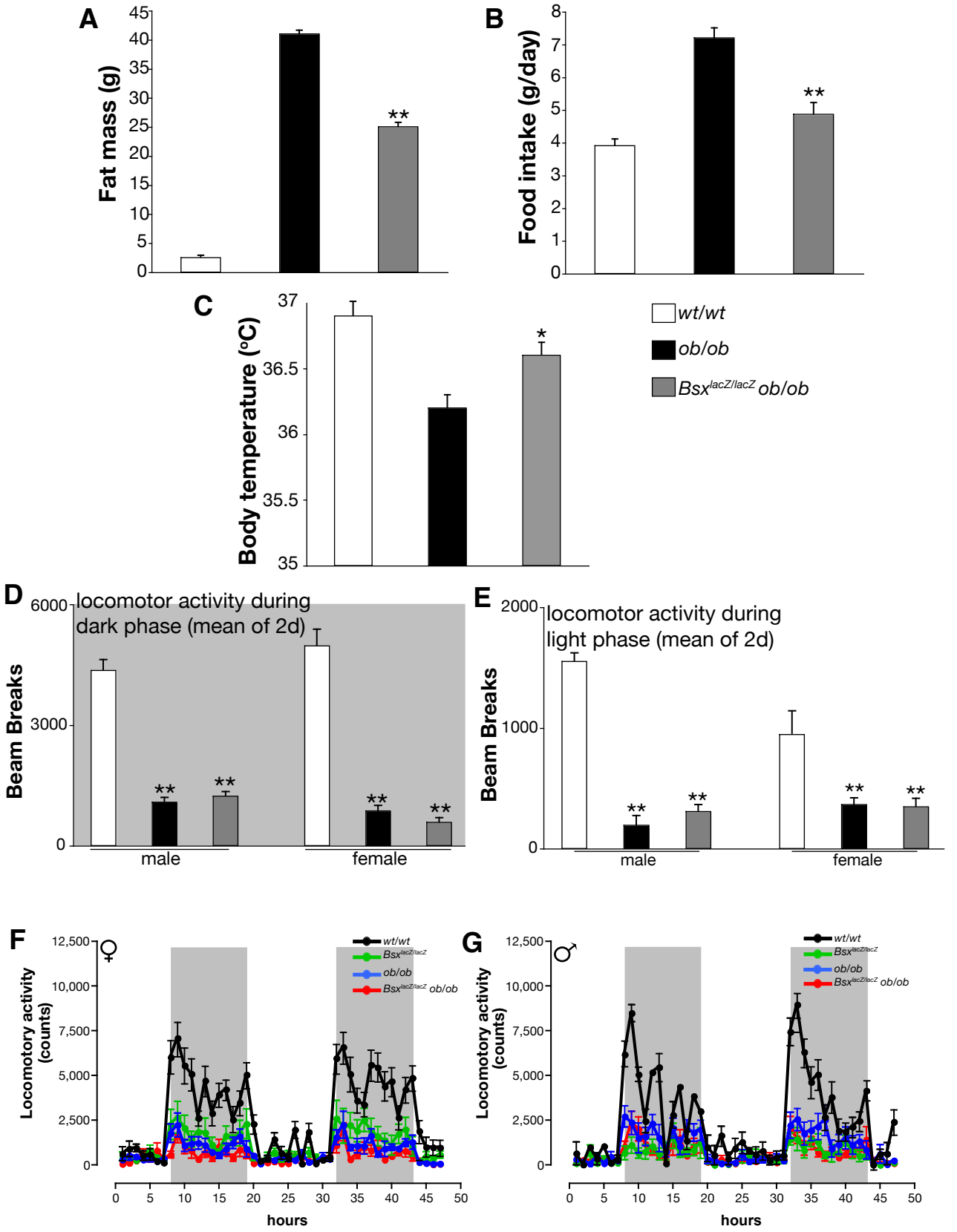

Figure 2.7.2 Physiological measurements of the compound *Bsx*$^{lacZ/lacZ}$ *ob/ob* and comparison with *wt/wt* and *ob/ob* mice. (A) Fat mass of the mice as measured by NMR at the age of 15 weeks;n>12 for each genotype, values represent mean ±SEM, **P<0.001. (B) Food intake measured over 2 days and averaged; n>15 for each genotype, values are the mean ± SEM, **P<0.001. (C) Body temperature as measured from mice of all three genotypes; n>15 for each genotype, values are the mean ±SEM, *P<0.01. (D, E, F, G) Locomotor activity calculated as the number of beam breaks in dark and light phase for both males and females, white represents the light pahse and grey the dark phase; n>15 for each genotype of both sexes, values are

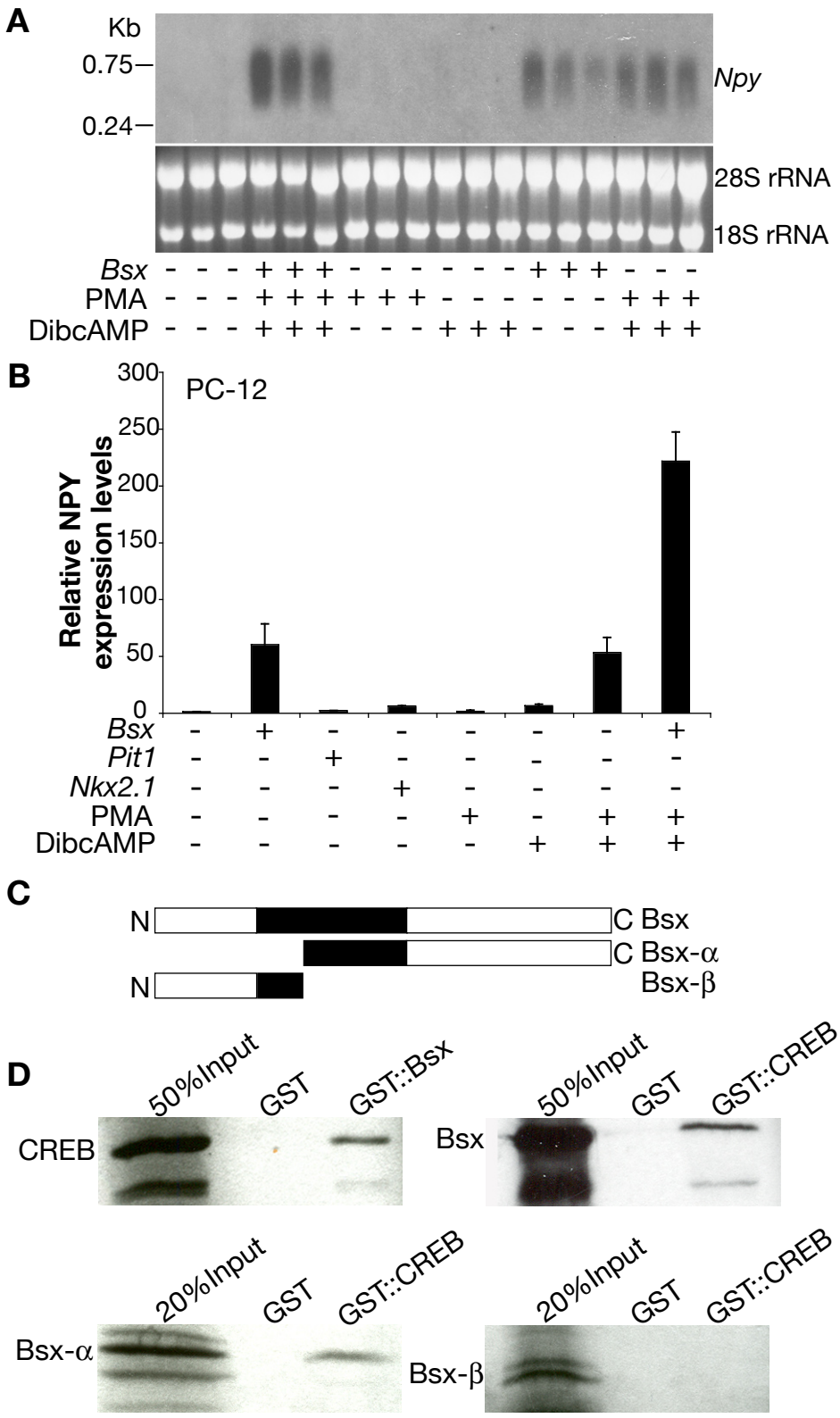

Figure 2.8.1 Cooperative interaction between Bsx and phosphorylated CREB in activating *Npy* transcription. (A) Analysis of *Npy* mRNA by Northern bloting on RNA isolated by PC-12 cells transfected with Bsx in combination with 0.4 μMphorbol, myristate acetate (PMA) and 1 mM N^6,2'-*O*-dibutyryl cAMP (DibcAMP). The bottom panel is the same gel prior bloting stained with ethidium bromide and used as control for the loaded RNA. (B) Quantitative RT-PCR for *Npy* on RNA isolated by PC-12 cells Bsx transfected in combination with treatement of PMA and DibcAMP. Values represent mean ±SEM, data were normalized with *TBP*. (C) Schematic representation of the 3 construct that have been used for in vitro translation in (D) pull-down interaction essays with purified GST::CREB protein. The first panel is a pull down essay performed with in vitro translated and labeled CREB with purified GST::Bsx.

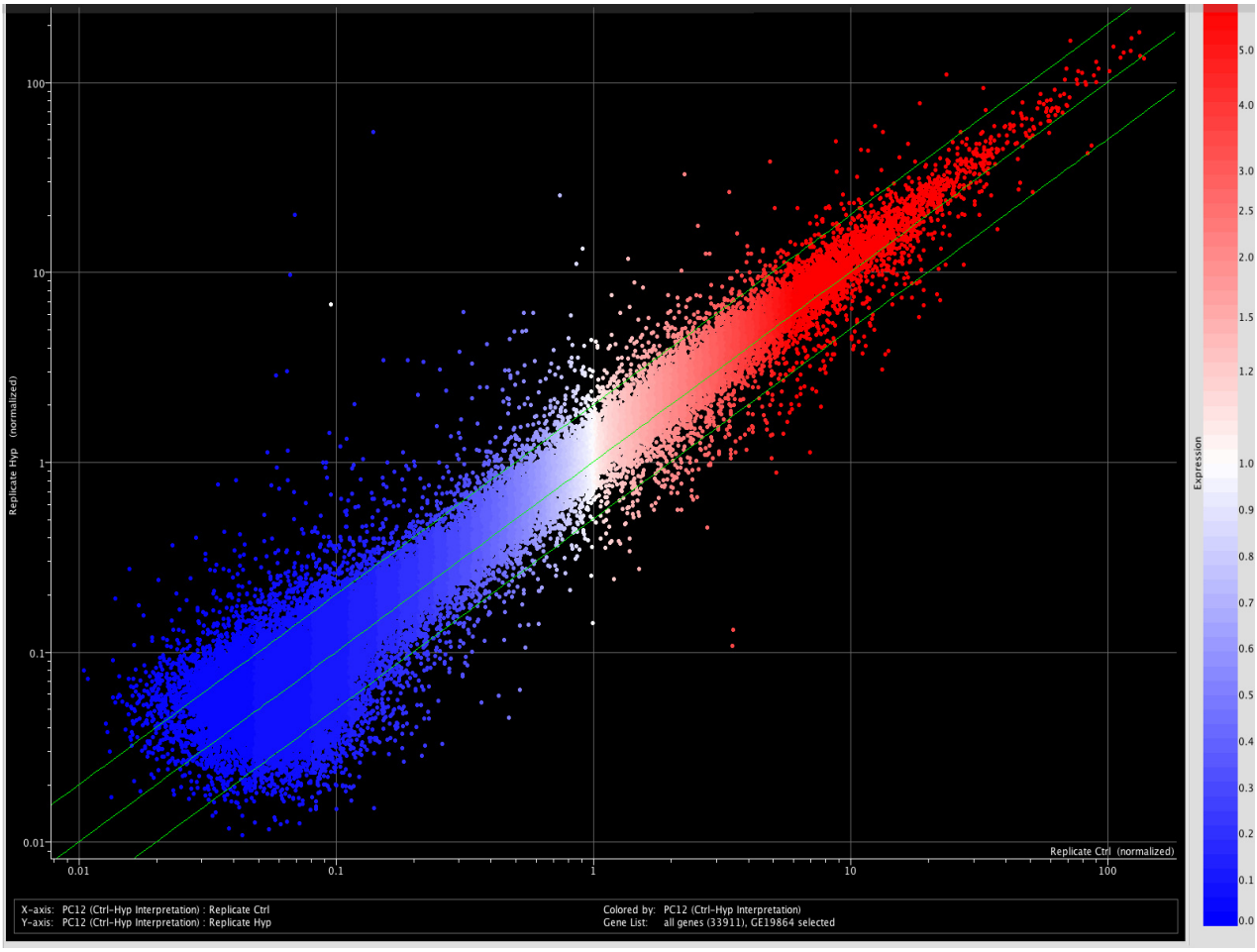

Figure 2.8.2 Gene expression profiling on Bsx and mock transfected PC-12 cells. Scatterplot of biological replicates. More than 98% of the genes expressed in the PC-12 cells fall within the lines indicating two fold difference. Gene expression profiling was performed on RNA from 10 cm diameter Bsx transfected plates using the CodeLink Rat whole Genome Bioarrays that contains probes for 35000 individual rat genes. Three biological replicates were done for VP16::Bsx and mock transfected cells. The data from the microarrays were imported from the CodeLink software into the Genespring and normalised to the 50th percentile of all spots on each array (per chip normalisation or scaling). Scatterplot between 3 VP16::Bsx transfected plates (Y axis) and 3 mock transfected plates (X axis). Note that the axis are logarithmic.

A

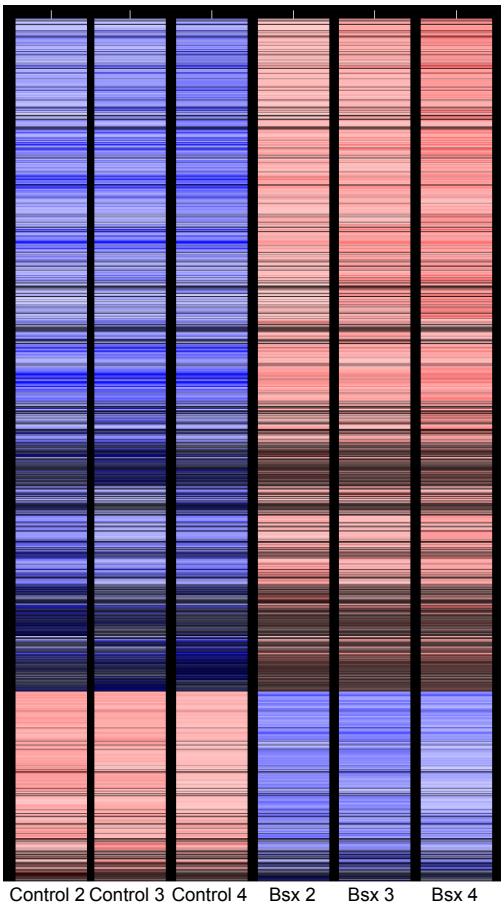

Figure 2.8.3 Gene expression profiling of Bsx and mock transfected cells. Biological replicates cluster together, suggesting that Bsx overexpression in the PC-12 cells is the primary cause of change in the gene expression profiling. Condition tree. Three biological replicates were done using RNA from three different independently Bsx and mock transfected PC-12 cell plates. The microarray data were analysed in Genespring. All 33911 genes were normalised to the 50th percentile of all spots on each array (per chip normalisation or scaling). (A) The samples were clustered in a condition tree using spearman correlation. Each gene is represented with a bar. The color of the bar indicates the normalised intensity of the gene of each microarray. Red represents the highest intensity and blue the lowest. The three mock transfected and the three Bsx transfected samples cluster together, which means that the overall differences are biggest between mock and Bsx transfected plates. This suggests that the main cause of change in gene expression profile is due to Bsx overexpression. (B) Correlation coefficiencies between all 6 arrays. The standard correlation between all pairs of microarrays were calculated in Genespring. All biological replicates are between 95.8 and 96.2 percent identical for the Bsx transfected plates and between 95.3 and 95.7 percent identical for the mock transfected plates. The correlation between all pairs of Bsx-mock transfected cells were between 94.5 and 94.8 percent.

B

	Control 2	Control 3	Control 4	Bsx 2	Bsx 3	Bsx 4
Control 2	1	0.954	0.957	0.948	0.948	0.946
Control 3	0.954	1	0.953	0.945	0.946	0.946
Control 4	0.957	0.953	1	0.947	0.948	0.945
Bsx 2	0.948	0.945	0.947	1	0.958	0.959
Bsx 3	0.948	0.946	0.948	0.958	1	0.962
Bsx 4	0.946	0.946	0.945	0.959	0.962	1

Gene/description	Fold up VP16::Bsx vs mock
Matrix metalloproteinase 3	353.5
Matrix metalloproteinase 10	269.2
Neuropeptide Y	**71.8**
Tissue-type transglutaminase	49.7
Lectin galactose binding soluble 3	34.6
S100 calcium-binding protein A9	22.6
FXYD domain-containing ion transportregulator 2	19.7
Brain-enriched SH3 domain Besh3	17.7
Aldose reductase-like protein	15.6
Relaxin 3	15.2
NGFI-B Immediate early gene transcription factor	12.7
Urotensin 2	12.4
Similar to protein tyrosine phosphatase, non receptor	12.3
Kruppel-like factor 4	9
Similar to Neurotensin/neuromedin N precursor	7.5
Regulator of G-protein signaling protein 2	6.5
Melanocyte specific gene 1 protein	6.4
Early growth response 1 Erg1	5.9
Transcribed locus similar to cfos	5.2
Synapsin 2	4,8
Glycoprotein hormones, alpha subunit	4.7
VGF nerve growth factor inducible	4.6
Potassium channel, subfamily V, member 1 Kcnv1	4.5
MAD homolog 3 Madh3	4.5
Immediate early response 3	4.5
Synapsin 2	4.3
Fos-like antigen Fosl1	4.3
Insulin receptor substrate 1 Irs1	3.9
Chloride channel K1 Clcnk1	3.5
PKC-delta binding protein	3.4
Chloride channel 5 Clcn5	3.4
Immediate early response 5 Ier5	3
Sodium channel, voltage gated, type III, alpha polypeptide Scn3a	2.8
Potassium intermediate/small conductance Kcnn1	2.8
Benzodiazepin receptor	2.7
Similar to class I cytokine receptor	2.7

Gene/description	Fold down VP16::Bsx vs mock
Chemokine receptor LCR1	3.9
BE112048	6.6
BQ206081	6.1
BE108409	5.3
CyclinA2 Ccna2	3.9
Neuronatin Nnat	3.7
Cell cycle protein p55CDC Cdc20	3
Forkhead box M1 FoxM1	2.8
Dopamine beta hydroxylase	2.8
Rab3B protein Rab3b	2.7
Neuropilin Nrp	2.7
Cyclin F Ccnf	2.7
BE113443	2.7
AI549424	2.6
Timeless (Drosophila) homolog	2.3

Table 2.8.4

A

AAAGCTGAGCTCACGCGGTGGCGGCCGCTCTAGAGATTGTTTCCTAGACAAGTTA-
CAAAAAGTTAAAGGTGAATGCAAGTCCAGTAATCTGGGTACATTGACAGGTACCCA
ACTGAGTGTGATGATGTATTGCTAACCAAGGACTGAGTGATCTCTGTGTAATTAAGT
GTGCTCCTATGTGGCTGAAATATGGGAGCGGCATGTCAGCACTGAGTGAAGGTAA
GATTGTTTGGTCTCTGTGGCATGGAGAATTTCATGTGCCTGCGTGGGTGCAGGCT
TTCTTTTTCTTTTTTTTAAAAAAATAAACCACTTTAGATCGTGTCGCCTCCCCTCACT
TCTGTGATTGATTTTGCGAGGCTAATGGTGCGTAAAAGCACTGGTGAGATCTGGGG
GCGCCTCCTTGGCTGACGTCAGAGAGAGAGTTTAAAAAGGGGAGACCGTGGAGA
GCTCCATAGCGGCTGAAGGAGACGCTACCGAAGCCGTCGCTGCTGCCTGAAGCT
TATCGATACCGTCGACCTCGAGGGGGGGCCCGGTACCCAATTCGCCTATAGTGAG
TCGTATTACAATTCACTGGCCGTCGTTTTACAACGTCGTGACTGGGAAAACCCTGG
CGTTACCCAACTTAATCGCTTGCAGCACATCCCCTTTCGCCAGCTGGCGTAATAGC
GAAGAGGCCCGACGATCGCCTTCCA

B

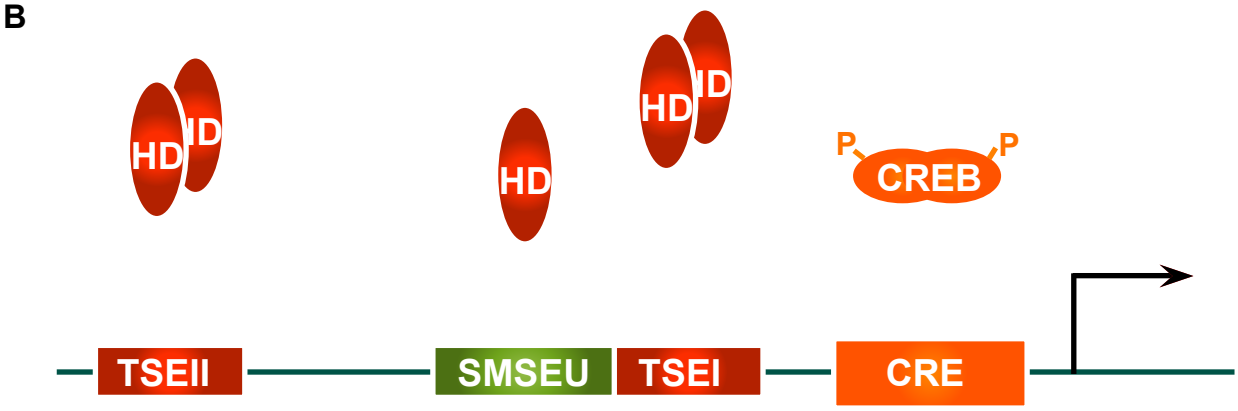

Figure 2.8.5 ***Somatostatin*** **(*Sst*) expression in the Arc nucleus of *Bsx*$^{lacZ/lacZ}$ mice is abolished.** (A) Sequence of the promoter area upstream the 5' of Sst and (B) schematic representation of the promoter structure and the characterized binding motifs.

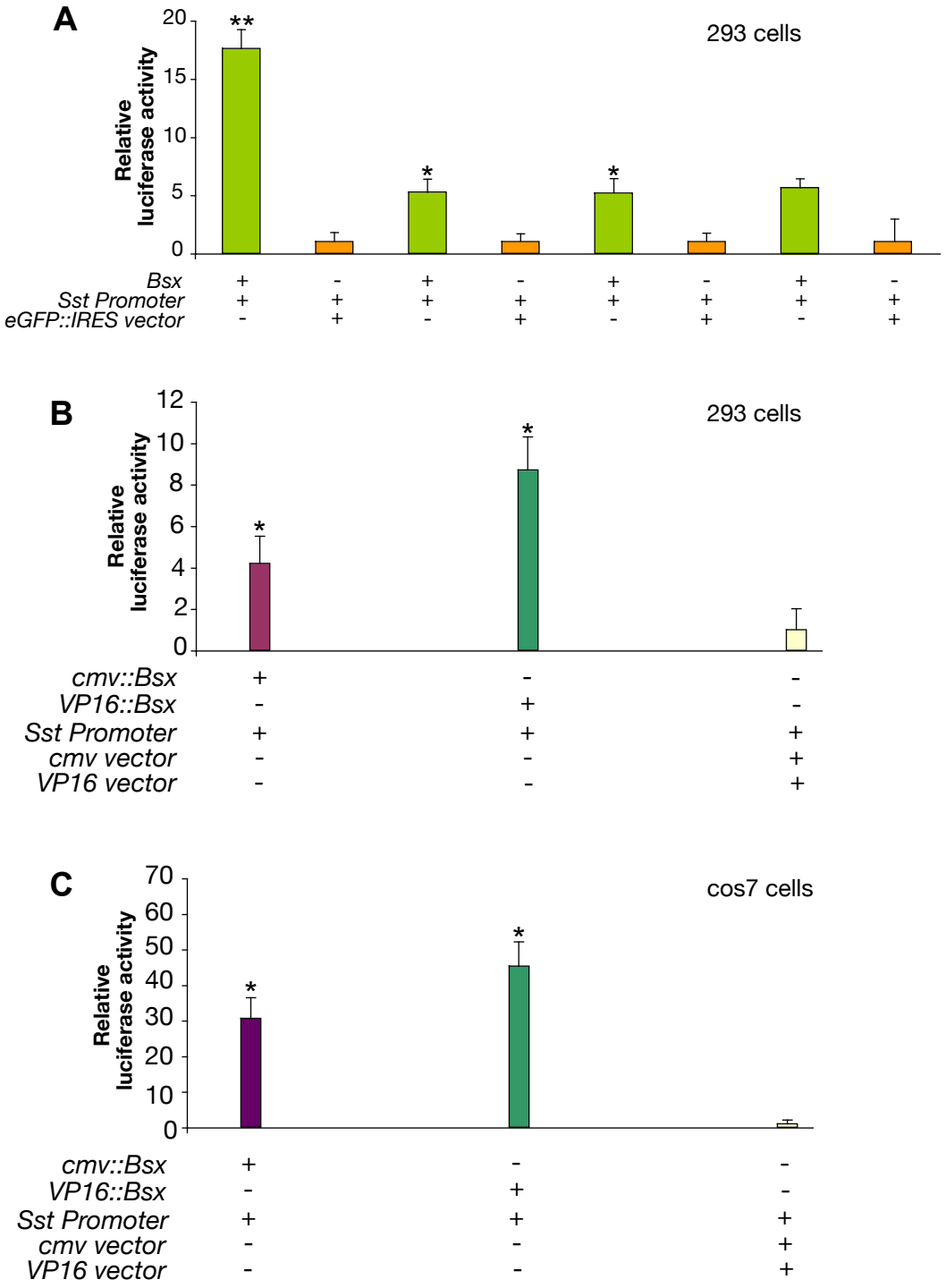

Figure 2.8.6 Bsx activates directly the *Somatostatin (Sst)* promoter. (A) Transactivation by Bsx of the Somatostatin promoter-luciferase construct in 293 kidney cells. The reporter construct was either transfected with the IRES-eGFP vector as control or with the Bsx-eGFP construct. (B) Transactivation of the somatostatin promoter by Bsx in 293 kidney cells. The reporter construct was transfected either with Bsx downsream cmv promoter, or Bsx fused to VP16, or the empty vectors for control. (C) Transactivation of *Sst* promoter-luciferase by the Bsx constructs described at (B) in cos7 cells; n>12 for each transfection condition, values represent mean ±SEM, *P<0.05, **P<0.01.

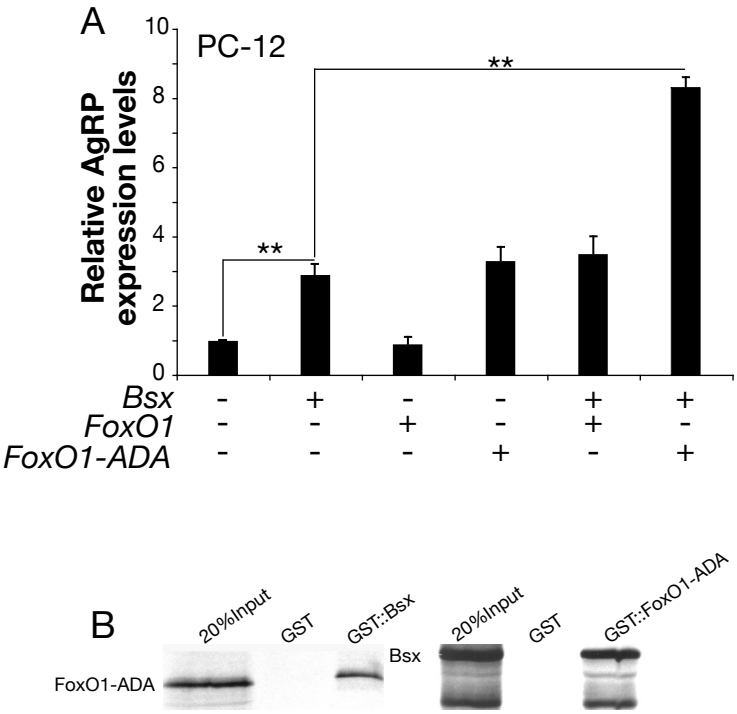

Figure 2.8.7 Cooperative interaction between Bsx and FoxO1 in activating *Agrp* transcription (A) Agrp expression analysis using quantitative RT-PCR from PC-12 cells transiently transfected with bsx and FoxO1 expression vectors; data were normalized for TBP (**P< 0.005). (B) GST pull-down interaction assay with GST::Bsx and in vitro translated full length FoxO1 protein and GST::FoxO1 with in vitro translated Bsx protein.

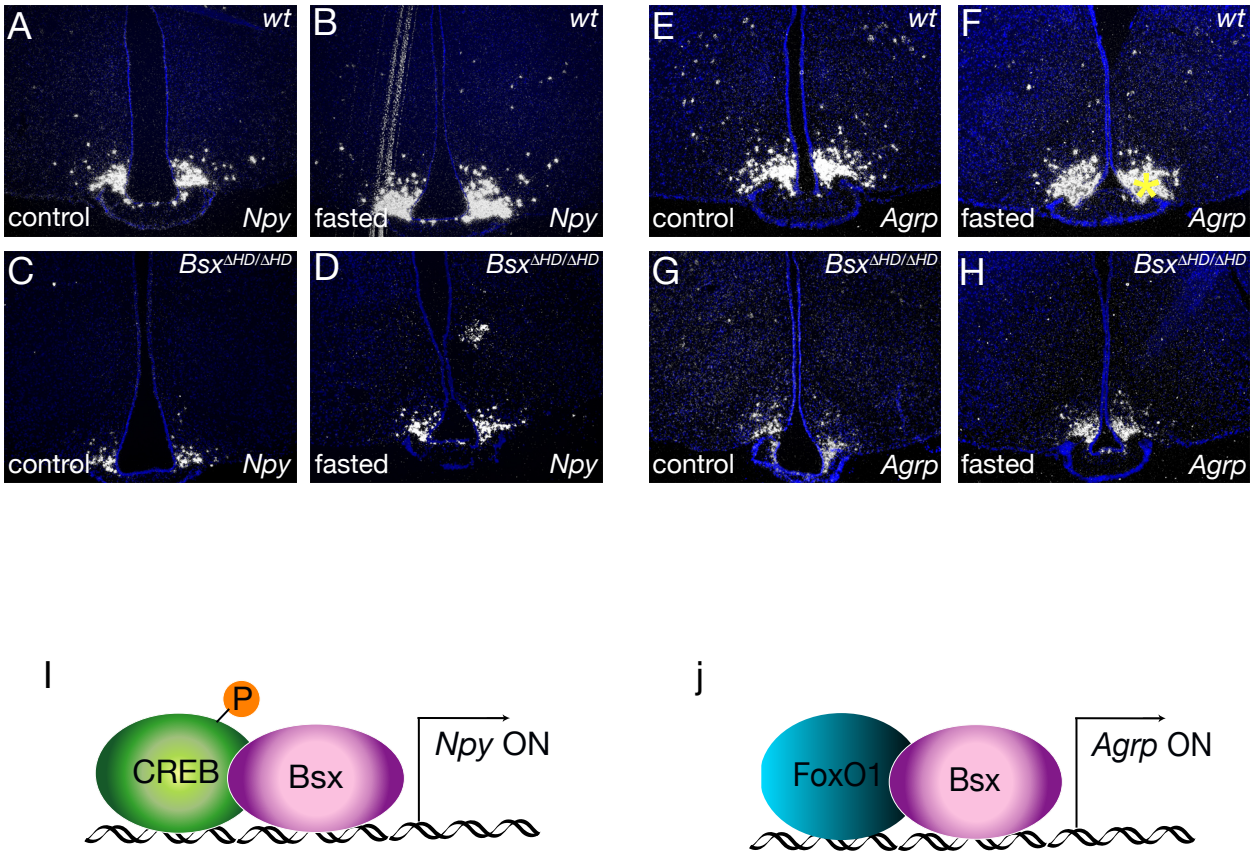

Figure 2.8.8 Bsx is required for fasting induced *Npy* and *Agrp* upregulation. (A-D) *Npy* ^{35}S-in situ expression analysis in non-fasted and 48h fasted control and *Bsx* mutant mice (E-H) *Agrp* ^{35}S-in situ expression analysis in non-fasted and 48h fasted control and *Bsx* mutant mice. (I) Model of *Npy* gene regulation. (J) Model of *Agrp* gene regulation.